

WFO-19246

# Developing, Mechanizing and Testing of a Digital Active Flutter Suppression System for a Modified B-52 Wind-Tunnel Model

John R. Matthew

**BOEING** MILITARY AIRPLANE COMPANY

A Division of The Boeing Company • Wichita, Kansas • 67210

Contract NAS1-14031  
March 1980

**NASA**

National Aeronautics and  
Space Administration

**Langley Research Center**  
Hampton, Virginia 23665  
AC 804 827-3966

# TABLE OF CONTENTS

	<u>Page</u>
1.0 SUMMARY . . . . .	1
2.0 INTRODUCTION . . . . .	3
3.0 FLUTTER SUPPRESSION SYSTEM DESIGN CRITERIA AND METHODOLOGY. . . . .	9
3.1 Ballast and Attachment Configuration . . . . .	9
3.2 Flutter Suppression System Synthesis . . . . .	10
3.3 Flutter Suppression System Implementation . . . . .	11
4.0 AEROELASTIC AND DYNAMIC ANALYSIS . . . . .	15
4.1 Structural Analysis . . . . .	15
4.1.1 Vibration . . . . .	15
4.1.2 Aerodynamics . . . . .	15
4.1.3 Equations of motion . . . . .	17
4.2 Flutter Analysis . . . . .	19
4.2.1 Configuration definition . . . . .	19
4.2.2 Flutter results . . . . .	20
4.2.3 Ballast design . . . . .	20
5.0 FLUTTER SUPPRESSION SYSTEM SYNTHESIS AND ANALYSIS . . . . .	23
5.1 Synthesis Criteria and Constraints . . . . .	23
5.1.1 Stability criteria . . . . .	23
5.1.2 System constraints . . . . .	23
5.2 Flutter Suppression System Synthesis . . . . .	23
5.2.1 Sensor and control surface selection . . . . .	23
5.2.2 Symmetric flutter suppression system synthesis . . . . .	27
5.2.3 Antisymmetric flutter suppression system synthesis . . . . .	34
5.2.4 System configuration . . . . .	34
5.3 Flutter Suppression System Performance Analysis . . . . .	34
5.3.1 Flutter damping performance . . . . .	34
5.3.2 System stability margins . . . . .	34
5.3.3 Control surface requirements . . . . .	35
6.0 FLUTTER SUPPRESSION SYSTEM IMPLEMENTATION . . . . .	53
6.1 System Configuration . . . . .	53
6.1.1 System requirements . . . . .	53
6.1.2 System interface . . . . .	54
6.1.3 Final configuration . . . . .	55
6.2 Hardware Design . . . . .	57
6.2.1 Analog voter design . . . . .	57
6.2.2 Interface panel design . . . . .	59
6.3 Software Design . . . . .	59
6.3.1 Software design requirements . . . . .	59
6.3.2 Computer and signal processing equipment . . . . .	59
6.3.3 Selection of linear-to-discrete transform . . . . .	59
6.3.4 Flutter suppression system filter implementation . . . . .	61
6.3.5 Failure detection and indication . . . . .	67

## TABLE OF CONTENTS (Concluded)

	<u>Page</u>
6.4      System Performance . . . . .	68
6.4.1   Filter frequency response . . . . .	69
6.4.2   Analog voter performance . . . . .	69
6.4.3   Failure detection performance . . . . .	69
7.0      TEST SUPPORT AND RESULTS . . . . .	75
7.1      Flutter Suppression System Preparation and Model Modifications . . . . .	75
7.1.1   Flutter suppression system preparation . . . . .	75
7.1.2   Model modifications . . . . .	76
7.2      Test Results . . . . .	77
7.2.1   Flutter mode damping performance . . . . .	77
7.2.2   Degraded system performance . . . . .	77
7.3      Post Test Analysis . . . . .	81
7.3.1   Changes to structural model . . . . .	81
7.3.2   Comparison with test results . . . . .	81
8.0      CONCLUSIONS AND RECOMMENDATIONS . . . . .	87
8.1      Conclusions . . . . .	87
8.2      Recommendations . . . . .	87
9.0      REFERENCES . . . . .	89

## APPENDIX

A	FLUTTER SUPPRESSION SYSTEM PERFORMANCE . . . . .	A-1
B	FLUTTER SUPPRESSION SYSTEM IMPLEMENTATION . . . . .	B-1

# LIST OF FIGURES

Figure No.	Title	Page
2-1	Plan View of B-52E Aeroelastic Model . . . . .	3
2-2	Block Diagram of Flutter Suppression System . . . . .	5
2-3	Symmetric and Antisymmetric Flutter Suppression System Damping Performance. . . . .	6
2-4	Redundant Digital Flutter Suppression System Signal Paths . . . . .	7
3-1	Configuration Design Methodology . . . . .	10
3-2	Flutter Suppression System Synthesis Methodology . . . . .	11
3-3	Hardware/Software Design Methodology . . . . .	12
4-1	Aerodynamic Paneling . . . . .	20
4-2	Symmetric Flutter Characteristics. . . . .	21
4-3	Antisymmetric Flutter Characteristics . . . . .	22
5-1	Plan View of the B-52E Aeroelastic Model . . . . .	24
5-2	Zero Root Locus of Various Control Surfaces and Sensors . . . . .	26
5-3	Symmetric and Antisymmetric Flutter Mode Damping Versus Dynamic Pressure . . . . .	28
5-4	Flutter Suppression System Filter Frequency Response . . . . .	29
5-5	Root Locus of the Symmetric Flutter Suppression System, Dynamic Pressure = 3112 N/m <sup>2</sup> (65 psf) . . . . .	30
5-6	Root Locus of the Symmetric Flutter Suppression System Dynamic Pressure = 4309 N/m <sup>2</sup> (90 psf) . . . . .	32
5-7	Root Locus of the Antisymmetric Flutter Suppression System Dynamic Pressure = 3112 N/m <sup>2</sup> (65 psf) . . . . .	36
5-8	Root Locus of the Antisymmetric Flutter Suppression System Dynamic Pressure = 4309 N/m <sup>2</sup> (90 psf) . . . . .	38
5-9	Block Diagram of Flutter Suppression System . . . . .	40
5-10	Block Diagram of Alternate Flutter Suppression System . . . . .	41
5-11	Symmetric Flutter Mode Characteristics with the Flutter Suppression System On and Off . . . . .	42
5-12	Antisymmetric Flutter Mode Characteristics with the Flutter Suppression System On and Off . . . . .	43
5-13	Gain/Phase Root Locus of the Symmetric Flutter Suppression System, Dynamic Pressure = 4309 N/m <sup>2</sup> (90 psf) . . . . .	46
5-14	Minimum Gain Margins of the Flutter Suppression System . . . . .	48
5-15	Minimum Phase Margins of the Flutter Suppression System . . . . .	49
5-16	Symmetric Control Surface Requirements . . . . .	50
5-17	Antisymmetric Control Surface Requirements . . . . .	51
6-1	System Interface Configuration . . . . .	54
6-2	Interface Panel Signal Paths . . . . .	55
6-3	Redundant Digital Flutter Suppression System Signal Paths . . . . .	56
6-4	Analog Voter Circuit . . . . .	57
6-5	Analog Voter Box External Details . . . . .	58
6-6	Interface Panel Front Details and Wiring Diagram . . . . .	60
6-7	Parallel Expansion of the Flutter Suppression System Filter. . . . .	66
6-8	Parallel Expansion of the Partial Flutter Suppression System Filter . . . . .	67
6-9	Frequency Response of Symmetric Flutter Suppression System . . . . .	70
6-10	Frequency Response of Antisymmetric Flutter Suppression System . . . . .	71

## LIST OF FIGURES (Concluded)

<u>Figure No.</u>	<u>Title</u>	<u>Page</u>
6-11	Frequency Response of Symmetric Flutter Suppression System with Each Channel Failed . . . . .	72
6-12	Frequency Response of Antisymmetric Flutter Suppression System with Each Channel Failed . . . . .	73
7-1	Model Response with Flutter Suppression System On and Off . . .	78
7-2	Acceleration Frequency Response with Flutter Suppression System On and Off . . . . .	79
7-3	Symmetric Flutter Characteristics - Modified Stiffness . . . .	82
7-4	Root Locus of Flutter Suppression System using Updated Equations, Dynamic Pressure = $3831 \text{ N/m}^2$ (80 psf) . . . . .	83
7-5	Flutter Suppression System Flutter Mode Damping Performance .	85

# LIST OF TABLES

<u>Table No.</u>	<u>Title</u>	<u>Page</u>
4-I	Model Scale Factors . . . . .	.16
5-I	Symmetric Modal Frequency and Damping . . . . .	.44
5-II	Antisymmetric Modal Frequency and Damping . . . . .	.45
6-I	Comparison of Discrete Transforms . . . . .	.62
6-II	Difference Equations for Common Filter Elements . . . . .	.63
6-III	Difference Equations for the Flutter Suppression System Filter.	.65
6-IV	Difference Equations for the Parallel Flutter Suppression System Filter . . . . .	.66
6-V	Difference Equations for the Partial Parallel Flutter Suppression System Filter . . . . .	.68
7-I	Comparison of GVT and Analytical Frequencies . . . . .	.76
7-II	Voter Outputs with Degraded Inputs . . . . .	.80

## SYMBOLS

$A_I$	Aerodynamic Influence Coefficient Matrix
A-to-D	Analog-to-Digital
$B_i, G_i$	Lift Growth Parameters
BM	Bending Moment, N-m (in-lb)
BS	Body Station, m (inch)
$C_i, D_i$	Aerodynamic Parameters
$C_\theta, C_z, C_w$	Linearized Boundary Condition Matrices
CCV	Control Configured Vehicle
D-to-A	Digital-to-Analog
dB	Decibel
DC	Direct Current
Deg.	Degree
EI, GJ	Stiffness Parameters
F	Force, N (lb)
FN	Froude Number
FSS	Flutter Suppression System
g	Normalized Acceleration
GVT	Ground Vibration Test
Hz	Hertz
I	Mass Inertia, $\text{kg-m}^2$ (lb-in-sec <sup>2</sup> )
$\bar{I}$	Area Inertia, $\text{m}^4$ (in <sup>4</sup> )
j	Square Root of -1 ( $\sqrt{-1}$ )
$K_i$	Difference Equation Gains
kg	Kilogram
KTAS	Knots True Airspeed
$\ell$	Length, m (in)
lb	pound
m	meter
M	Mach number
$\bar{M}$	Mass, kg (lb-sec <sup>2</sup> /in)
N	Newton
PSD	Power Spectral Density
psf	Pounds per Square Foot
q	Dynamic Pressure, $\text{N/m}^2$ (lb/ft <sup>2</sup> )

# SYMBOLS (Concluded)

$q(s), q(j\omega)$	Rigid body, Structural and Control Surface Degrees of Freedom
$R$	Resistance, Ohm
$R_i$	Gust Coefficient
Rad	Radian
RMS	Root Mean Square
$s$	Second
$S$	Laplace Transform Variable, radians/second
$T$	Sample Time, seconds
$U_0$	True Airspeed, m/s (in/sec)
$V$	Velocity, m/s (in/sec)
$V_A, V_B, V_C$	Voter Input Voltages, volts
$V_A', V_B', V_C'$	Voter Intermediate Voltages, volts
$V_{CC}$	Power Supply Voltage, volts
$V_g$	Lateral Gust, m/s (in/sec)
$V_o$	Output Voltage, volts
$W$	Weight, kg (lb)
WBL	Wing Buttock Line, m (in)
$W_g$	Vertical Gust, m/s (in/sec)
$X_i$	Difference Equation Input
$Y_i$	Difference Equation Output
$\ddot{Z}$	Vertical Acceleration, $m/s^2$ (in/sec <sup>2</sup> )
$\delta$	Control Surface Deflection, rad (deg)
$\Delta$	Time Delay Operator
$\zeta$	Damping Ratio
$\rho$	Air Density, $kg/m^3$ (in-sec <sup>2</sup> /in <sup>4</sup> )
$\sigma$	Stress, $N/m^2$ (lb/in <sup>2</sup> )
$\omega$	Frequency, rad/s



## 1.0

### SUMMARY

This study was performed under NASA Contract NAS1-14031 to define a configuration for the B-52E aeroelastic wind tunnel model that would produce high-frequency symmetric and anti-symmetric flutter modes with violent onset, synthesize a flutter suppression system (FSS) capable of stabilizing these modes and implement the FSS using digital computers. The system was then tested in the Transonic Dynamics Tunnel at NASA Langley Research Center.

For the past ten years the Boeing Military Airplane Company has assisted NASA Langley in demonstrating the feasibility of active control systems designed to augment or suppress low frequency structural modes. During the B-52 CCV program a 1/30 scale B-52 aeroelastic wind tunnel model was used to predict and verify the performance of the ride control and flutter suppression systems. The results of the wind tunnel and flight tests showed good correlation to analytical results, verifying the usefulness of this methodology.

The flutter mode on the B-52 CCV program was a symmetric, low-frequency (2.4 Hz) mode with mild onset. For the current study, the B-52E aeroelastic model was modified to produce symmetric and antisymmetric flutter modes with violent onset at higher frequencies (13 Hz to 25 Hz model frequencies; 2.4 to 4.6 Hz airplane frequencies). A flutter suppression system was then synthesized to extend the flutter dynamic pressure of the modified model at least 44 percent. The resulting FSS feedback filters were mechanized using digital computers with three channel redundancy to provide fail-operate capability.



This document is the final report of Contract NAS1-14031 entitled "Stability Augmentation System for Aeroelastic Wind Tunnel Models." The primary result of this program was a flutter suppression system implemented digitally which was capable of stabilizing the flutter modes of the modified B-52E aeroelastic wind tunnel model. This system was successfully tested in the Transonic Dynamics Tunnel at NASA Langley Research Center.

The work began with the definition of the structural changes required for the existing 1/30-size, full-span, cable-mounted, free-flying model of the B-52 CCV airplane to obtain the flutter characteristics required for this study. (Descriptions of the original B-52 model and previous wind tunnel tests results are presented in references 1, 2, 3, and 4). For the modified model, flutter was to consist of two modes, symmetric and antisymmetric, that exhibited violent onset and had frequencies in the range of 13 Hz to 25 Hz (model frequency). To allow testing above the flutter speed without exceeding the design limit of the model the flutter modes were required to occur below  $3831 \text{ N/m}^2$  (80 psf). A configuration which satisfied these requirements was defined that had wing ballast replacing the engine nacelles and external fuel tanks and was sting mounted at the wing attach point as illustrated on Figure 2-1.

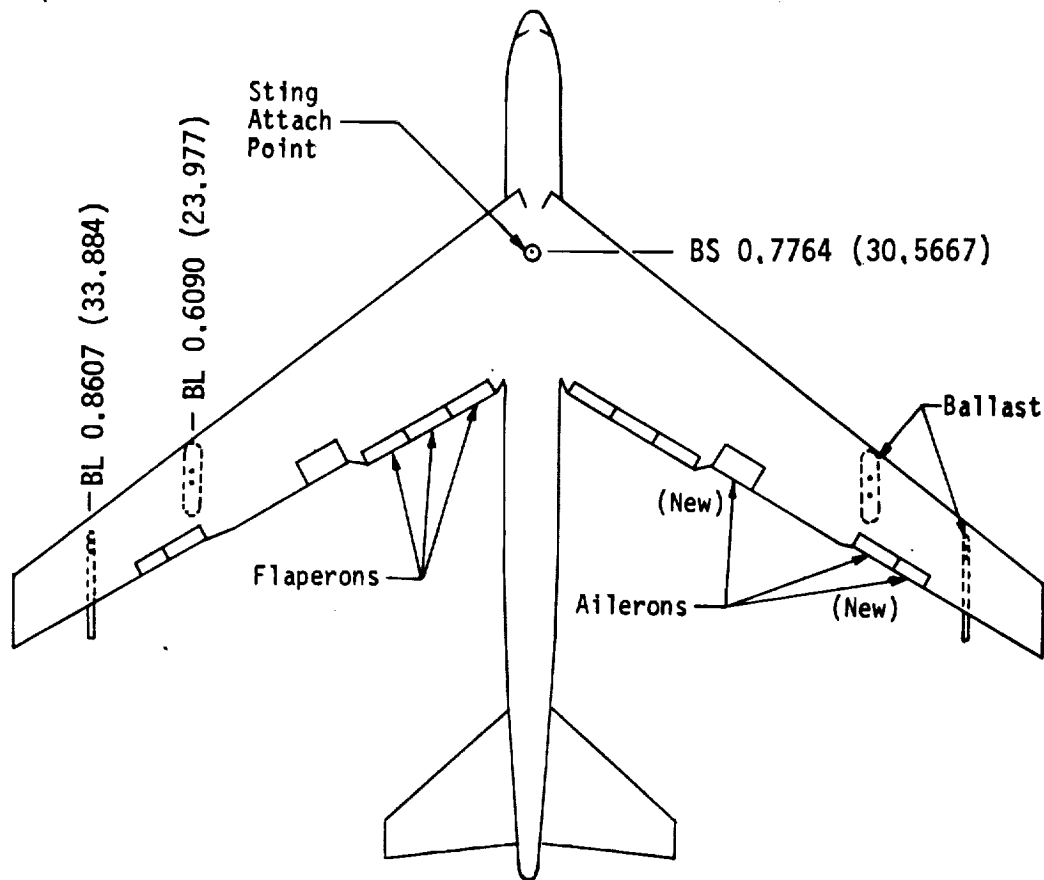


FIGURE 2-1 - PLAN VIEW OF B-52E AEROELASTIC MODEL

The flutter suppression system was synthesized to produce a 44 percent increase in flutter dynamic pressure with  $\pm 6$  dB gain margin and  $\pm 0.7854$  rad (45 degrees) phase margin at speeds below the flutter velocity. Due to the similarity of the symmetric and antisymmetric flutter modes the final symmetric and antisymmetric feedback filters were identical, as shown on Figure 2-2. The final system was predicted to extend the flutter dynamic pressure more than the required 44 percent as illustrated on Figure 2-3.

The FSS was implemented using digital computers in a three channel, redundant arrangement. The filters were transformed from analog form into difference equations using the bi-linear transform (Tustin's method) and implemented in parallel form using scaled integer arithmetic operations. The system performed failure detection using a circular comparison technique where each computer compared the voter output to another computer's output. The final form of the FSS is shown on Figure 2-4.

The wind tunnel test of the model equipped with the FSS was conducted in 95 percent freon with a density of  $2.58 \text{ kg/m}^3$  ( $0.005 \text{ lb-sec}^2/\text{ft}^4$ ) at 6400 m (21 000 feet) equivalent air-plane altitude. Although the flutter dynamic pressure was considerably above the predicted value,  $3926 \text{ N/m}^2$  (82 psf) instead of  $2873 \text{ N/m}^2$  (60 psf), the FSS performed as predicted, stabilizing the flutter modes up to  $4884 \text{ N/m}^2$  (102 psf). In addition, the FSS was evaluated with various induced failures and degradations. These tests proved the fail-operate capability of the FSS and the ability of the system to reduce the effects of a channel degradation when another channel had failed. Post-test analysis revealed that improved flutter speed prediction resulted when measured wing torsional stiffness and sting flexibility were incorporated in the mathematical model.

The excellent nominal and degraded performance of the FSS indicated that digital implementation of control systems was a viable alternative and was capable of supporting multiple advanced control concepts. Discrete time and optimal control techniques represent the next logical step in the synthesis and implementation of active control systems.

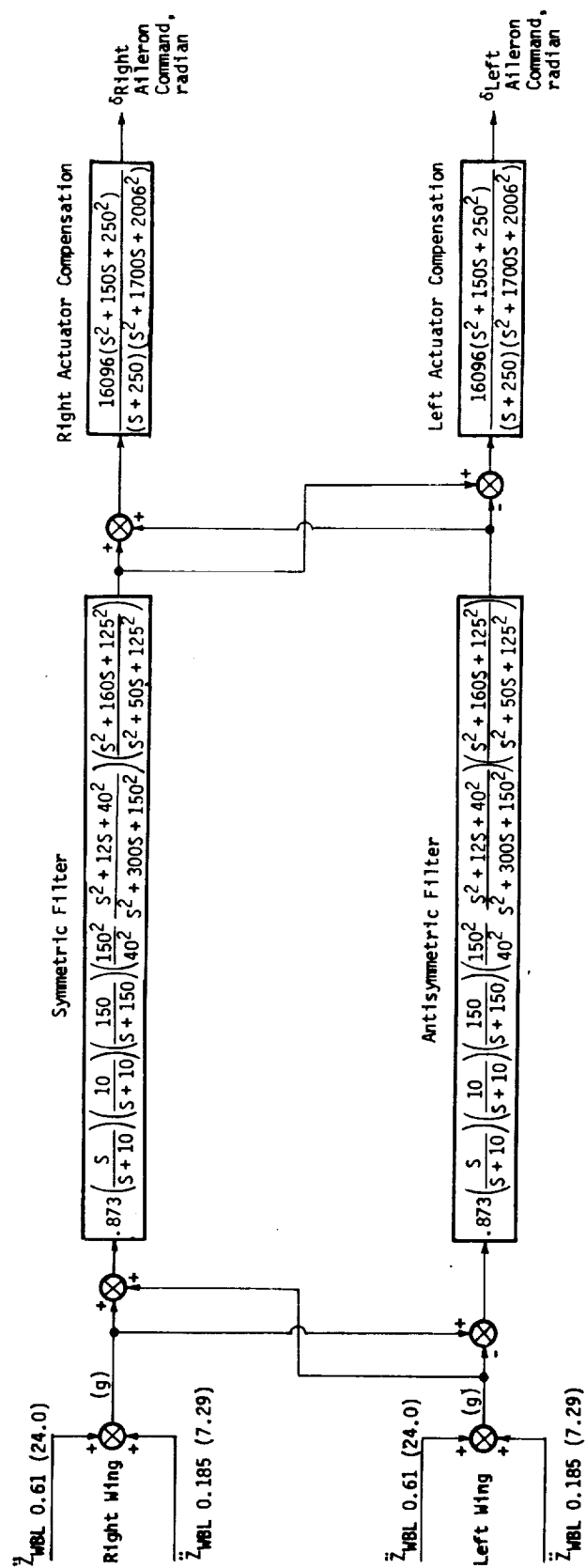


FIGURE 2-2 - BLOCK DIAGRAM OF FLUTTER SUPPRESSION SYSTEM

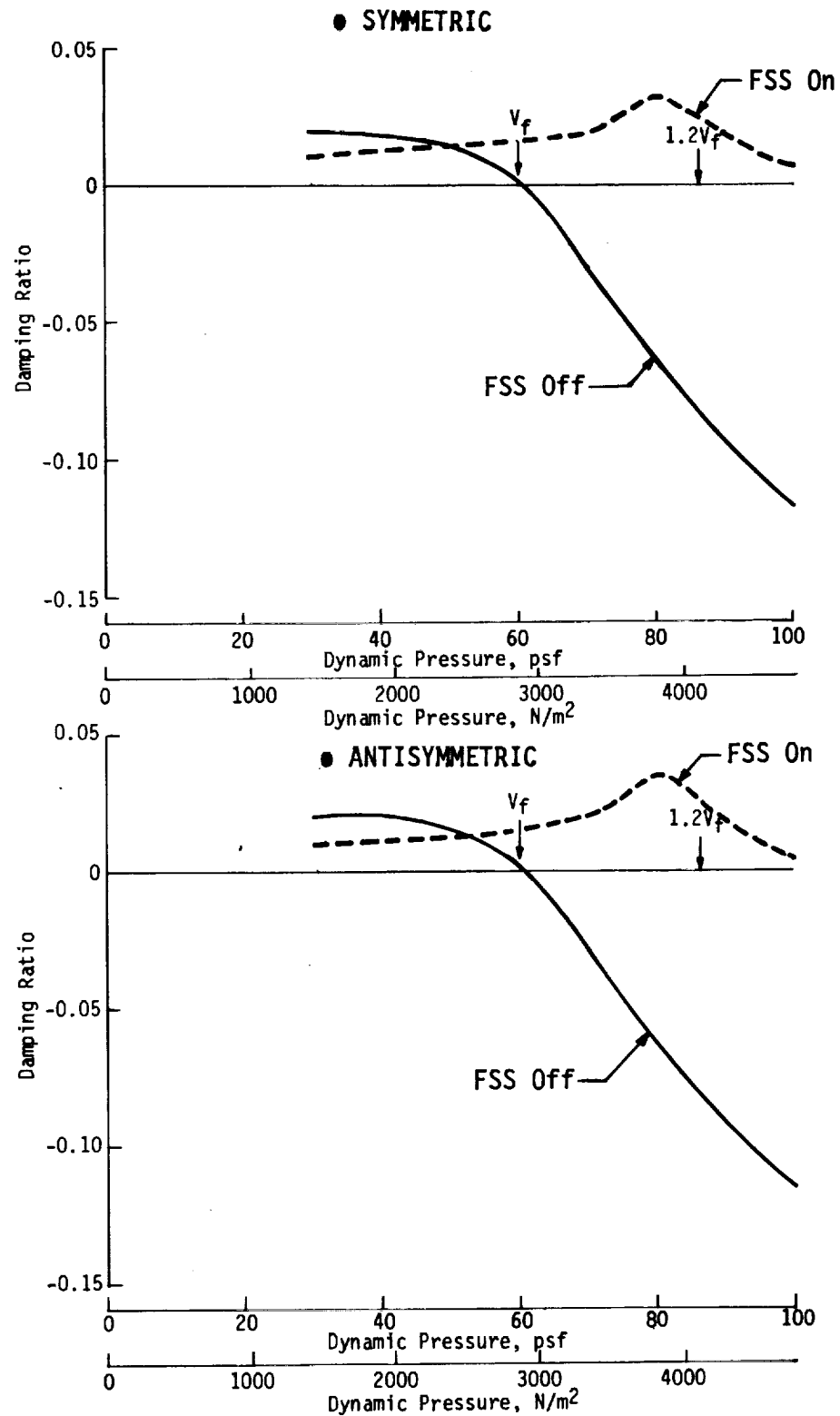


FIGURE 2-3 - SYMMETRIC AND ANTISYMMETRIC FLUTTER SUPPRESSION SYSTEM DAMPING PERFORMANCE

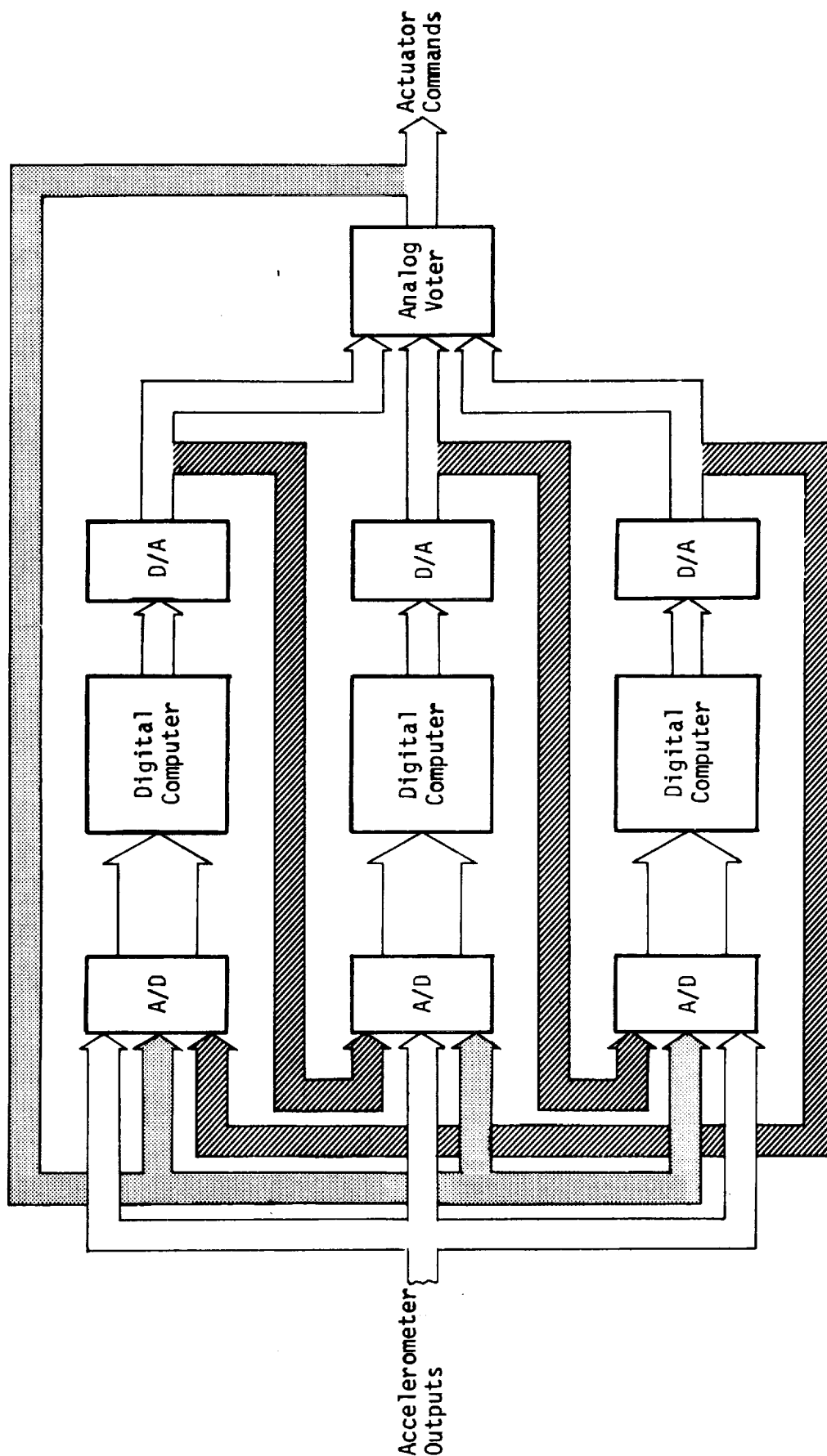


FIGURE 2-4 - REDUNDANT DIGITAL FLUTTER SUPPRESSION SYSTEM SIGNAL PATHS





### 3.0 FLUTTER SUPPRESSION SYSTEM DESIGN CRITERIA AND METHODOLOGY

This section describes the design criteria and methodology used to develop and implement a flutter suppression system capable of stabilizing the flutter modes of the B-52E aeroelastic model. Paragraph 3.1 presents the criteria and methods used in selecting the ballast and sting attachment configuration. Similar information is given for the control law synthesis and system implementation in Paragraphs 3.2 and 3.3, respectively.

#### 3.1 Ballast and Attachment Configuration

The initial effort in the program centered around the structural configuration of the model necessary to produce the desired flutter characteristics. The constraints imposed on the flutter characteristics were as follows:

- The flutter modes were to exhibit a violent onset, with the structural damping slope at flutter to be between approximately 0.001 and 0.003 per m/s (0.002 and 0.006 per KTAS airplane scale).
- The flutter modes were to have frequencies between 13 Hz and 25 Hz.
- No flutter modes other than the primary wing flutter modes (symmetric and antisymmetric) were to exist at dynamic pressures below 4788 N/m<sup>2</sup> (100 psf).
- Wind tunnel testing was to be conducted in 95 percent freon with a mass density of 2.58 kg/m<sup>3</sup> (0.005 lb-sec<sup>2</sup>/ft<sup>4</sup>) (equivalent to 6400 m (21 000 feet) atmospheric altitude).
- In order not to exceed the model design limit dynamic pressure of 4788 N/m<sup>2</sup> (100 psf) the model was to be configured to flutter at dynamic pressures below 3831 N/m<sup>2</sup> (80 psf).

Using these constraints the methodology illustrated on Figure 3-1 was used to define an acceptable configuration. To begin the process a start-up configuration was chosen and equations of motion were generated. The flutter characteristics of the model were then compared to the flutter criteria to determine whether the present configuration was acceptable or needed to be changed. If a change was indicated the ballast and/or sting attachment were updated and the process started over. When the flutter criteria were satisfied the structural modifications (ballast and/or sting attachment) were designed and transmitted to NASA for implementation. Synthesis of the flutter suppression system control laws was then ready to begin.

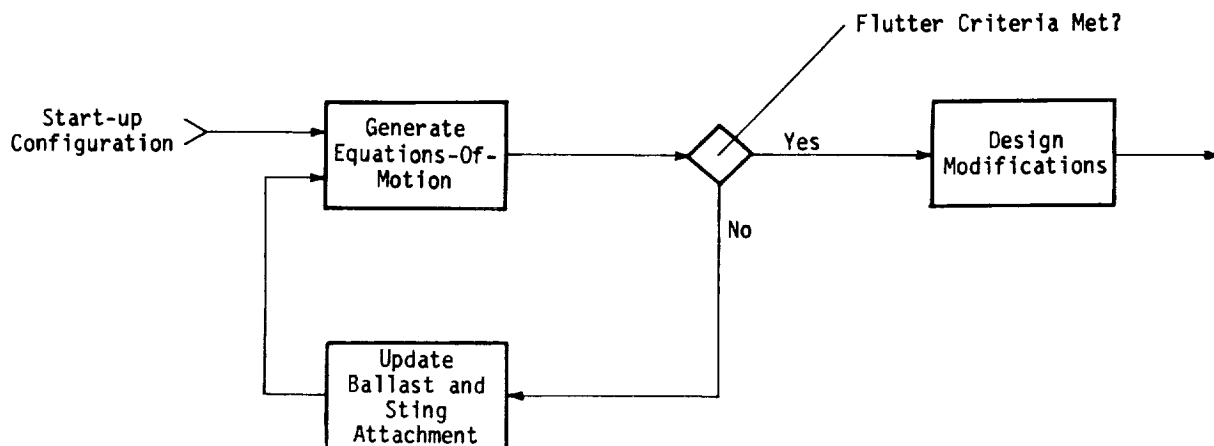


FIGURE 3-1 - CONFIGURATION DESIGN METHODOLOGY

### 3.2 Flutter Suppression System Synthesis

Synthesis of the flutter suppression system (FSS) was centered around two tasks, selection of the sensor(s) and control surface(s) and synthesis of the control laws. The criteria used in synthesizing the FSS were as follows:

- The FSS was to be synthesized in the continuous time domain.
- The FSS should extend the flutter dynamic pressure at least 20 percent while maintaining the stability of all other modes (both structural and those due to the FSS).
- The FSS should possess  $\pm 6$  dB of gain margin and  $\pm 0.7854$  rad (45 degrees) of phase margin at and below the flutter velocity.
- For digital implementation purposes, the FSS should not have modes higher in frequency than approximately 100 Hz.

With these criteria the methodology illustrated in Figure 3-2 was used to define the FSS. This methodology consisted of two major steps, selection of control surface and sensor parameters and synthesis of the control law. The process was started using an initial configuration of control surface and sensors which was updated until the desired modal coupling was achieved. The next step was to synthesize the control laws using an iterative process until the required stability characteristics were obtained. During the control law synthesis the modal coupling characteristics were reviewed with the option of returning to the control surface/sensor selection step with revised modal coupling criteria. After all criteria had been met, the next step was implementation of the resulting control law(s).

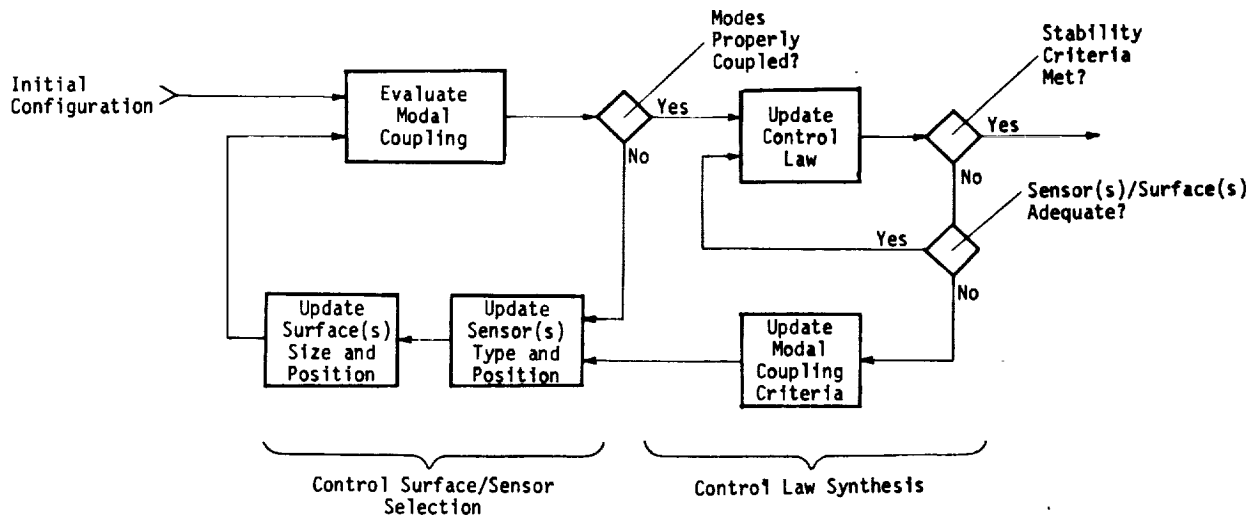


FIGURE 3-2 - FLUTTER SUPPRESSION SYSTEM SYNTHESIS METHODOLOGY

### 3.3 Flutter Suppression System Implementation

Implementation of the FSS consisted of designing and implementing both hardware and software in essentially two parallel, but inter-dependent tasks as shown on Figure 3-3. The design criteria used in this methodology were as follows:

- The FSS was to be implemented on digital computers using difference equations to represent the filters.
- The frequency response of the FSS should have no significant deviation from the ideal around the flutter frequency.
- The FSS was to have a single fail-operate capability.
- The FSS should be capable of detecting when a failure had occurred and indicating this fact to the operator.
- The sensors and control surfaces were to have no redundancy due to size limitations.

Due to the limitations on the end-to-end redundancy of the system the following failures were used in the failure analysis as those constituting a single failure.

- A single computer failing to update or incorrectly updating it's output.
- A single failed channel of an A-to-D or D-to-A converter.
- A complete failure of an A-to-D or D-to-A converter unit.
- A failure in an analog voting device.

The FSS was required to operate with all but the last failure.

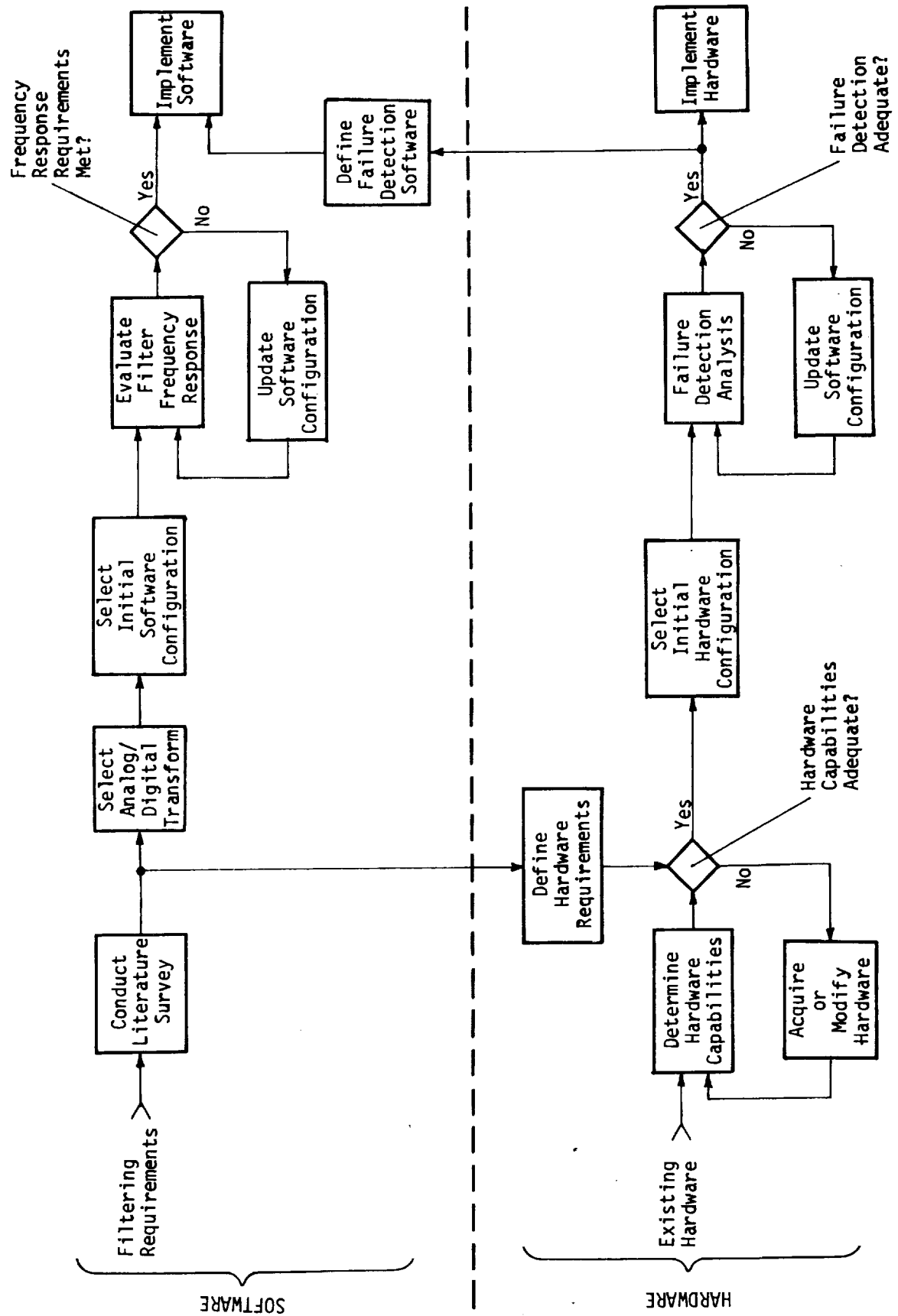


FIGURE 3-3 - HARDWARE/SOFTWARE DESIGN METHODOLOGY

The first step in both the hardware and software design was to determine the most accurate and efficient means of implementing the FSS. The output of this effort was the information necessary to select the analog to discrete filter transform and to define the hardware requirements. From this initial step the hardware capable of meeting the hardware requirements and the initial configuration could be selected. Failure detection analysis was then conducted and the hardware configuration modified until all failures could be detected. The resulting hardware design was then ready to be implemented.

Design of the software configuration proceeded in parallel with the hardware design after the initial requirements were determined. After a transform was selected an initial software configuration was chosen and an iterative process was followed until the frequency response of the digital filter met the frequency response criteria. After a satisfactory digital filter was found, the failure detection software was defined using the constraints imposed by the hardware configuration. This software, along with any support software, was then consolidated and implemented.



## 4.0 AEROELASTIC AND DYNAMIC ANALYSIS

This section describes the development of structural and aerodynamic mathematical models from which equations of motion were produced for the B-52E aeroelastic wind tunnel model. Flutter analyses were then conducted to define a configuration that met the criteria set forth in Section 3.0. Structural analysis, including development of the equations of motion, is presented in Paragraph 4.1 and flutter analysis in Paragraph 4.2.

### 4.1 Structural Analysis

Using the methodology presented in Paragraph 3.1, mathematical models were developed that describe the vibrational and aerodynamic characteristics of the wind tunnel model. These math models, developed initially in airplane scale, were used to produce equations of motion which were reduced to model scale using the scale factors in Table 4-I.

- 4.1.1 Vibration - Elastic and inertia characteristics of the airplane were represented with a lumped parameter idealization. Inertia properties (mass, and first and second moments of mass) were lumped at the appropriate elastic axis stations. Structural stiffness properties were defined by specifying the beam stiffness parameters EI and GJ at each end and the center of each beam connecting the elastic axis stations. Tapered beam element stiffness representations for the elastic axis were generated using the three sets of stiffness properties specified for each beam. Cantilevered vibration modes were computed for each of the airplane components plus a semi-rigid component representing the wind tunnel sting mount. The airplane components included the forward and aft body, wing, horizontal stabilizer, vertical fin, and wing ballast (when added). The vertical fin and horizontal stabilizer were treated as rigid components with their mass lumped on the aft body. The forward and aft body and wing represented airplane components.

Coupled vibration modes were determined using a sufficient number of cantilevered component modes to adequately represent the desired low frequency response of the airplane. The equations of motion and flutter analyses were based on 32 coupled modes.

- 4.1.2 Aerodynamics - Unsteady aerodynamic forces were generated using a three-dimensional plate doublet finite element solution. This theory accounts for Mach number and finite span effects and includes aerodynamic coupling between airplane components. The unknown pressure distribution was determined for each airplane mode by considering pressure to be a constant over a given aerodynamic panel and solving for the pressure based on a specified reduced

TABLE 4-I  
MODEL SCALE FACTORS

Scale	Symbol	Formula	Factor
Dimension	$\frac{\ell_M}{\ell_A}$	Selected	$\frac{1}{30}$
Density	$\frac{\rho_M}{\rho_A}$	Tunnel = .00499 Airplane Alt. = .0012249	4.07
Froude No.	$\frac{FN_M}{FN_A}$		1.0
Mass Ratio	$\frac{M_M}{M_A}$	$\frac{W_M}{W_A} \cdot \left(\frac{\rho_A}{\rho_M}\right) \left(\frac{\ell_A}{\ell_M}\right)^3$	1.0
Velocity	$\frac{V_M}{V_A}$	$\left(\frac{\ell_M}{\ell_A}\right)^{\frac{1}{2}}$	.183
Dynamic Pressure	$\frac{q_M}{q_A}$	$\frac{\rho_M}{\rho_A} \cdot \left(\frac{V_M}{V_A}\right)^2$	.136
Mach No.	$\frac{M_M}{M_A}$	$\frac{V_M}{V_A} \cdot \frac{a_A}{a_M}$	.375
Frequency	$\frac{\omega_M}{\omega_A}$	$\frac{V_M}{V_A} \cdot \frac{\ell_A}{\ell_M}$	5.48
Weight	$\frac{W_M}{W_A}$	$\frac{\rho_M}{\rho_A} \cdot \left(\frac{\ell_M}{\ell_A}\right)^3$	$151 \times 10^{-6}$
Mass Inertia	$\frac{I_M}{I_A}$	$\frac{\rho_M}{\rho_A} \cdot \left(\frac{\ell_M}{\ell_A}\right)^5$	$.168 \times 10^{-6}$
Stiffness	$\frac{EI_M}{EI_A} = \frac{GJ_M}{GJ_A}$	$\frac{\rho_M}{\rho_A} \cdot \left(\frac{\ell_M}{\ell_A}\right)^4 \left(\frac{V_M}{V_A}\right)^2$	$.168 \times 10^{-6}$
Area Inertia	$\frac{\bar{I}_M}{\bar{I}_A}$	$\left(\frac{\ell_M}{\ell_A}\right)^4$	$1.23 \times 10^{-6}$
External Loads	$\frac{F_M}{F_A}$	$\frac{q_M}{q_A} \cdot \left(\frac{\ell_M}{\ell_A}\right)^2$	$151 \times 10^{-6}$
Bending Moment	$\frac{BM_M}{BM_A}$	$\frac{F_M}{F_A} \cdot \frac{\ell_M}{\ell_A}$	$5.03 \times 10^{-6}$
Stress	$\frac{\sigma_M}{\sigma_A}$	$\frac{BM_M}{BM_A} \cdot \left(\frac{\ell_A}{\ell_M}\right)^3$	.136



frequency and Mach number. The airplane was modeled with trapezoidal panels arranged in strips parallel to the free-stream. The panel arrangement is shown on Figure 4-1.

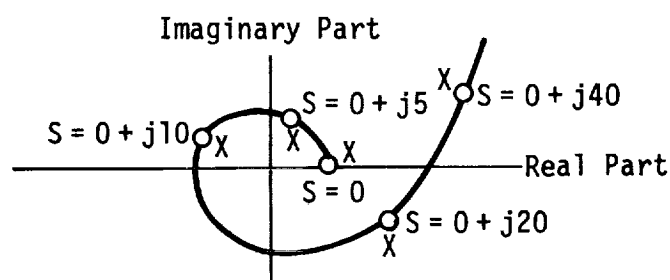
- 4.1.3 Equations of motion - Initial equations of motion were formed using complex oscillatory aerodynamic coefficients generated for specific values of the frequency parameter,  $\omega/U_0$ . Final equations of motion were formulated in terms of real matrices through introduction of an "interpolating" or "approximating" function.

The original equations were the standard form:

$$\begin{aligned} & \left( -(j\omega)^2 [\text{Mass}] + (j\omega) [\text{Damping}] + [\text{Stiffness}] \right) \{q(j\omega)\} \\ & + \rho U_0^2 \left[ A_I \left( \frac{j\omega}{U_0} \right) \right] \left( [C_\theta] \{q(j\omega)\} + \frac{j\omega}{U_0} [C_Z] \{q(j\omega)\} \right. \\ & \left. + \frac{1}{U_0} [C_W] \left\{ \frac{W_g(j\omega)}{V_g(j\omega)} \right\} \right) = 0 \end{aligned}$$

where  $q$  is the generalized coordinate and  $A_I$  is an aerodynamic influence coefficient matrix which can be evaluated for specific values of  $\omega/U_0$ . The matrices,  $C_\theta$ ,  $C_Z$ , and  $C_W$  prescribe the usual linearized boundary conditions.

If one of the elements of the complex matrix  $A_I$  is plotted, as  $\omega$  takes on selected values from 0 to 40 radians/second (airplane scale), the result appears as the X's on the sketch below.



The solid line in the sketch is an approximating function, chosen as a rational polynomal function of the complex variable  $S$ . The circles are values of the approximating function at values of  $S$  for which the X's are plotted. The approximating function was chosen to permit accurate approximation of the time delays inherent in the unsteady aerodynamics subject to the following restrictions:

- It must have complex conjugate symmetry
- It must have denominator roots in the left half-plane

- It must approximate the value of the complex coefficient when  $S = 0 + j\omega$ , for those values of  $\omega$  analyzed.

The approximating function for each element in the aerodynamic influence coefficient matrix was determined after analysis at twelve discrete frequencies. When the approximating functions are substituted in the equations of motion for the complex aerodynamic coefficients, a new set of equations results, whose coefficients are coefficients of the approximating function. After rearrangement, the final form of the equations of motion with variable density  $\rho$  and velocity  $U_0$  and without gust penetration is:

$$\begin{aligned} & (S^2[\text{Mass}] + S[\text{Damping}] + [\text{Stiffness}])\{q(S)\} \\ & + \left( S^2\rho[C_1] + S\rho U_0[C_2] + \rho U_0^2[C_3] + \rho U_0^2 \sum_{i=1}^4 [D_i] \frac{S}{S + U_0 B_i} \right) \{q(S)\} \\ & + \left( \rho U_0[R_0] + \rho U_0 \sum_{i=1}^4 [R_i] \frac{S}{S + U_0 G_i} \right) \begin{Bmatrix} W_g(S) \\ V_g(S) \end{Bmatrix} = \{0\} \end{aligned}$$

The items in the first line of the above equation are structural coefficients; items in the second line are aerodynamic coefficients; items in the third line are gust velocity coefficients; where:

$S$	= Laplace variables
$\rho$	= Air density
$U_0$	= True airspeed
$[\text{Mass}]$	= Structural mass
$[\text{Damping}]$	= Structural damping
$[\text{Stiffness}]$	= Structural stiffness
$[C_1], [C_2], [C_3]$	= Aerodynamic parameters
$[D_1], [D_2], [D_3], [D_4]$	= Aerodynamic parameters
$[B_i], [G_i],$	= Lift growth parameters
$[R_0], [R_1], [R_2], [R_3], [R_4]$	= Vertical and lateral gust coefficients
$q(S)$	= Rigid body, structural and control surface freedoms
$W_g(S)$	= Vertical Gust
$V_g(S)$	= Lateral gust

Because of the continuity of the aerodynamic coefficients as  $\omega$  varies (no aerodynamic poles or zeroes in the vicinity of the imaginary axis) these equations are considered to be a good approximation of the Laplace transformed equations. They should not be depended upon for values of  $S$  too remote from the imaginary axis or above the highest frequency analyzed (100 Hz; model scale). The generalized equations of motion were augmented with an additional degree of freedom for each control surface. The control surfaces defined for the model were inboard, midspan and outboard flaperons, an inboard aileron and two outboard ailerons.

## 4.2 Flutter Analysis

Using the equations of motion developed in the previous paragraph, analysis was conducted to define a configuration that satisfied the flutter criteria. The model modifications (wing ballast and/or sting attachment) were then designed and transmitted to NASA for implementation.

4.2.1 Configuration definition - All analyses were conducted using a model scale air density of  $2.58 \text{ kg/m}^3$  ( $0.005 \text{ lb-sec}^2/\text{ft}^4$ ) 6400 m (21 000 feet) equivalent airplane altitude. The initial configuration had the engine nacelles and external fuel tanks removed from the wing and the sting mount located at the existing cable mount block. Though this configuration exhibited dual flutter modes with violent onset, the flutter speeds occurred well above  $4788 \text{ N/m}^2$  (100 psf) design dynamic pressure. Various ballast arrangements were then investigated in order to reduce the flutter velocity. Included in the investigation were masses located fore and aft of the elastic axis at the outboard nacelle and external fuel tank locations. The following ballast arrangement produced satisfactory symmetric flutter characteristics.

- 1.37 kg (3.01578 pounds) ballast attached to the elastic axis at the outboard nacelle attach point.
- 0.05443 kg (0.11974 pounds) ballast attached to the elastic axis at the external fuel tank location.

However, the antisymmetric axis exhibited three flutter modes one of which occurred well below the others at  $1915 \text{ N/m}^2$  (40 psf). This 4 Hz mode appeared to be wing chordwise bending coupling with fuselage side bending through the moment arm existing between the wing attach point (BS 0.05224 (20.5667)) and the sting mount (BS 0.7764 (30.5667)). The sting attach point was, therefore, moved to the wing attach point which produced satisfactory flutter characteristics in both axes.

- 4.2.2 Flutter results - Flutter characteristics were investigated for all dynamic pressures below  $4788 \text{ N/m}^2$  (100 psf). The frequency and damping ratio versus dynamic pressure for both symmetric and antisymmetric flutter modes are shown on Figures 4-2 and 4-3. Both flutter modes were made up of first wing torsion and second wing bending, with the torsion mode becoming unstable at  $2873 \text{ N/m}^2$  (60 psf). No other modes exhibited instability below  $4788 \text{ N/m}^2$  (100 psf) in either axis.
- 4.2.3 Ballast design - The two masses were designed to give the same inertia effects as those used in the analysis. Both had circular cross-sections to minimize aerodynamic effects and produce maximum rigidity. Attachment to the wing was achieved in the same fashion as the outboard nacelle and external fuel tank.

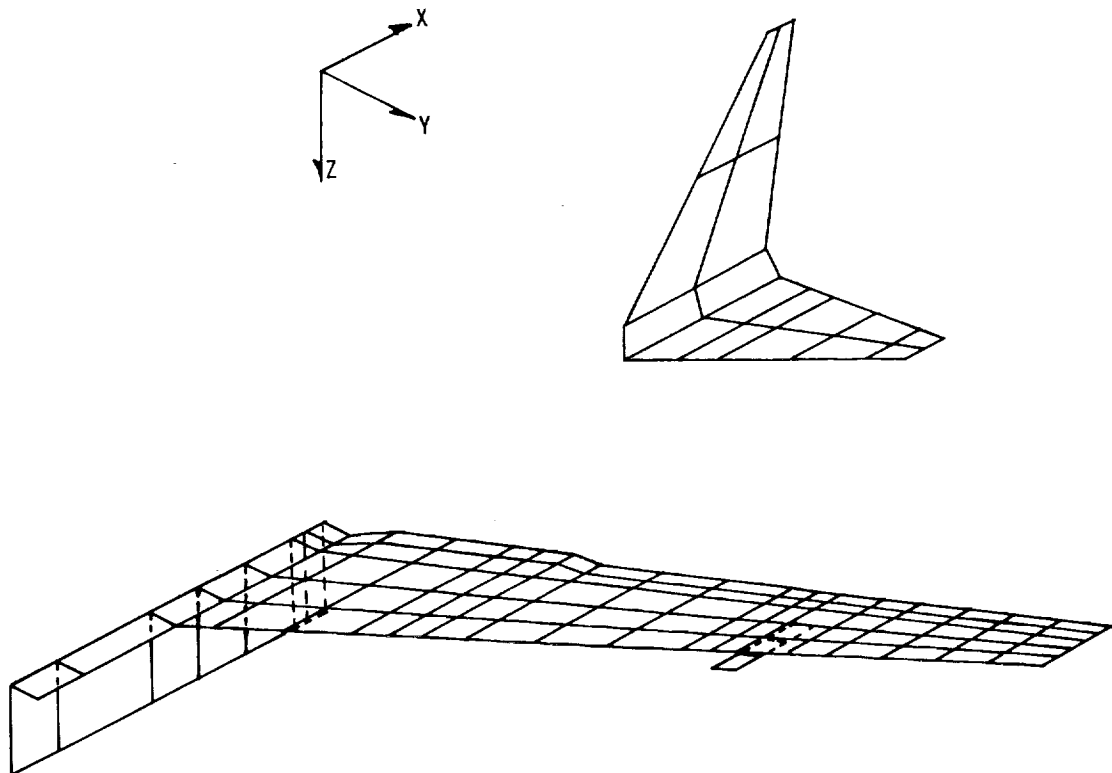


FIGURE 4-1 - AERODYNAMIC PANELING

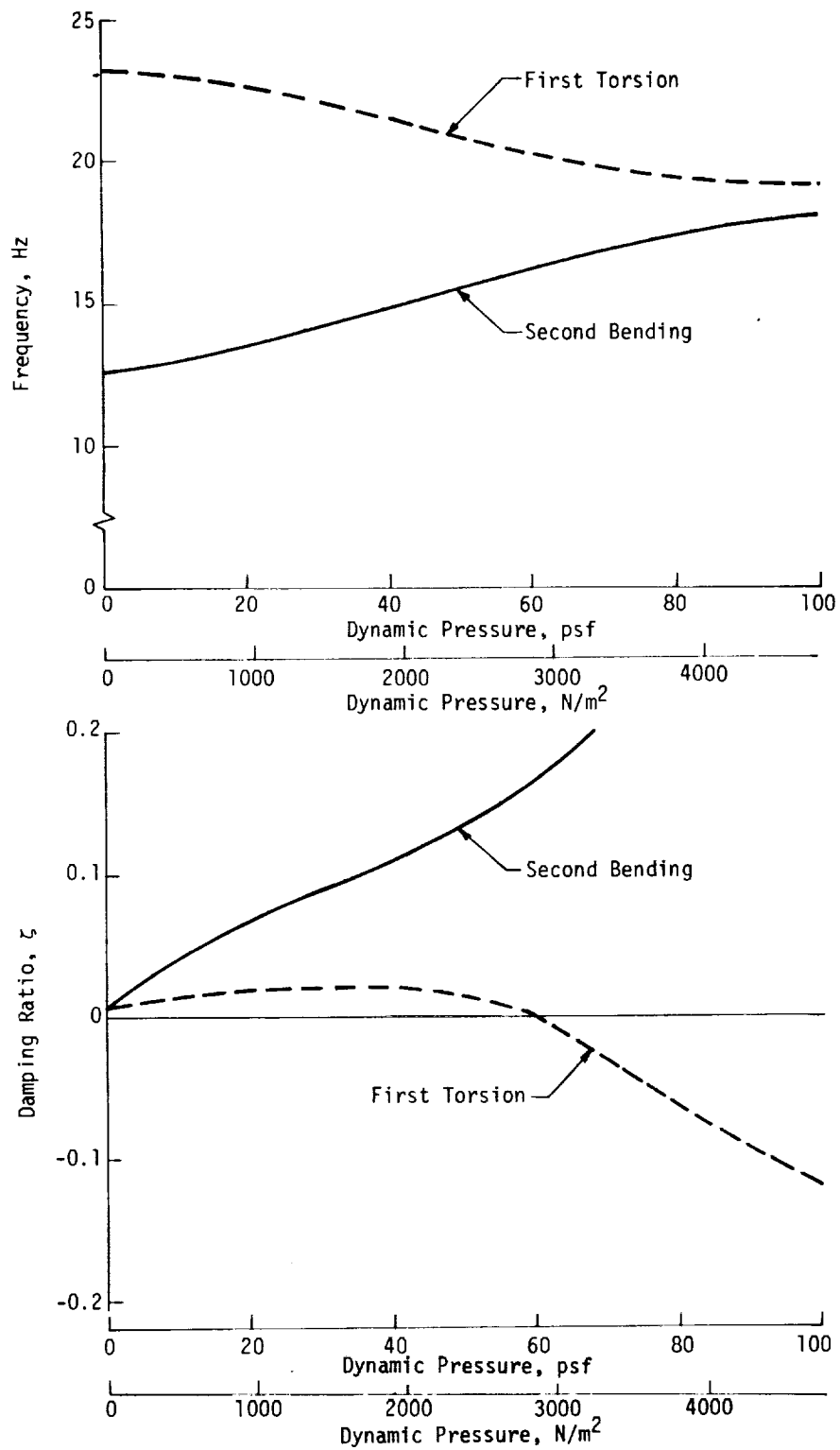


FIGURE 4-2 - SYMMETRIC FLUTTER CHARACTERISTICS

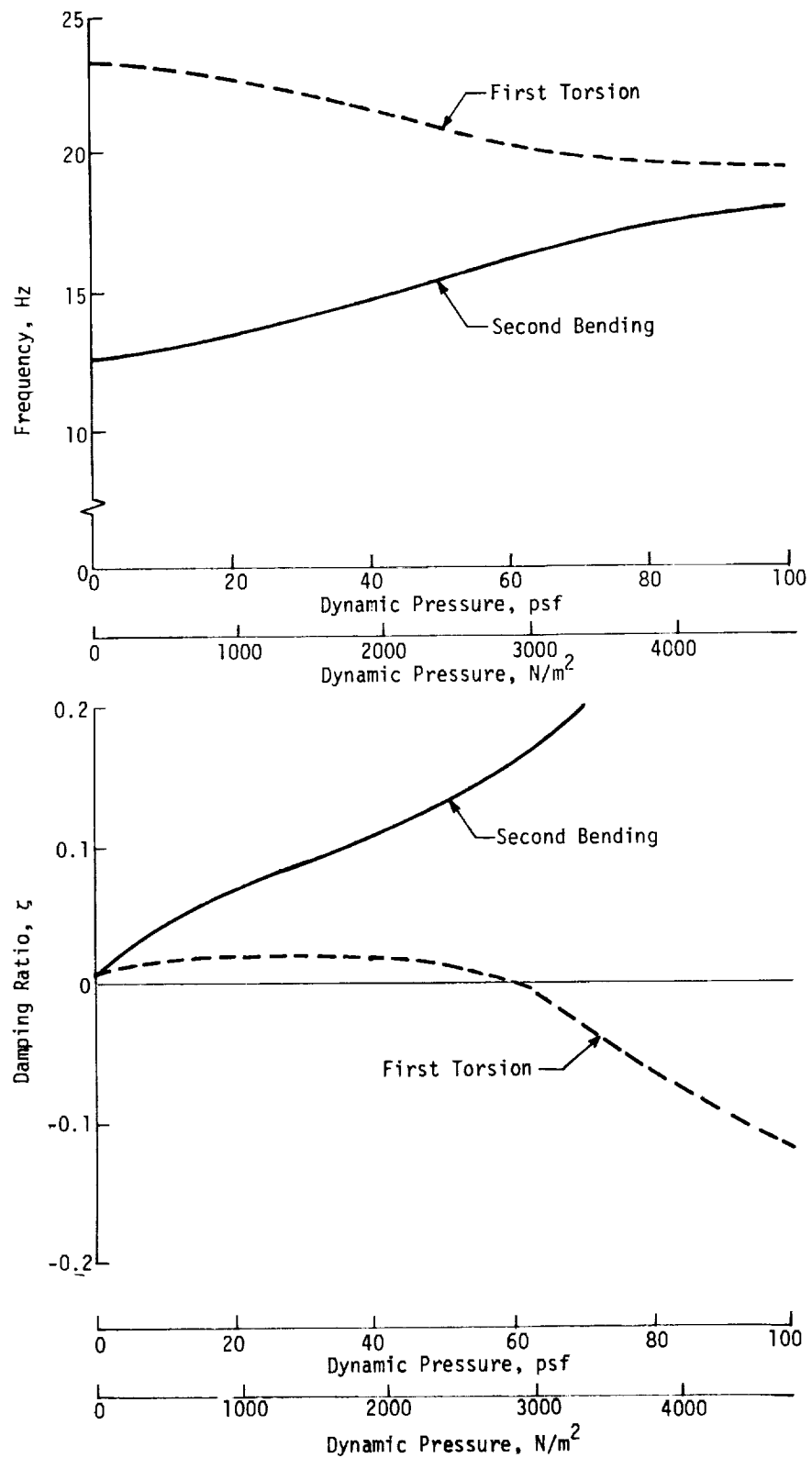


FIGURE 4-3 - ANTISYMMETRIC FLUTTER CHARACTERISTICS

## 5.0 FLUTTER SUPPRESSION SYSTEM SYNTHESIS AND ANALYSIS

This section describes the synthesis and performance analysis conducted for the B-52E aeroelastic model FSS. A review of the criteria used in the FSS synthesis is given in Paragraph 5.1. Detailed descriptions of the FSS synthesis and performance evaluation are presented in Paragraphs 5.2 and 5.3, respectively.

### 5.1 Synthesis Criteria and Constraints

The FSS was synthesized using the criteria and methodology described in Paragraph 3.2. A review of the criteria and constraints is presented in the following paragraphs.

#### 5.1.1 Stability criteria - The stability criteria used in synthesizing the FSS were as follows:

- The FSS should extend the flutter dynamic pressure at least 20 percent while not significantly degrading the damping of any other structural mode.
- The FSS should possess MIL-F-9490D stability margins below the flutter speed; that is  $\pm 6$  dB of gain margin and  $\pm 0.7854$  rad (45 degrees) of phase margin.

#### 5.1.2 System constraints - System constraints are usually constraints which arise due to physical limitations in the mechanization process. The constraints under which the FSS was synthesized are given as follows:

- All modes of the FSS were to be below approximately 100 Hz (model scale) to ease digital implementation.
- The control surface actuation systems were assumed to have certain dynamic properties based on experimental results on these systems (Reference 5).

### 5.2 Flutter Suppression System Synthesis

This paragraph describes the synthesis of the FSS for the B-52E aeroelastic wind tunnel model. Paragraphs 5.2.1 through 5.2.3 present the control surface and sensor selection and the control law synthesis. In Paragraph 5.2.4, the integrated configuration of the symmetric and antisymmetric flutter suppression system is presented.

#### 5.2.1 Sensor and control surface selection - Selection of the sensors and control surfaces was performed using the methodology described in Paragraph 3.2 and the math models defined in Section 4.0. Only wing control surfaces, both singularly and in combination, were investigated, since they are most effective in controlling flutter. Besides the existing three segment flaperons

and outboard aileron, two additional control surfaces were included in both the symmetric and antisymmetric math models. As shown on Figure 5-1, the two new control surfaces were an aileron located just outboard of the existing one between WBL 0.672 (26.47) and WBL 0.716 (28.17) and an inboard aileron between WBL 0.343 (13.50) and WBL 0.419 (16.50). Also shown on this figure is the sting attach point and the two flutter producing ballasts attached at the outboard nacelle and external fuel tank locations.

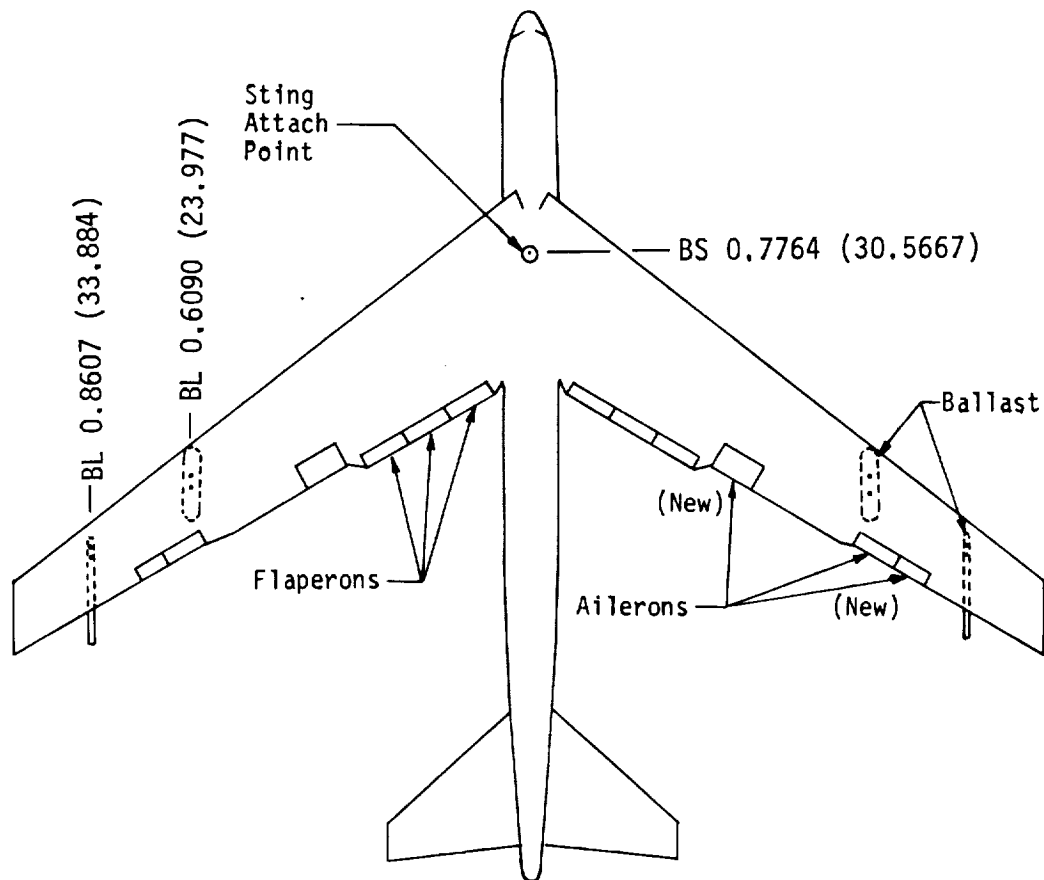


FIGURE 5-1 - PLAN VIEW OF B-52E AEROELASTIC MODEL

Since the flutter modes were primarily wing bending and torsion with very little fuselage or tail motion, only sensors located along the wing were investigated. Though other types of sensors were considered, vertical accelerometers were chosen as the primary sensor candidates because of size limitations and nature of the flutter modes.

Zero root locus techniques were used to evaluate modal coupling. This involved finding the zeroes (numerator root) of the transfer function of the sensor response due to a control surface input and comparing their locations to those of the open-loop poles (denominator roots) on the S-plane.



Using this technique, an extensive study was conducted to define the most promising combinations of sensors and control surfaces. The location of the vertical accelerometers was varied in conjunction with the following control surfaces:

- a. The existing outboard ailerons (WBL 0.597 (23.5) to WBL 0.672 (26.47))
- b. The new outboard ailerons (WBL 0.672 (26.47) to WBL 0.716 (28.17))
- c. The combination of the outboard ailerons (WBL 0.597 (23.5) to WBL 0.716 (28.17))
- d. The outboard segment of the existing three segment flaperons (WBL 0.227 (8.92) to WBL 0.297 (11.68))
- e. The full three segment flaperons (WBL 0.087 (3.42) to WBL 0.297 (11.68))
- f. The new inboard ailerons (WBL 0.343 (13.5) to WBL 0.415 (16.33)).

From this study the most promising combination appeared to be a vertical accelerometer at WBL 0.610 (24.0) coupled with the combined outboard ailerons (option c above). A zero root locus, illustrating this fact is shown on Figure 5-2 where both the combined and existing aileron zeroes are plotted as the accelerometer location is varied around the nominal position. Although the flutter mode is well coupled (by virtue of it's distance from any zeroes), mode  $q_8$  is also well coupled, which is undesirable. By summing the vertical acceleration at WBL 0.185 (7.29), with the outboard accelerometer, mode  $q_8$  is shown to be decoupled.

This study was conducted using the symmetric equations of motion at several dynamic pressures with good results in all conditions. The antisymmetric equations of motion behaved in essentially the same manner allowing the use of the same sensors and control surfaces for both systems. Therefore, the selected sensor/control surface configuration was the sum of the vertical accelerations at WBL 0.610 (24.0) and WBL 0.185 (7.29) fed back to the combined outboard ailerons.

The model was modified by NASA to incorporate the larger outboard ailerons. The existing outboard ailerons were removed and replaced with larger surfaces. From practical structural considerations it was necessary to make the new ailerons about 5 percent shorter in the spanwise direction than the ailerons used in the analysis. This reduction in area, of course, does decrease aileron effectiveness slightly, but it should not have a significant effect on the performance of the FSS. The aileron linkages were modified inside the fuselage so that each aileron was actuated independently. On the original model the ailerons were driven symmetrically by a single torque motor. On the modified model the original aileron motor was used to actuate the left aileron and what was formerly the right flaperon motor was used to actuate the right aileron.

- Existing Aileron
- Combined Aileron
- △ Combined Aileron with Inboard Sensor



5.2.2 Symmetric flutter suppression system synthesis - Synthesis of the FSS was conducted using the first (lowest frequency) 18 degrees of freedom of the math model developed in Section 4.0. The open loop flutter characteristics of this model are shown on Figure 5.3. Both axes have nearly identical flutter dynamic pressures of about 2873 N/m<sup>2</sup> (60 psf). Since the goal was to extend the flutter dynamic pressure at least 44 percent, synthesis of the FSS was performed at a point just above flutter, 3112 N/m<sup>2</sup> (65 psf), and just above 1.2 times the flutter dynamic pressure, 4309 N/m<sup>2</sup> (90 psf). The system was then evaluated at the other dynamic pressures as synthesis progressed.

The symmetric FSS was synthesized using root locus techniques. This iterative process involved synthesizing a filter that met gain and phase requirements as nearly as possible, evaluating it's effects as the feedback gain was varied, and then updating the filter equation to improve the results. Included in the feedback loop were the dynamics of the aileron actuation system as follows:

$$\frac{\theta_{\text{Actual}}}{\theta_{\text{Command}}} = \frac{62500}{s^2 + 150s + 62500} \frac{\text{Rad}}{\text{Rad}} \quad \text{Eq. 5-1}$$

During the synthesis it was noted that the fairly light damping ratio of the actuator mode was causing adverse coupling with modes in the same frequency range. This problem was solved by placing the following actuator compensation in series with the actuator.

$$C(s) = \frac{16096(s^2 + 150s + (250)^2)}{(s + 250)(s^2 + 1700s + (2006)^2)} \frac{\text{Rad}}{\text{Rad}} \quad \text{Eq. 5-2}$$

This has the effect of making the actuator behave as a first order lag at 250 rad/s.

Using this compensated actuator, the following symmetric FSS filter was derived which satisfied all stability criteria.

$$\frac{\delta_{\text{Ail Cmd}}}{\ddot{z}_{\text{WBL}}} = -0.873 \left( \frac{s}{s+10} \right) \left( \frac{10}{s+10} \right) \left( \frac{150}{s+150} \right) \times \left( \frac{150^2}{40^2} \frac{s^2 + 12s + 40^2}{(s+150)^2} \right) \left( \frac{s^2 + 160s + 125^2}{s^2 + 50s + 125^2} \right) \frac{\text{Rad}}{g} \quad \text{Eq. 5-3}$$

where  $\delta_{\text{Ail Cmd}}$  is defined as positive trailing edge down and  $\ddot{z}$  is positive down. An explanation of the filter terms follow:

- The first term in parenthesis is a washout which will remove any steady-state commands from the accelerometers.
- The second and third terms provide 40 dB/decade of high frequency gain attenuation.
- The fourth term provides additional gain and phase lead at the flutter frequency.
- The last term provides a gain peak at the flutter frequency.

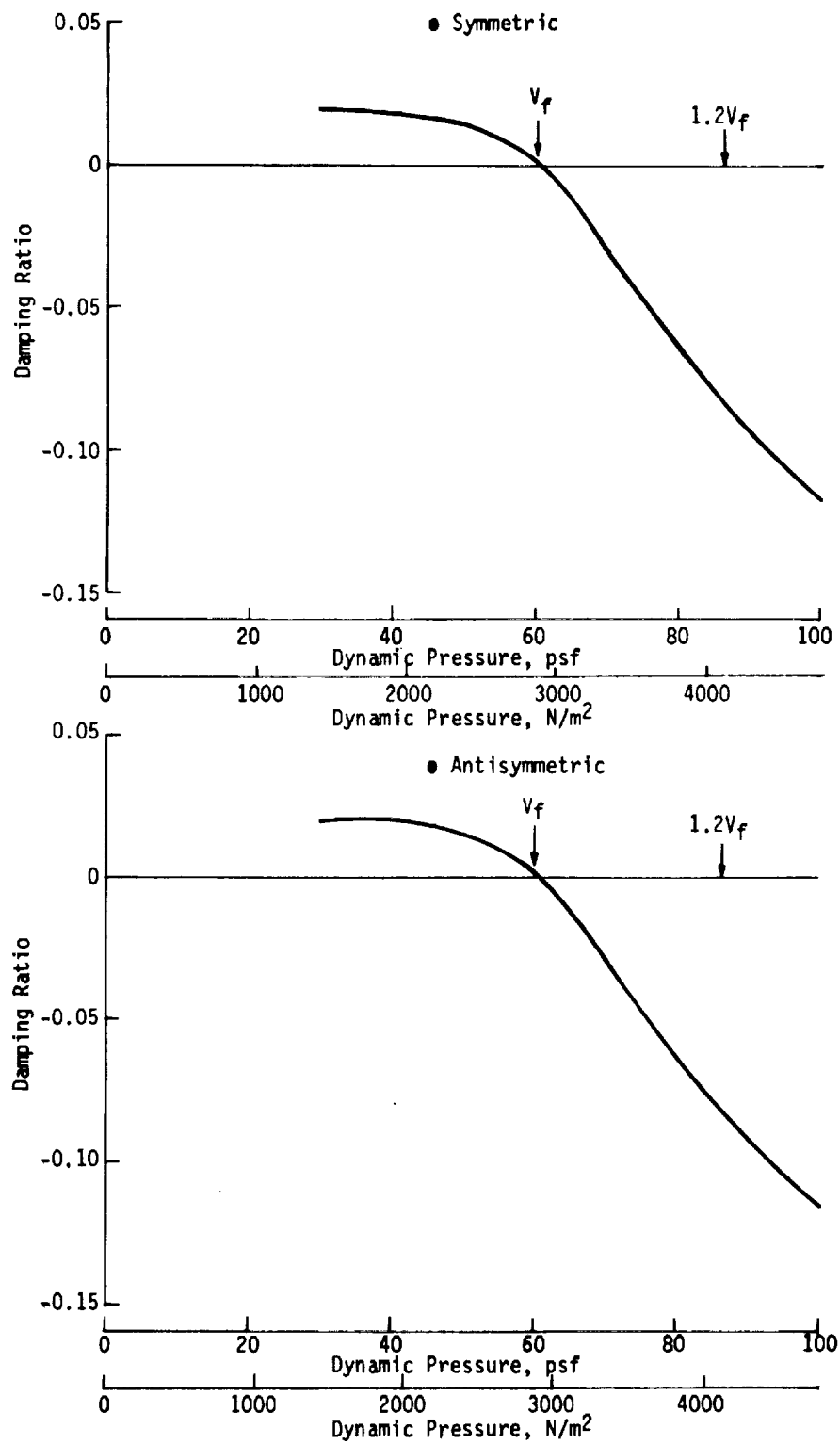


FIGURE 5-3 - SYMMETRIC AND ANTISYMMETRIC FLUTTER MODE DAMPING VERSUS DYNAMIC PRESSURE

Figure 5-4 shows the frequency response of the filter and illustrates the effect the last two terms in the filter have on the gain at the flutter frequency. Gain root loci of the symmetric FSS at 3112 N/m<sup>2</sup> (65 psf) and 4309 N/m<sup>2</sup> (90 psf) illustrating the effects of the system on the stability of all modes are shown on Figures 5-5 and 5-6.

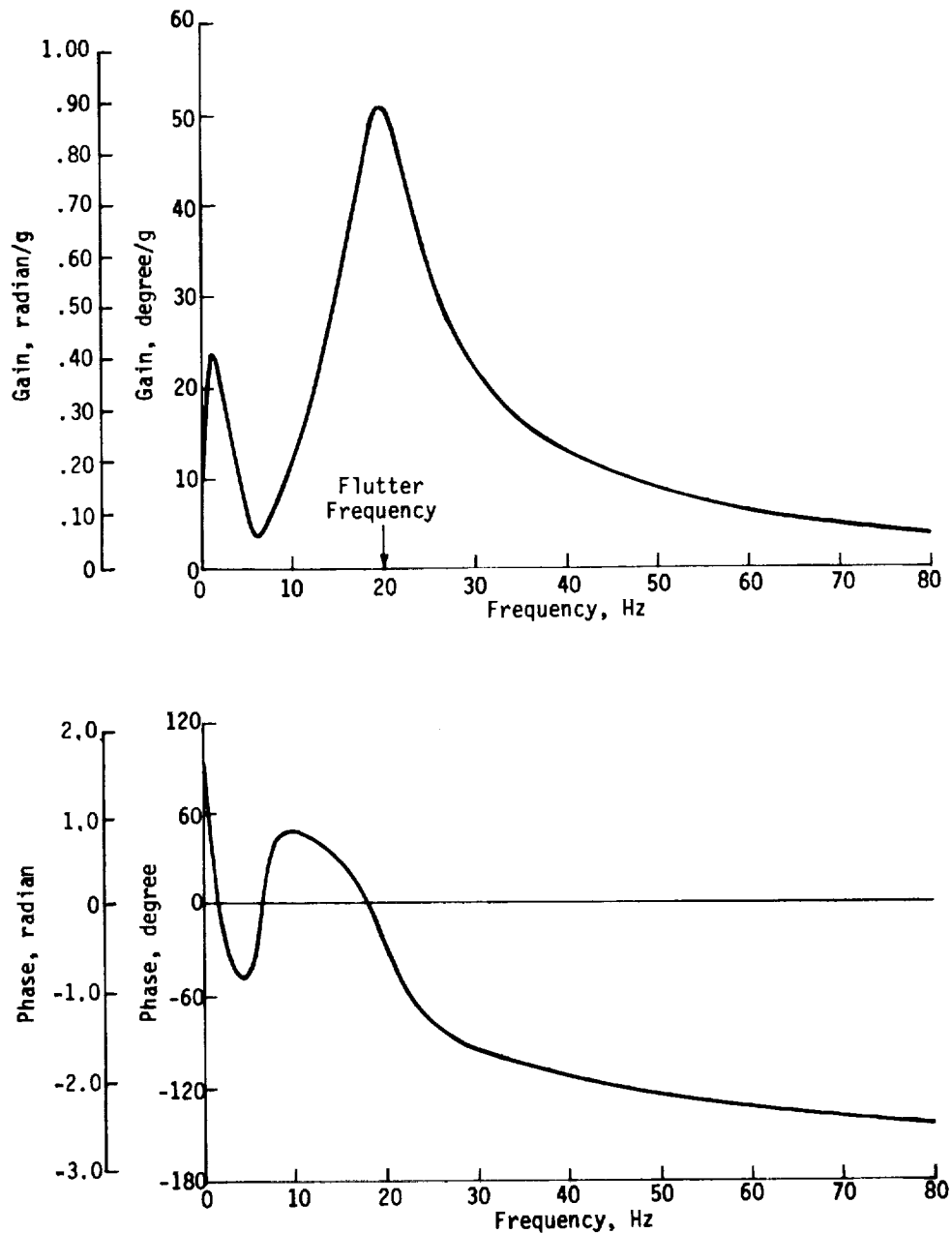


FIGURE 5-4 - FLUTTER SUPPRESSION SYSTEM FILTER FREQUENCY RESPONSE

Actuator and FSS: Equations 5-1, 5-2 and 5-3

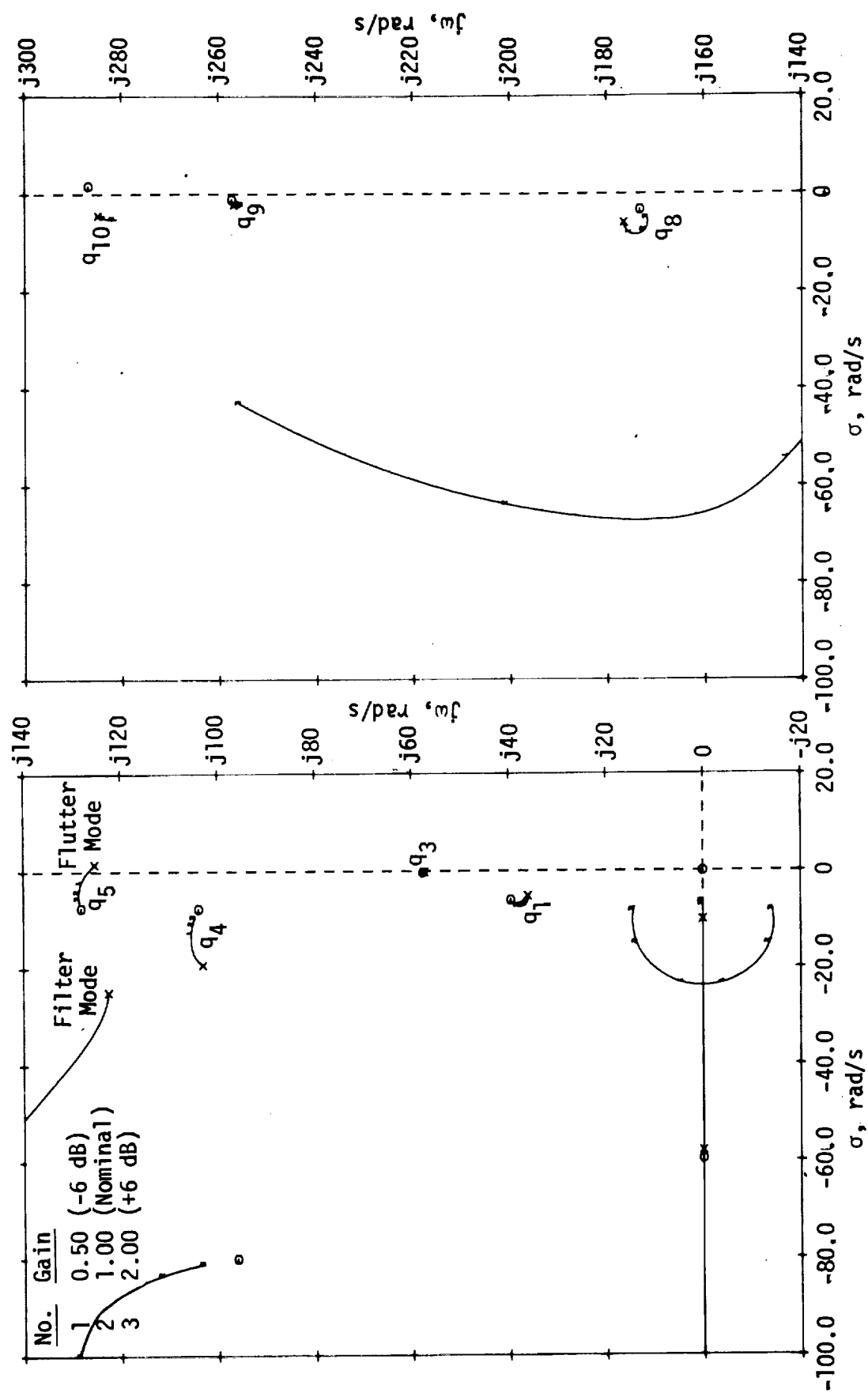


FIGURE 5-5 - ROOT LOCUS OF THE SYMMETRIC FLUTTER SUPPRESSION SYSTEM,  
DYNAMIC PRESSURE = 3112 N/m<sup>2</sup> (65 psf)

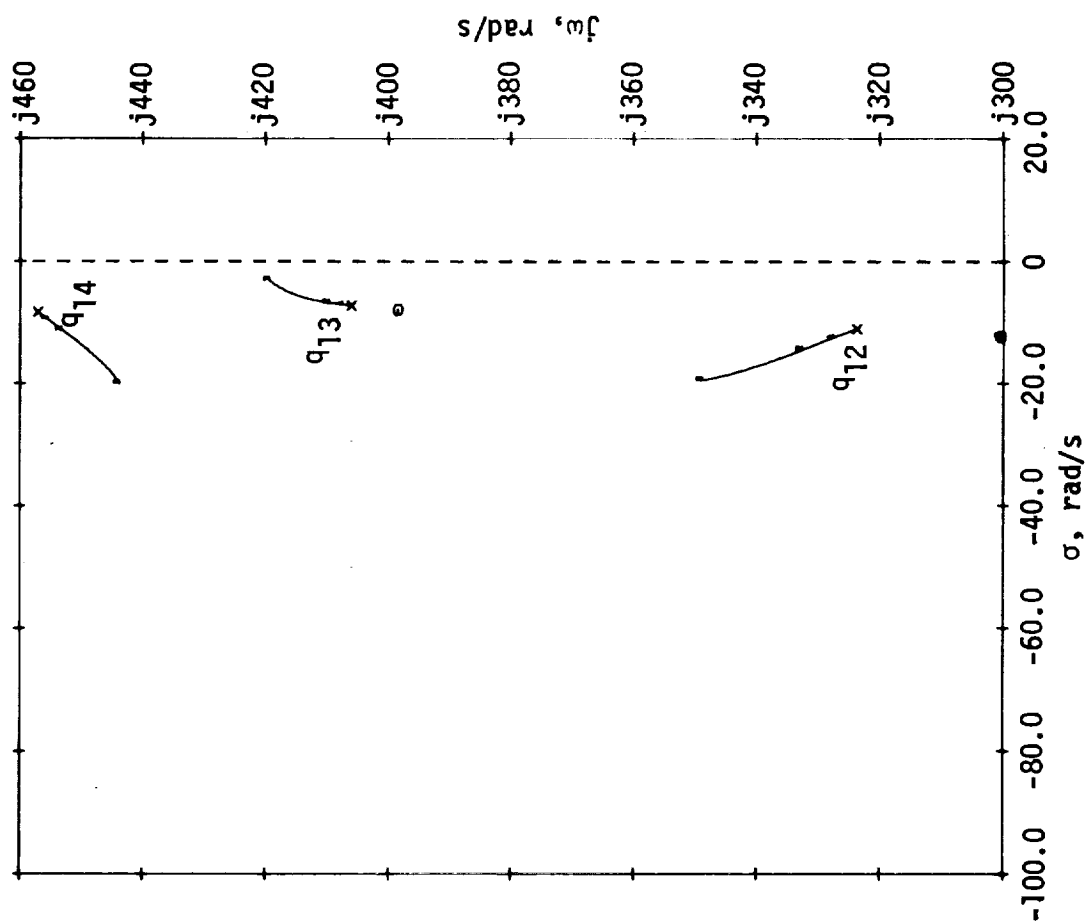


FIGURE 5-5 - ROOT LOCUS OF THE SYMMETRIC FLUTTER SUPPRESSION SYSTEM,  
DYNAMIC PRESSURE = 3112 N/m<sup>2</sup> (65 psf) (CONCLUDED)

Actuator and FSS: Equations 5-1, 5-2 and 5-3

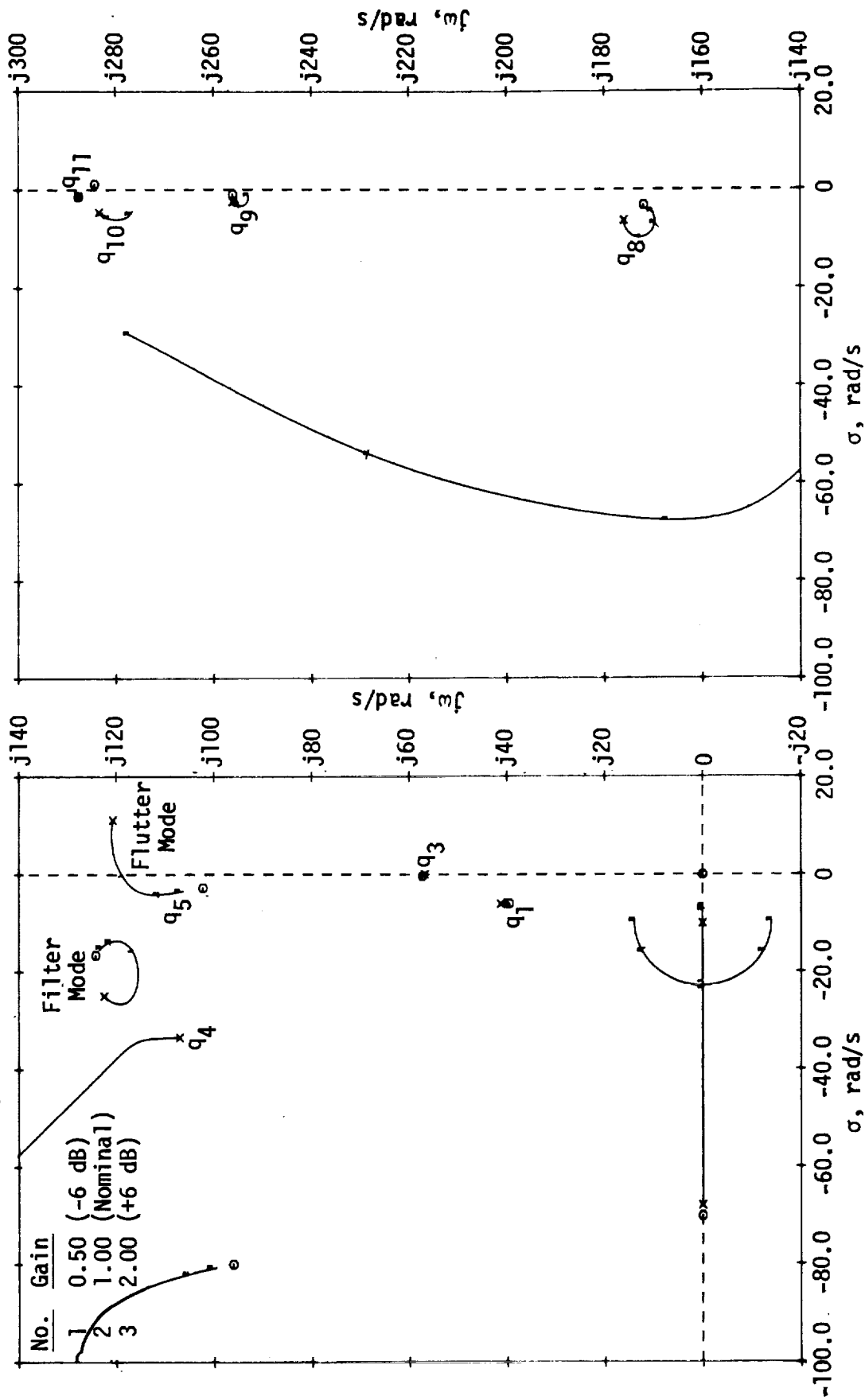


FIGURE 5-6 - ROOT LOCUS OF THE SYMMETRIC FLUTTER SUPPRESSION SYSTEM,  
DYNAMIC PRESSURE = 4309 N/m<sup>2</sup> (90 psf)



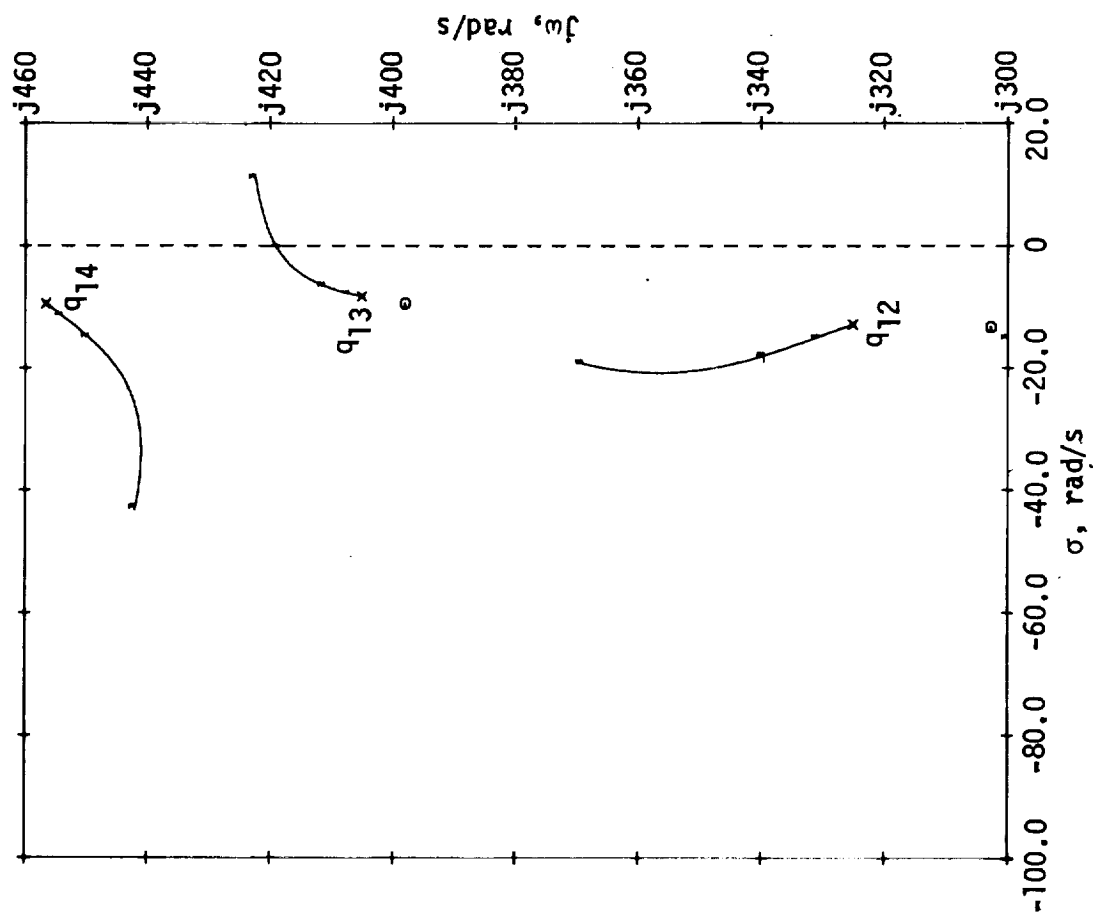


FIGURE 5-6 - ROOT LOCUS OF THE SYMMETRIC FLUTTER SUPPRESSION SYSTEM,  
DYNAMIC PRESSURE = 4309 N/m<sup>2</sup> (90 psf) (CONCLUDED)

5.2.3 Antisymmetric flutter suppression system synthesis - Since the basic flutter characteristics of the symmetric and antisymmetric axes were virtually identical, it was anticipated that the symmetric FSS filter would work for the antisymmetric axis. The symmetric system was evaluated on the 18 degree-of-freedom antisymmetric math model using the following sign convention:

- Vertical Acceleration - positive left wing down and right wing up.
- Aileron Displacement - positive left wing trailing edge down and right wing trailing edge up.

The performance was satisfactory as shown by the root loci of Figures 5-7 and 5-8.

5.2.4 System configuration - By performing the appropriate summing on the accelerometer signals and actuator commands the FSS can be put into the form shown on Figure 5-9. Because the filters are identical, a simplified configuration can be obtained which treats the flutter modes as left wing and right wing modes instead of symmetric and antisymmetric modes, shown on Figure 5-10.

### 5.3 Flutter Suppression System Performance Analysis

Analysis was conducted to determine the performance of the symmetric and antisymmetric flutter suppression systems. Conducted initially at the synthesis conditions of  $3112 \text{ N/m}^2$  (65 psf) and  $4309 \text{ N/m}^2$  (90 psf), this analysis was performed, after the control laws were selected, to verify satisfactory performance at all conditions below  $4788 \text{ N/m}^2$  (100 psf).

5.3.1 Flutter damping performance - The performance of the system in damping the flutter mode was evaluated by computing the characteristic roots of the model with the FSS operating. This analysis also allowed evaluation of the degradation in damping on the other structural modes.

Plots of damping ratio and frequency of the symmetric and antisymmetric flutter modes with the FSS on and off are given on Figures 5-11 and 5-12. Note that the flutter speed for both axes has been extended beyond  $4788 \text{ N/m}^2$  (100 psf), with very little change in flutter mode frequency. Tables 5-I and 5-II give the damping and frequency of all symmetric and antisymmetric modes at  $3831 \text{ N/m}^2$  (80 psf). Additional data at other dynamic pressures is presented in Appendix A.

5.3.2 System stability margins - During the synthesis process, system gain and phase margins were established by use of phase-gain root loci. These plots consist of the usual loci associated with variations in system gain and additional loci which have

been calculated with a given phase shift superimposed over the entire S-plane. An example of this type of plot is shown on Figure 5-13.

After the control laws had been selected the gain and phase margins for every condition below  $4788 \text{ N/m}^2$  (100 psf) was established using Bode techniques. This method involves evaluating the loop frequency response at the points where the phase is  $3.142 \text{ rad}$  (180 degrees) and the gain is 0 dB to determine gain and phase margins, respectively. Plots of the minimum gain and phase margins for the FSS are shown on Figures 5-14 and 15. Note that the margins required at and below  $2873 \text{ N/m}^2$  (60 psf) are met up to  $3352 \text{ N/m}^2$  (70 psf). At higher dynamic pressures, the FSS was intentionally designed to favor negative phase and gain margins. This decision was based on experience with other flutter systems where, in general, more phase lag will exist than expected and the control surfaces are less effective than predicted making it more desirable to have too much gain than too little.

- 5.3.3 Control surface requirements - Control surface displacement and rate requirements were generated using power spectral-density (PSD) techniques. Though little is known about the wind tunnel turbulence spectrum or amplitude, a rough estimate of the control surface requirements was made using a Von Karman spectrum with a gust length of 30.48 m (100 feet). By integrating the PSD of control surface displacement and rate the RMS values were obtained. This data for a 0.3048 m/s (1 ft/sec) RMS turbulence level is given on Figures 5-16 and 5-17. Since the requirements are fairly constant below  $3831 \text{ N/m}^2$  (80 psf), an indication of the expected control activity above the flutter velocity can be obtained at sub-critical speeds.

Actuator and FSS: Equations 5-1, 5-2 and 5-3

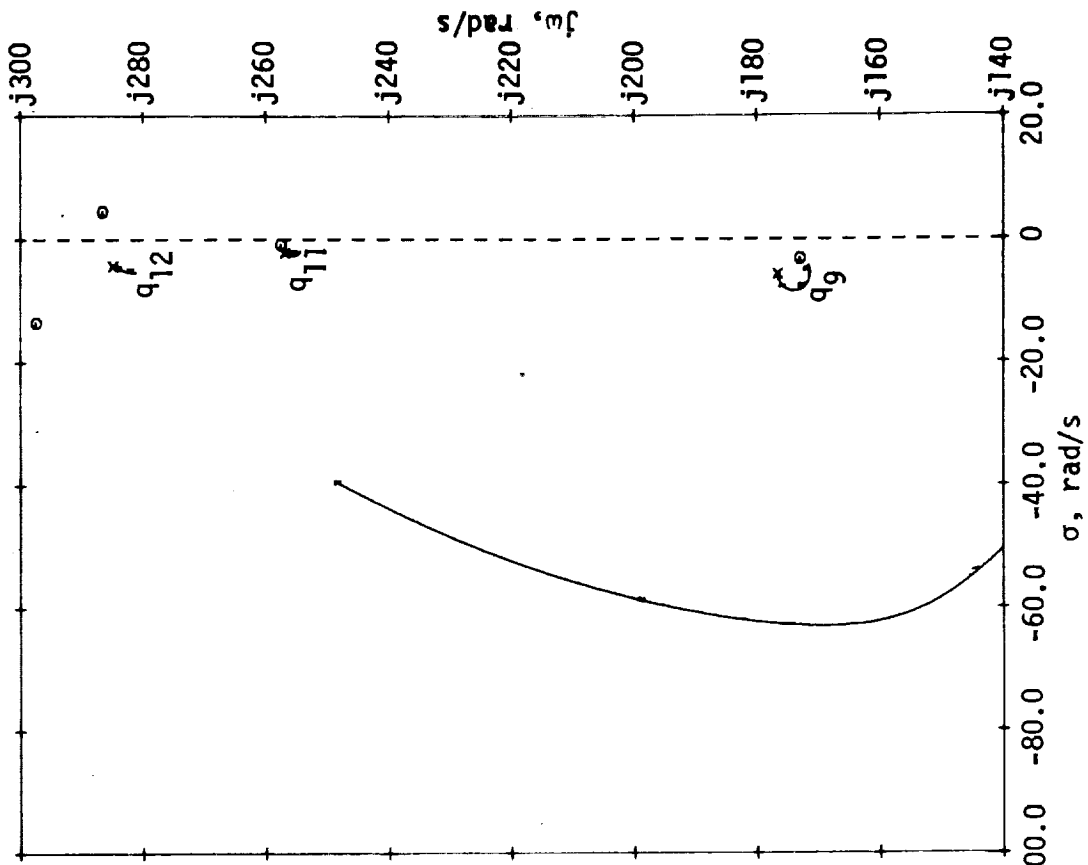
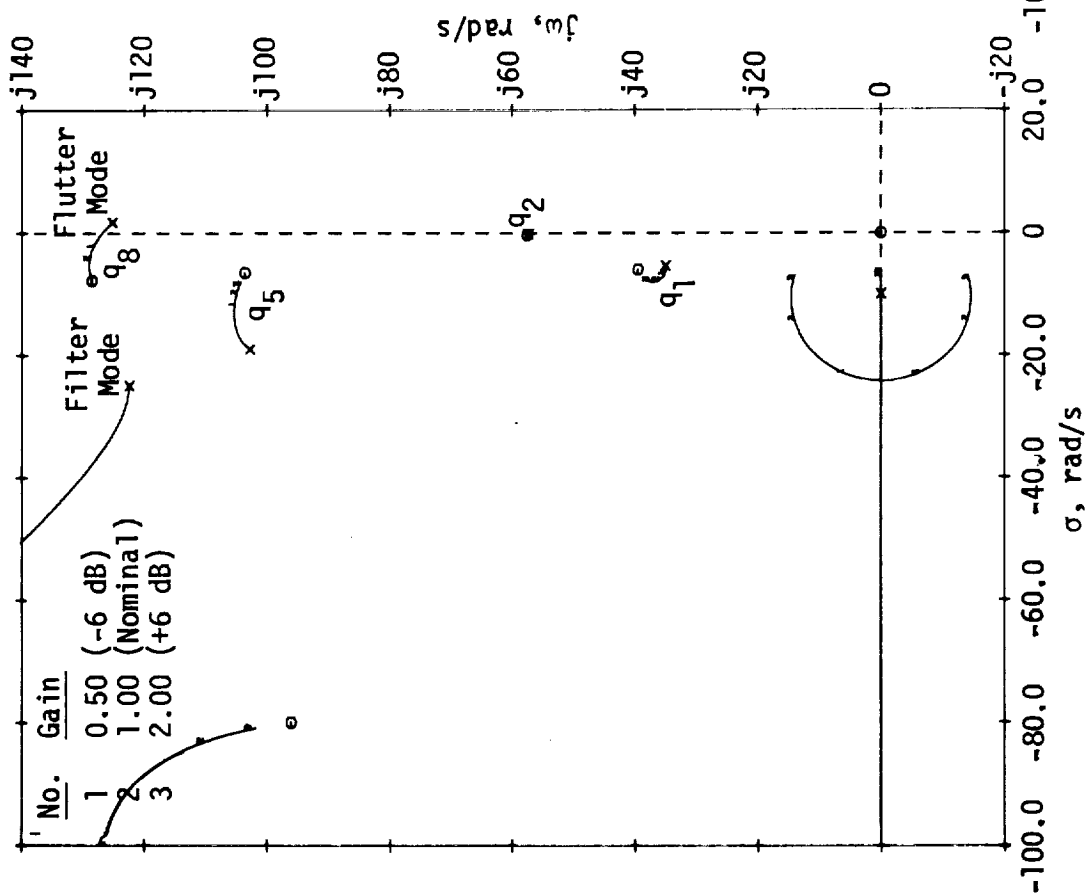


FIGURE 5-7 - ROOT LOCUS OF THE ANTISYMMETRIC FLUTTER SUPPRESSION SYSTEM, DYNAMIC PRESSURE = 3112 N/m<sup>2</sup> (65 psf)

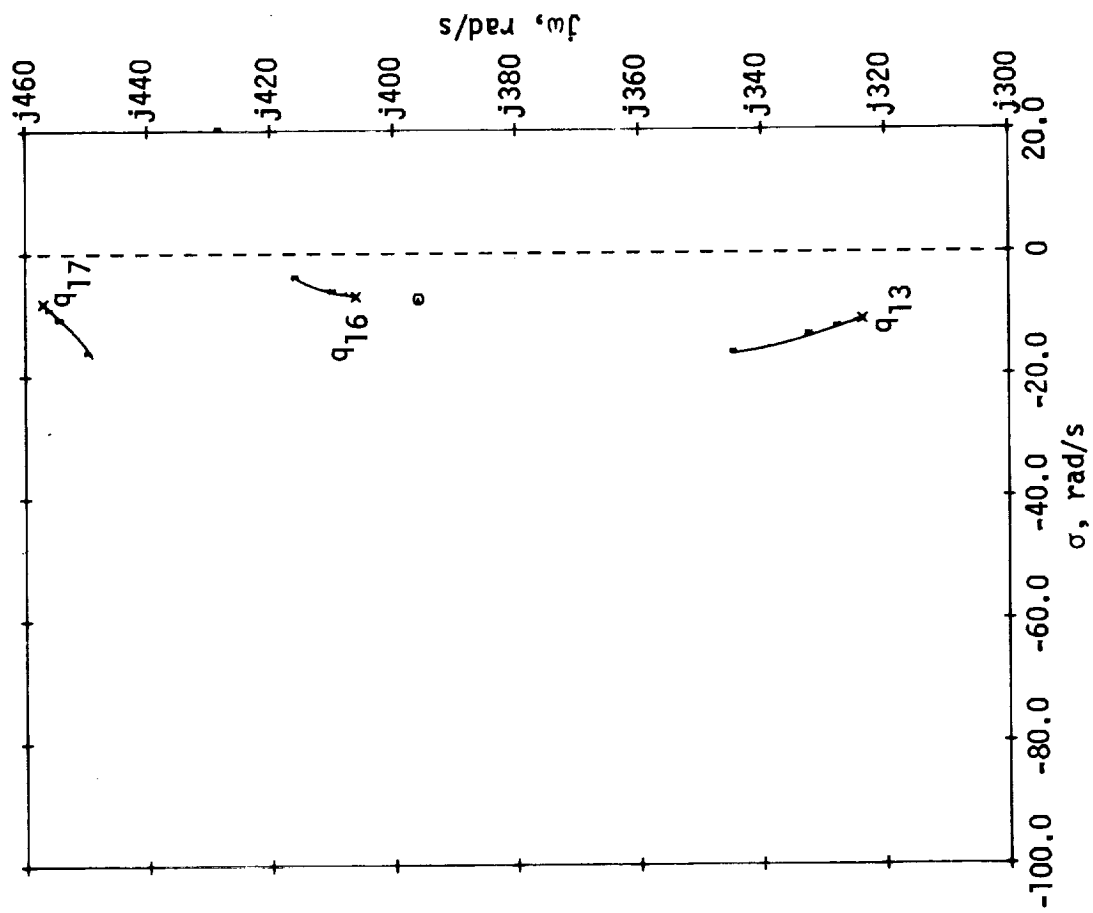


FIGURE 5-7 - ROOT LOCUS OF THE ANTISYMMETRIC FLUTTER SUPPRESSION SYSTEM,  
DYNAMIC PRESSURE =  $3112 \text{ N/m}^2$  (65 psf) (CONCLUDED)

Actuator and FSS: Equations 5-1, 5-2 and 5-3

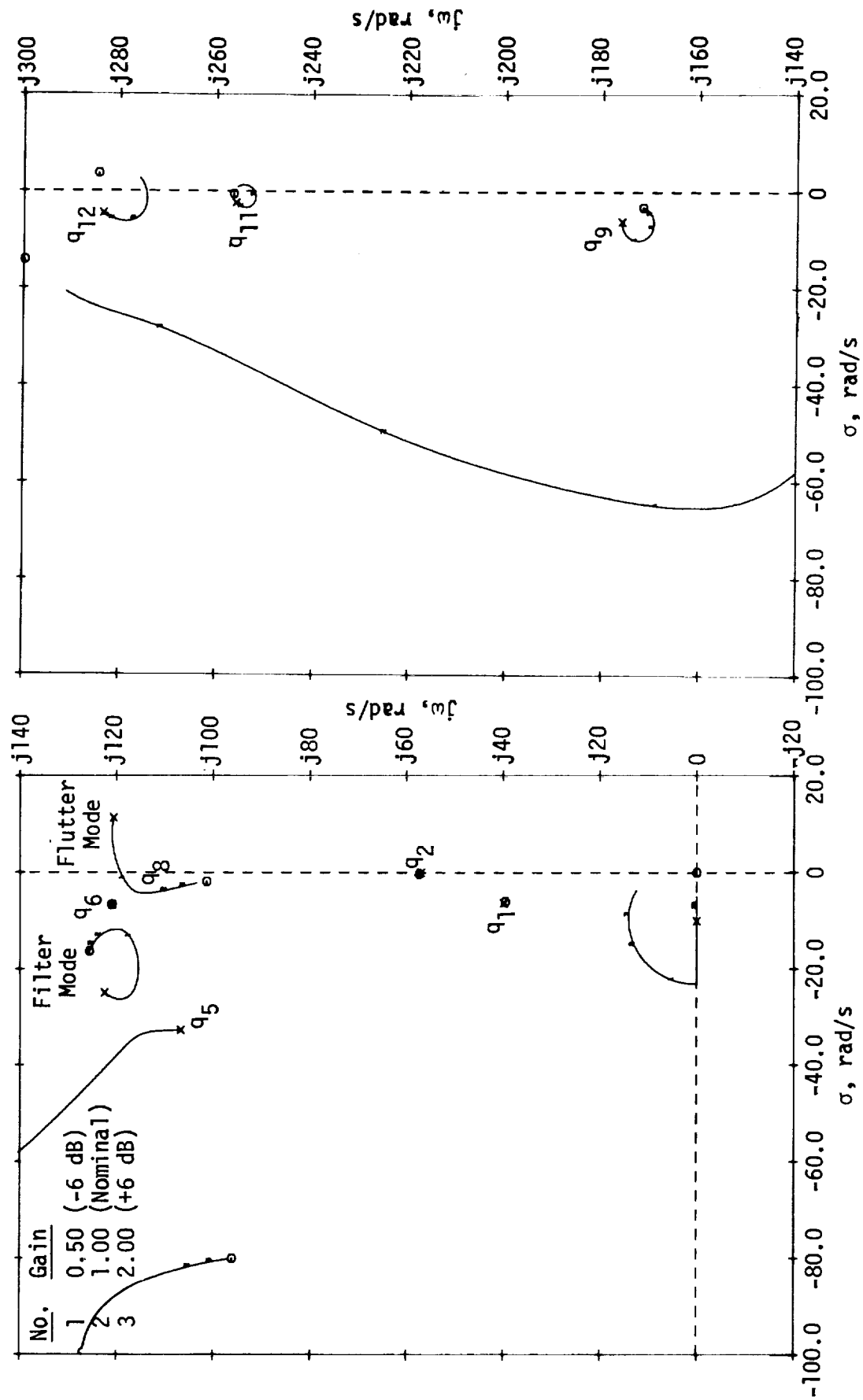


FIGURE 5-8 - ROOT LOCUS OF THE ANTISYMMETRIC FLUTTER SUPPRESSION SYSTEM,  
DYNAMIC PRESSURE = 4309 N/m<sup>2</sup> (90 psf)

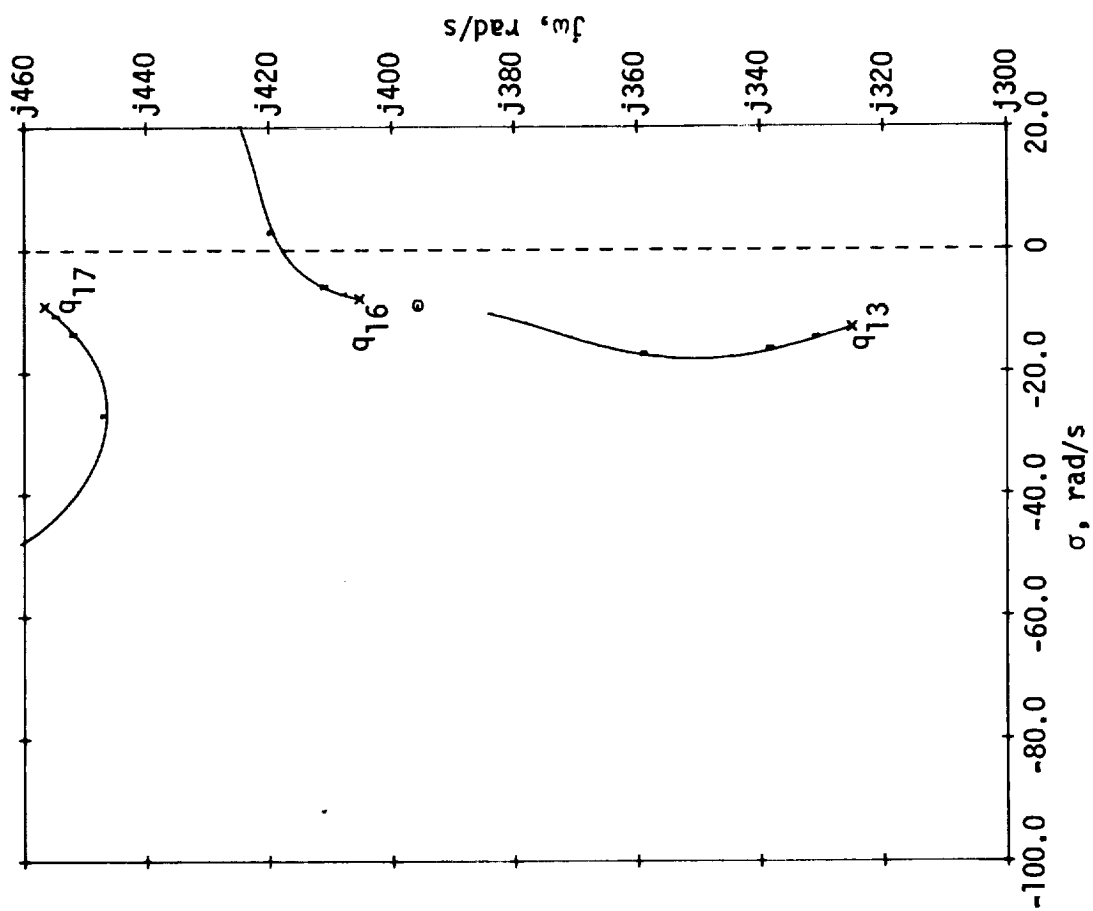


FIGURE 5-8 - ROOT LOCUS OF THE ANTISYMMETRIC FLUTTER SUPPRESSION SYSTEM,  
DYNAMIC PRESSURE = 4309 N/m<sup>2</sup> (90 psf) (CONCLUDED)

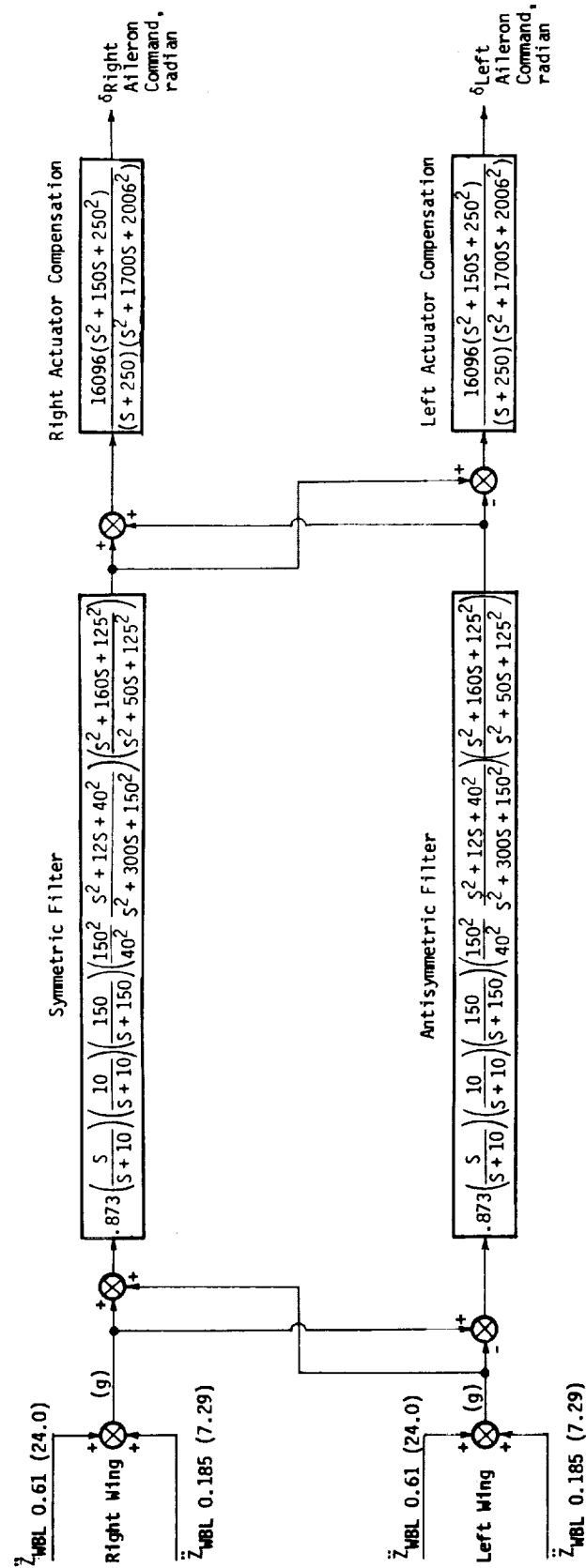


FIGURE 5-9 - BLOCK DIAGRAM OF FLUTTER SUPPRESSION SYSTEM



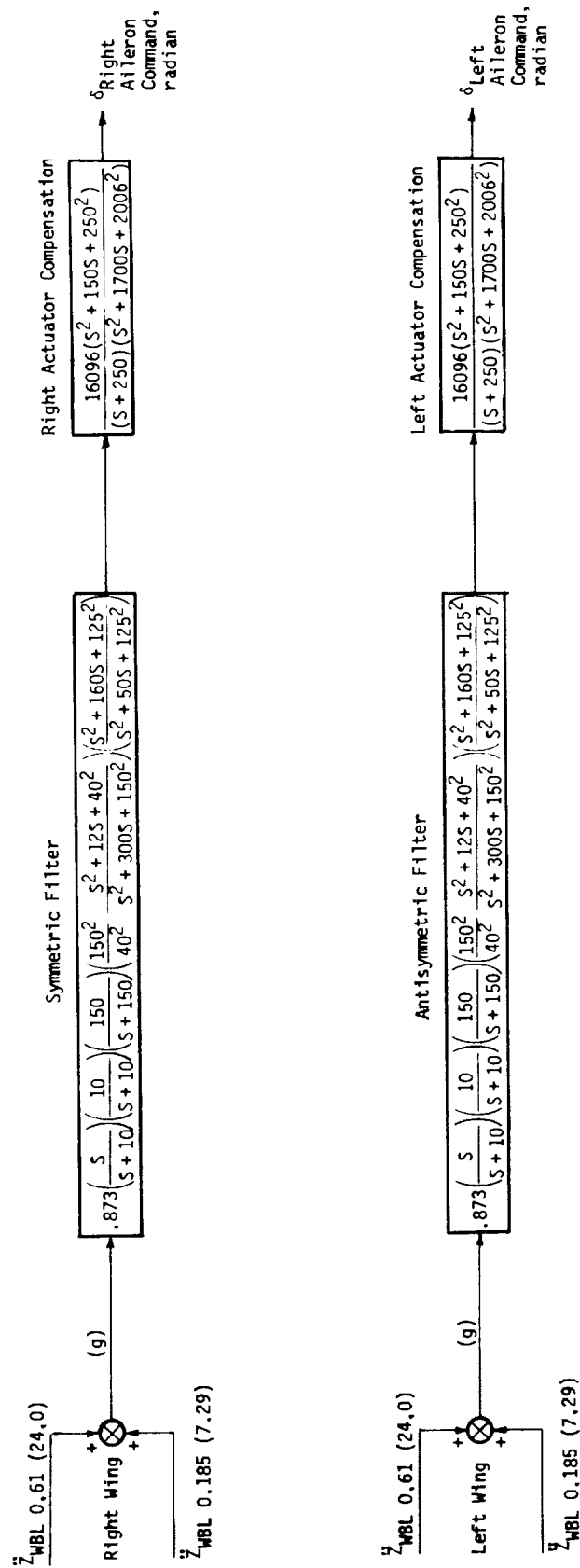


FIGURE 5-10 - BLOCK DIAGRAM OF THE ALTERNATE FLUTTER SUPPRESSION SYSTEM

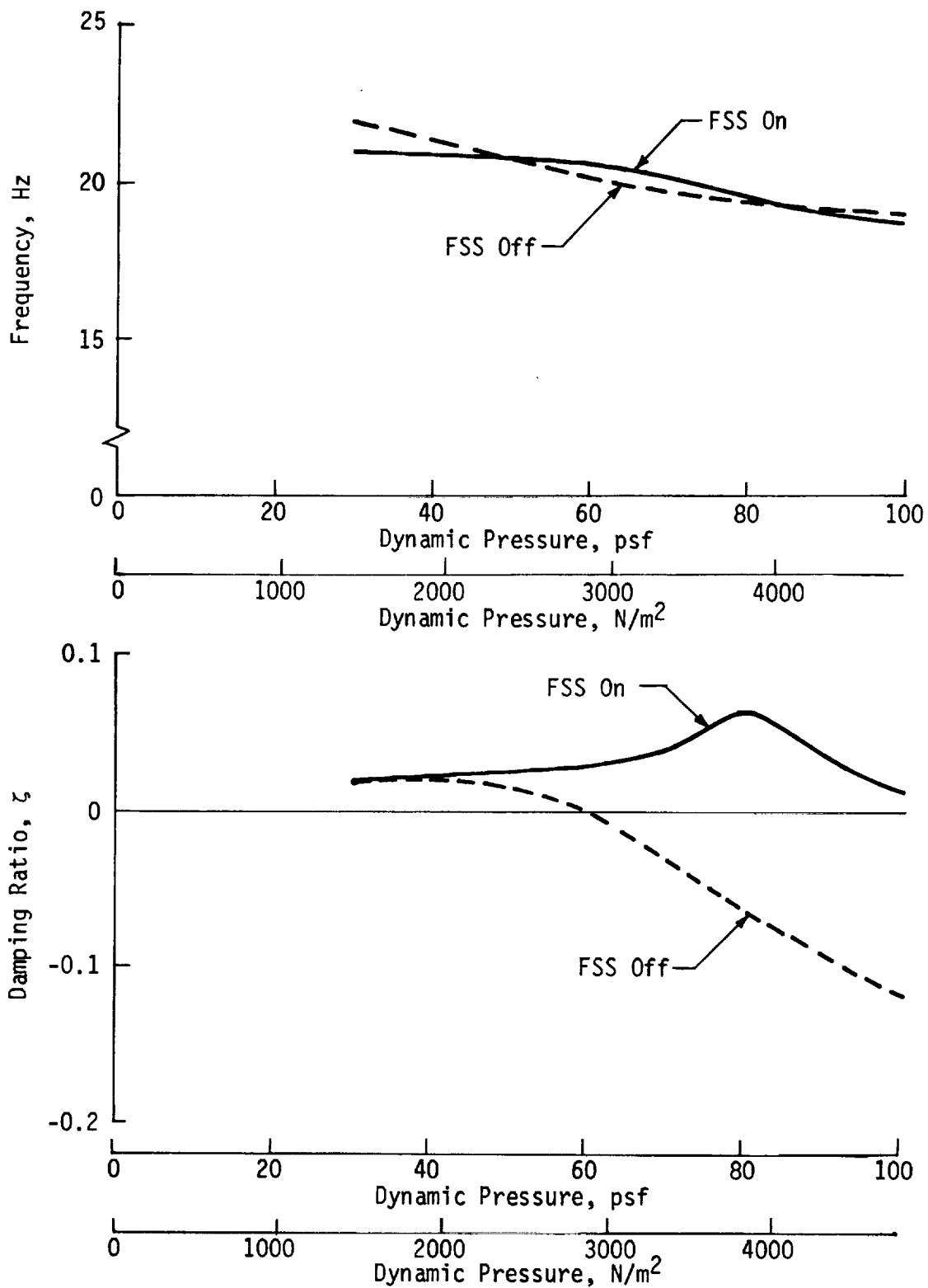


FIGURE 5-11 - SYMMETRIC FLUTTER MODE CHARACTERISTICS WITH THE FLUTTER SUPPRESSION SYSTEM ON AND OFF

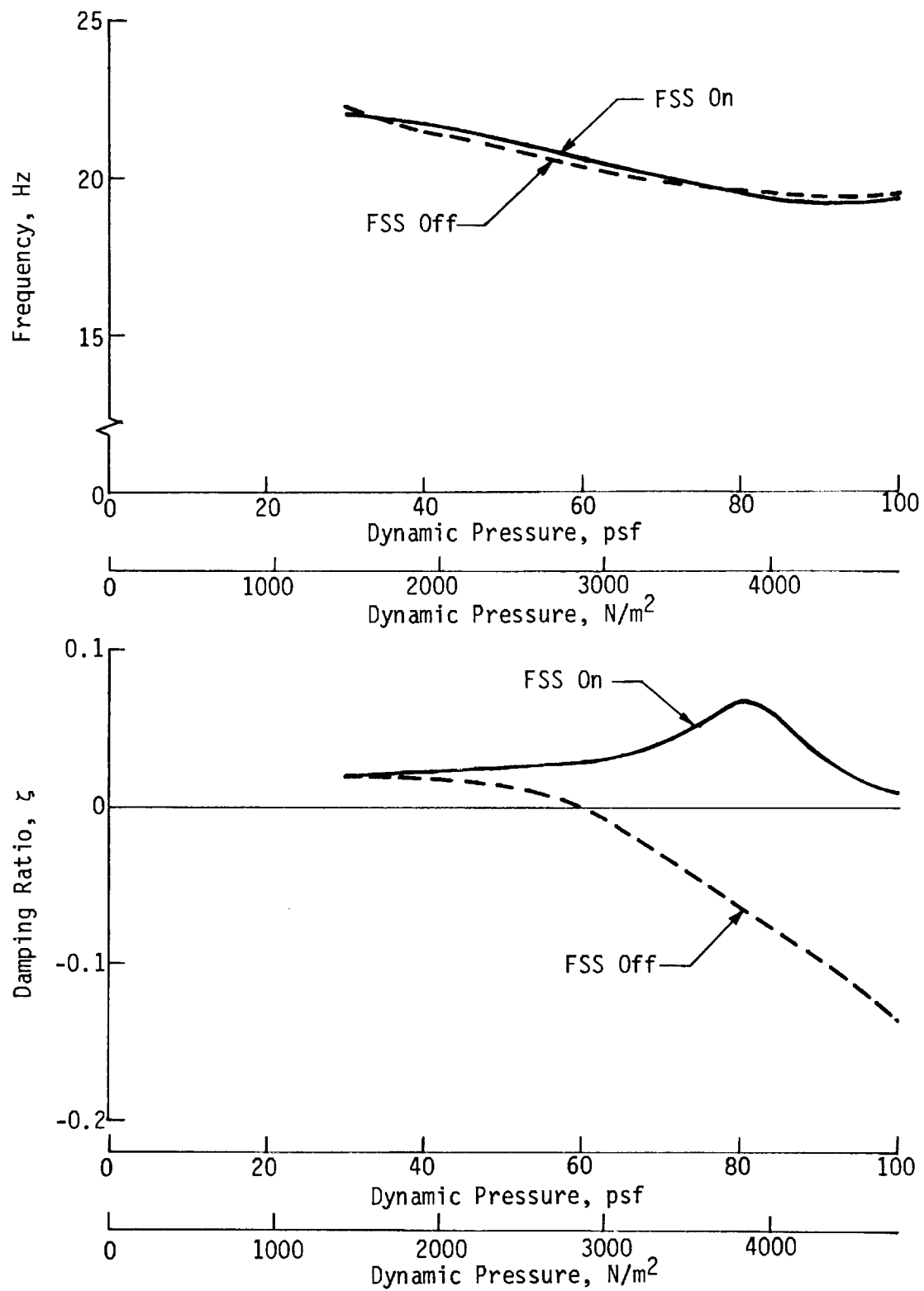


FIGURE 5-12 - ANTISYMMETRIC FLUTTER MODE CHARACTERISTICS WITH THE FLUTTER SUPPRESSION SYSTEM ON AND OFF

TABLE 5-I  
SYMMETRIC MODAL FREQUENCY AND DAMPING

• Symmetric

• Dynamic Pressure =  $3831 \text{ N/m}^2$  (80 psf)

Mode Number	FSS Off		FSS On	
	Frequency, Hz	Damping Ratio, $\zeta$	Frequency, Hz	Damping Ratio, $\zeta$
1	6.30	.144	6.30	.151
2	8.79	.129	8.79	.128
3	9.07	.0025	9.10	.0057
4	17.51	.256	17.64	.0827
5	19.40	-.0627	19.57	.0624
6	25.52	.0169	25.52	.0169
7	27.50	.0078	27.50	.0078
8	28.05	.0353	27.17	.0419
9	40.80	.0093	40.66	.0117
10	45.20	.0161	44.94	.0194
11	45.90	.0051	45.90	.0051
12	51.68	.0373	53.74	.0503
13	64.54	.0192	65.41	.0164
14	72.72	.0197	71.78	.0299
15	79.87	.0069	79.06	.0072
16	84.94	.0071	84.94	.0071
17	99.77	.0138	98.55	.0144
18	106.3	.0076	106.3	.0076
Filter	---	---	36.49	.255

TABLE 5-II  
ANTISYMMETRIC MODAL FREQUENCY AND DAMPING

- Antisymmetric
- Dynamic Pressure =  $3831 \text{ N/m}^2$  (80 psf)

Mode Number	FSS Off		FSS On	
	Frequency, Hz	Damping Ratio, $\zeta$	Frequency, Hz	Damping Ratio, $\zeta$
1	6.11	.154	6.22	.172
2	7.12	.105	7.12	.105
3	9.09	.0023	9.11	.0052
4	17.44	.252	17.47	.0693
5	17.36	.109	17.37	.111
6	19.59	.0629	19.79	.0699
7	19.40	-.0645	19.59	.0567
8	21.95	.0078	21.95	.0078
9	28.07	.0339	27.19	.0443
10	32.02	.0146	32.02	.0146
11	40.80	.0092	40.65	.0116
12	45.21	.0159	44.93	.0191
13	51.68	.0371	53.47	.0473
14	58.91	.0114	58.91	.0114
15	59.99	.0085	59.99	.0085
16	64.57	.0187	65.32	.0160
17	72.72	.0191	72.00	.0282
18	77.03	.0075	77.03	.0075
Filter	---	---	35.70	.250

Actuator and FSS: Equations 5-1, 5-2 and 5-3

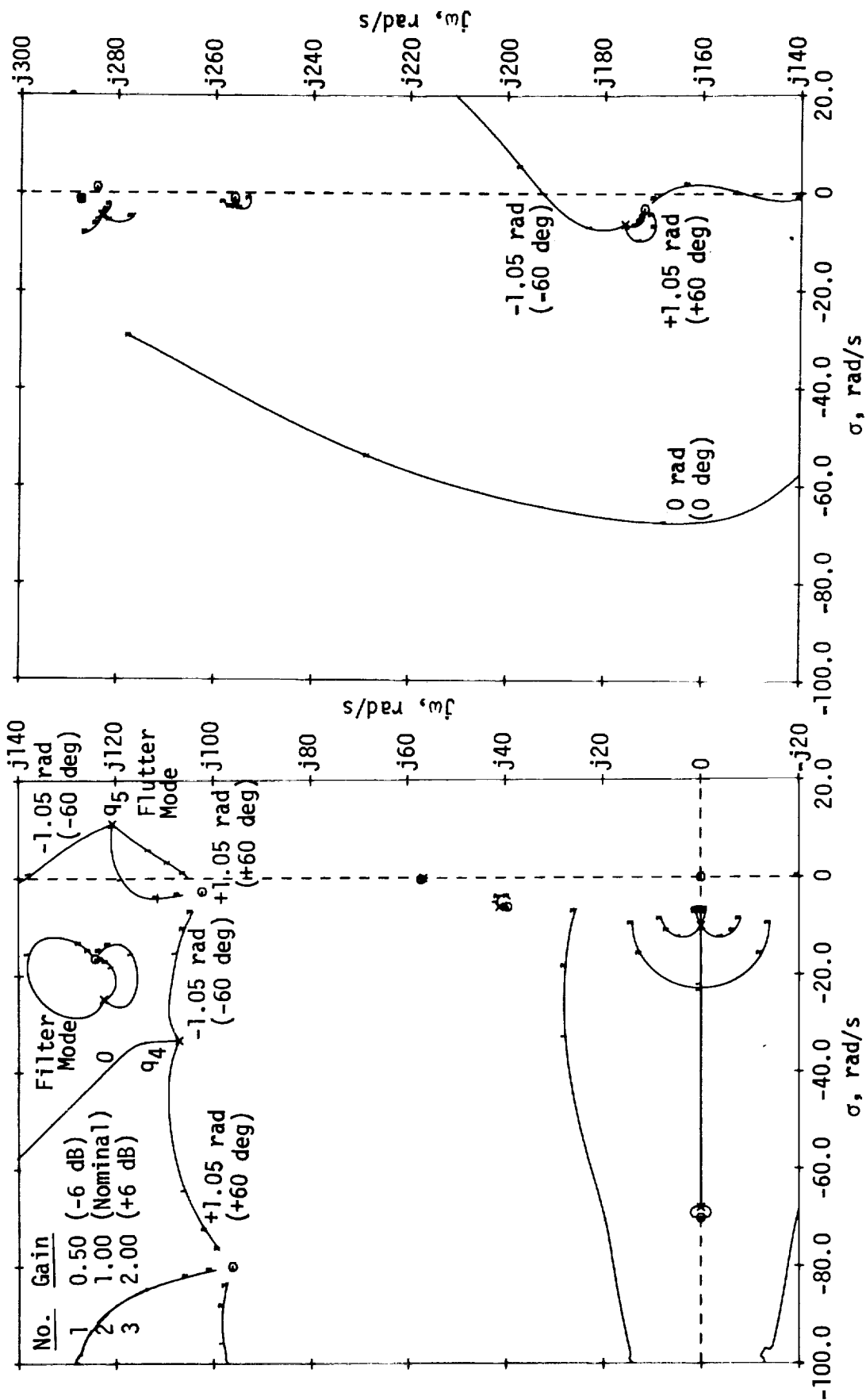


FIGURE 5-13 - GAIN/PHASE ROOT LOCUS OF THE SYMMETRIC FLUTTER SUPPRESSION SYSTEM,  
DYNAMIC PRESSURE = 4309 N/m<sup>2</sup> (90 psf)

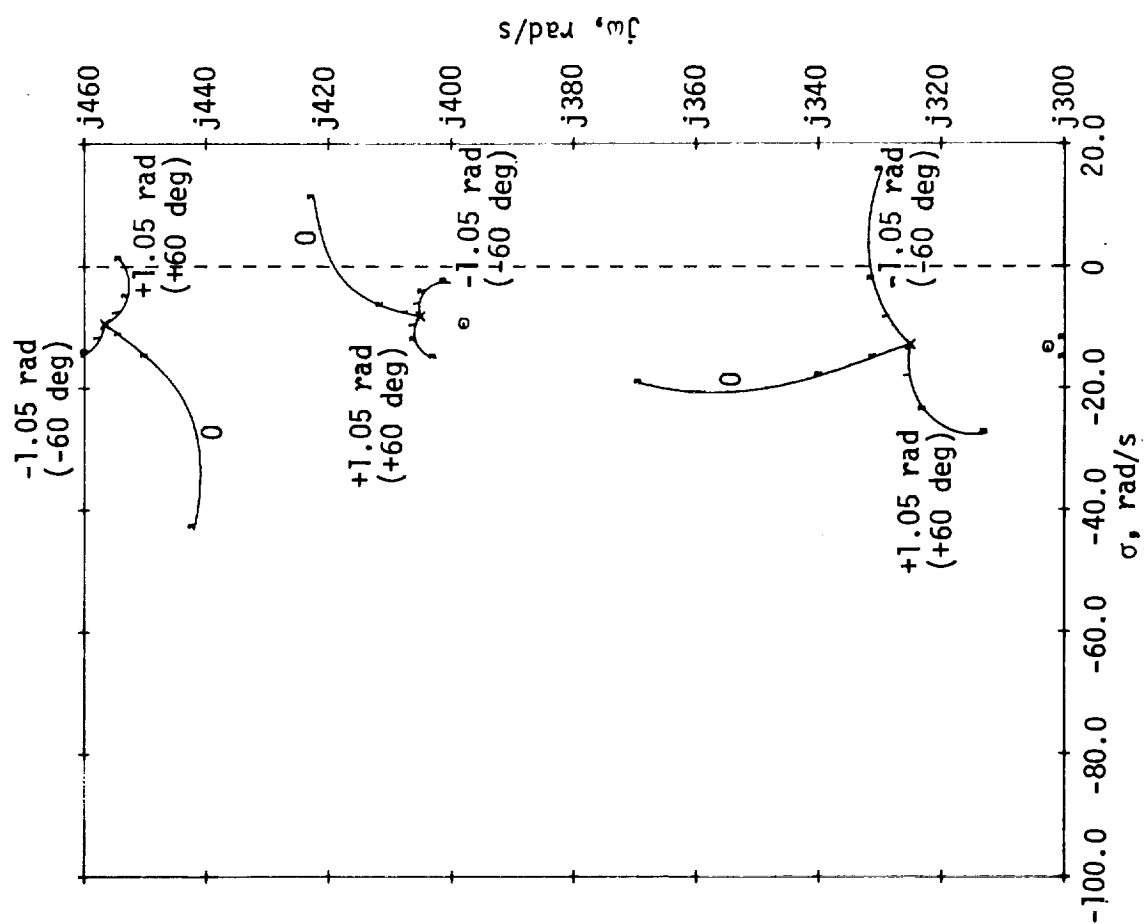


FIGURE 5-13 - GAIN/PHASE ROOT LOCUS OF THE SYMMETRIC FLUTTER SUPPRESSION SYSTEM,  
DYNAMIC PRESSURE = 4309 N/m<sup>2</sup> (90 psf) (CONCLUDED)

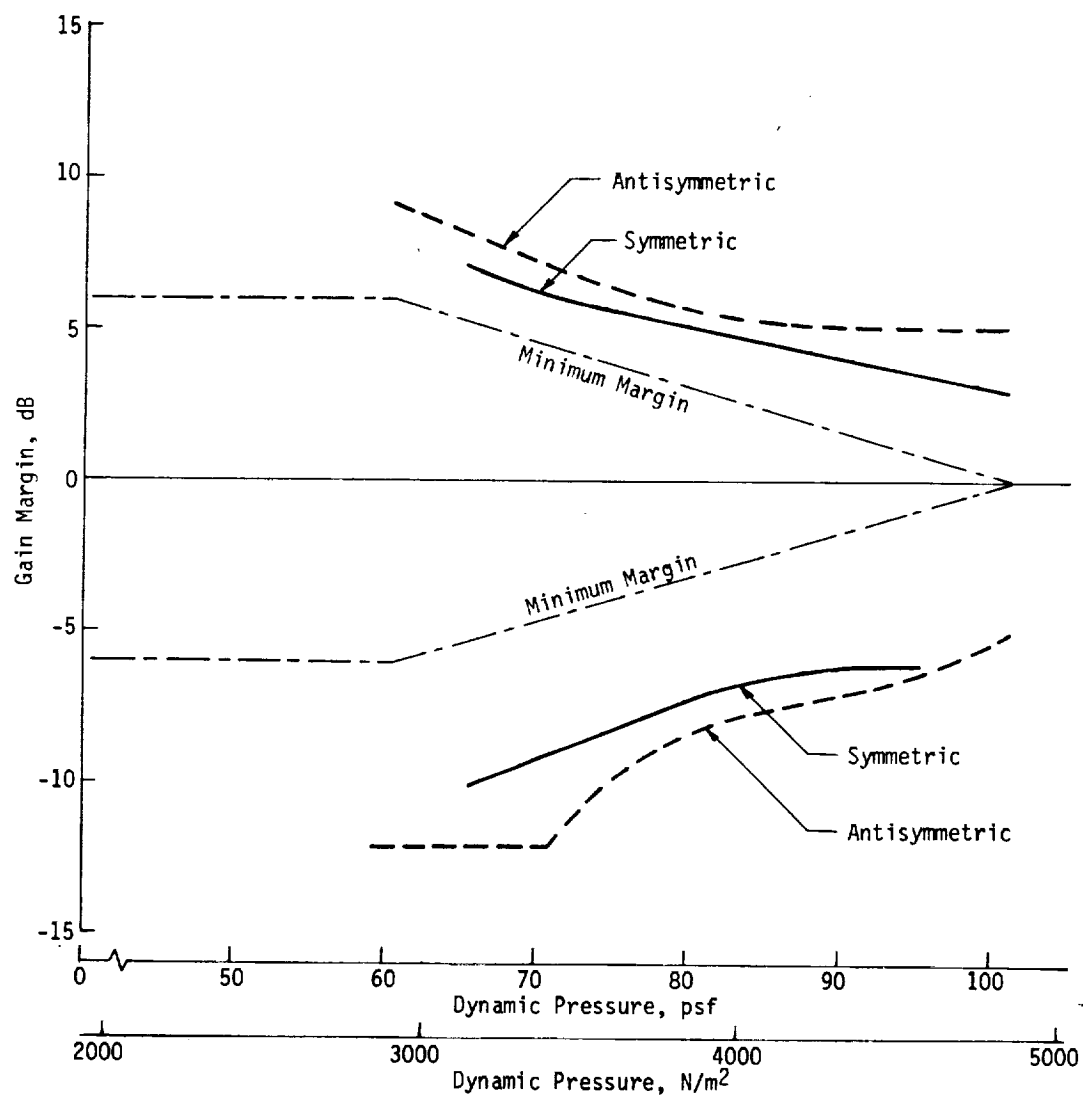


FIGURE 5-14 - MINIMUM GAIN MARGINS OF THE FLUTTER SUPPRESSION SYSTEM



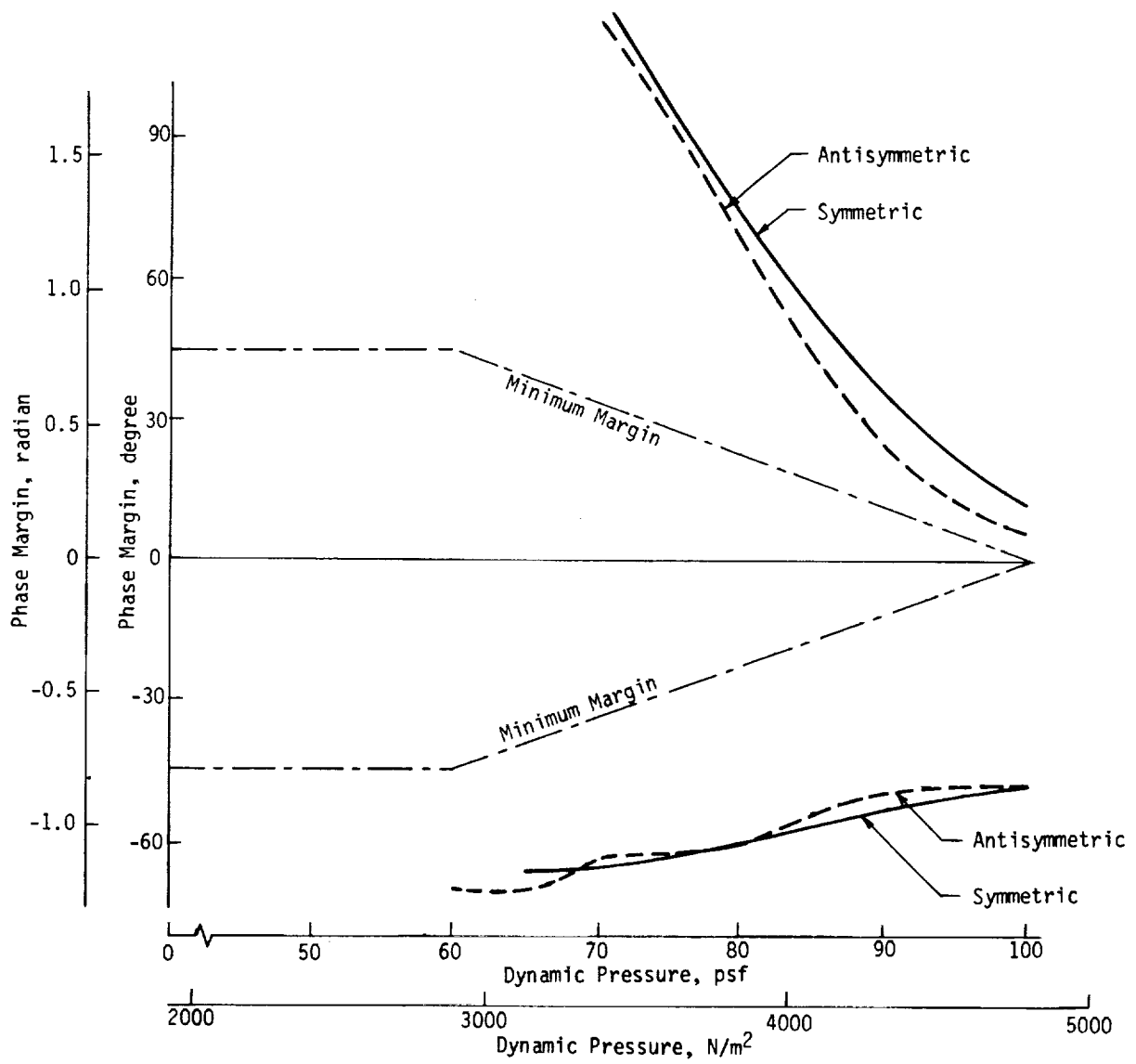


FIGURE 5-15 - MINIMUM PHASE MARGINS OF THE FLUTTER SUPPRESSION SYSTEM

- Symmetric
- Gust Length = 30.48m (100 ft.)
- 0.3048 m/s (1 ft/sec) RMS Random Turbulence

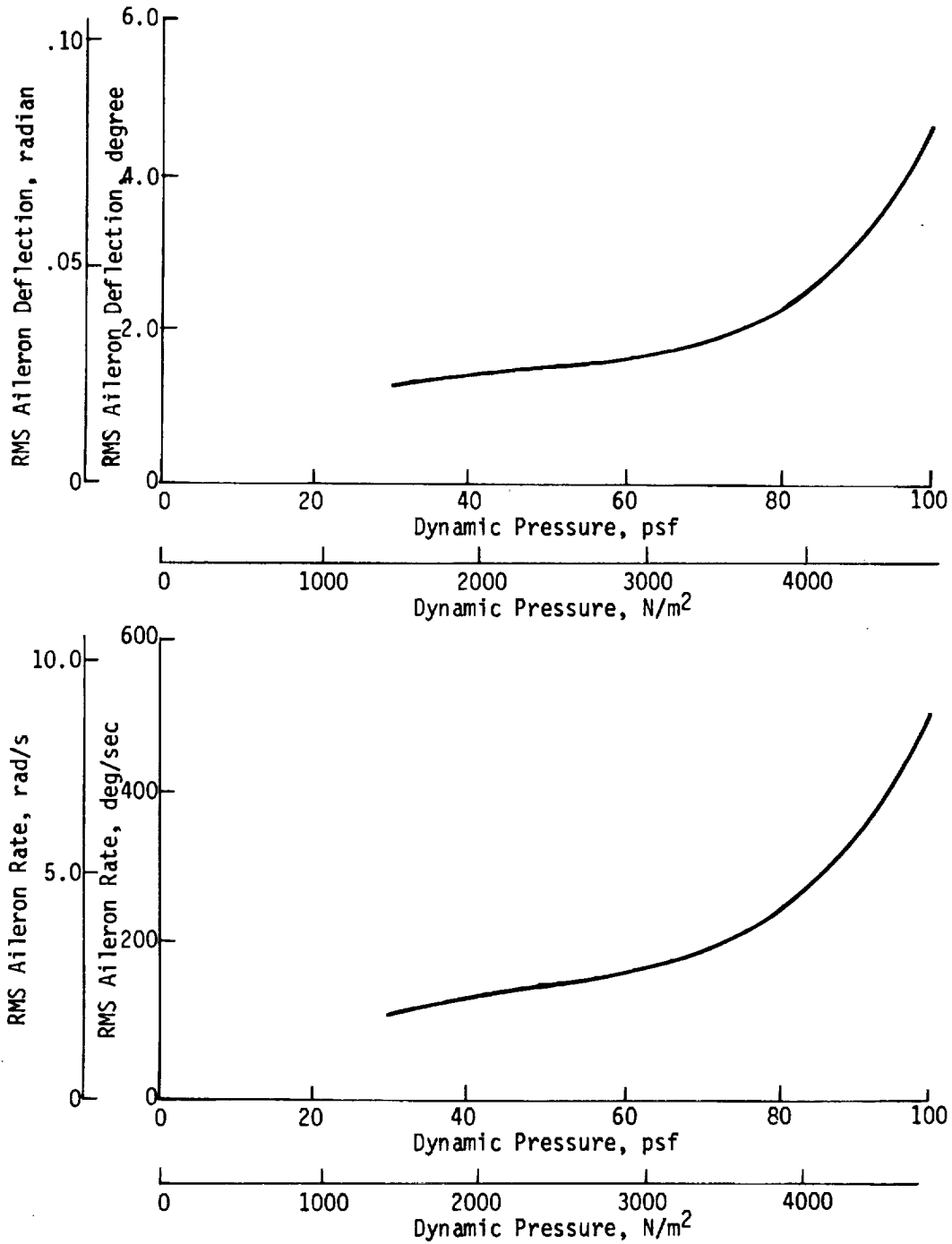


FIGURE 5-16 - SYMMETRIC CONTROL SURFACE REQUIREMENTS

- Antisymmetric
- Gust Length = 30.48m (100 ft.)
- 0.3048 m/s (1 ft/sec) RMS Random Turbulence

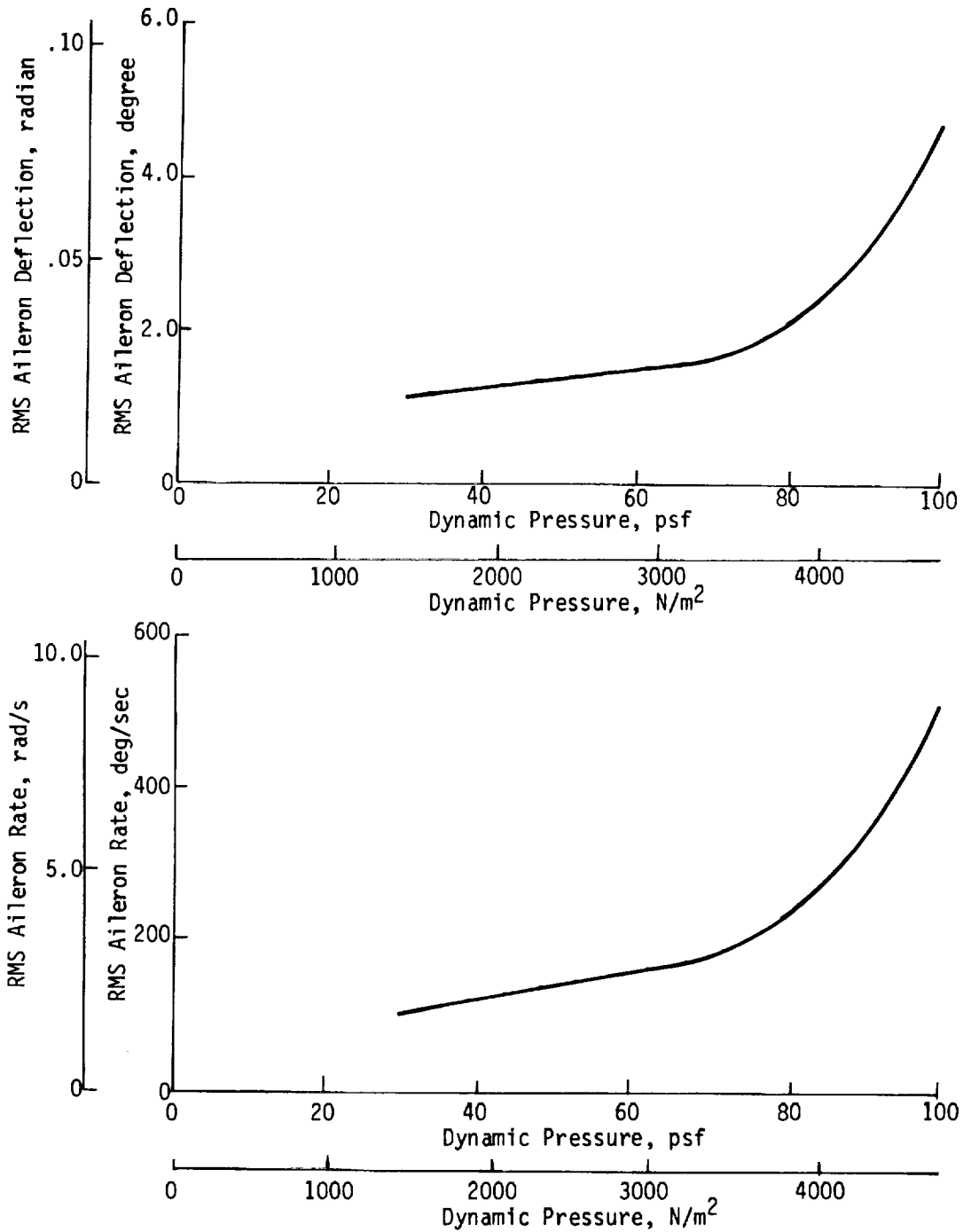


FIGURE 5-17 - ANTISYMMETRIC CONTROL SURFACE REQUIREMENTS



## 6.0 FLUTTER SUPPRESSION SYSTEM IMPLEMENTATION

This section describes the mechanization of the FSS control laws and fail-operational capability. The control laws, which were synthesized in the continuous time domain, were to be implemented using discrete time techniques and digital computers. The system was to have sufficient redundancy to allow non-degraded operation with, and detection of, a single failure.

The overall system requirements and the selected configuration are presented in Paragraph 6.1 and the hardware and software design are described in Paragraphs 6.2 and 6.3, respectively. System performance is presented in Paragraph 6.4 including filter frequency response and failure detection.

### 6.1 System Configuration

The methodology presented in Paragraph 3.3 was followed to define a configuration which satisfied the design requirements. Initially, specific requirements for the hardware were established such as computer word length and sample rate. These criteria, together with the overall design criteria, were then used to specify the hardware and define the FSS configuration.

#### 6.1.1 System requirements - Some of the more specific configuration design criteria, restated from Paragraph 3.3, are as follows:

- The FSS was to have single fail-operate capability
- The FSS should be capable of detecting when a failure has occurred and indicating this fact to the operator
- The sensors and control surfaces were to have no redundancy

Since the entire system could not be made redundant, a single, detectable failure was assumed to be one of the following:

- A single computer failing to update or incorrectly updating its output
- A single failed channel of an A-to-D or D-to-A converter
- A complete failure of an A-to-D or D-to-A converter unit
- A failure in an analog voting device

A literature survey was conducted to aid in selecting computer word length, sample rate, and continuous-to-discrete filter transform. As a consequence of this study the following was concluded.

- The sample rate of the FSS should be at least twice the highest frequency expected at its input (250 Hz)
- A computer word length of 16 bits is adequate for systems that use scaled integer arithmetic
- The best filter transform, in terms of filtering fidelity and computation time, is the Bilinear transform (Tustin's method).

A survey of the current methods of implementing redundant control systems was also conducted to aid in selecting a redundancy scheme that was uncomplicated yet effective. From this study came the following requirements:

- The system must be triply redundant to produce a fail-operate capability
- From the reliability and simplicity standpoint, selection of one good signal out of three (one possibly bad) is best performed with an analog device.

6.1.2 System interface - The FSS interfaces with the wind tunnel model via the accelerometer signals and aileron commands. In order to provide the proper scaling of these signals and minimize the number of A-to-D input channels an analog computer was utilized. This interface configuration, shown on Figure 6-1, also provided for any pre-or post scaling that was required and an interface to aileron excitation generations and data analyzers.

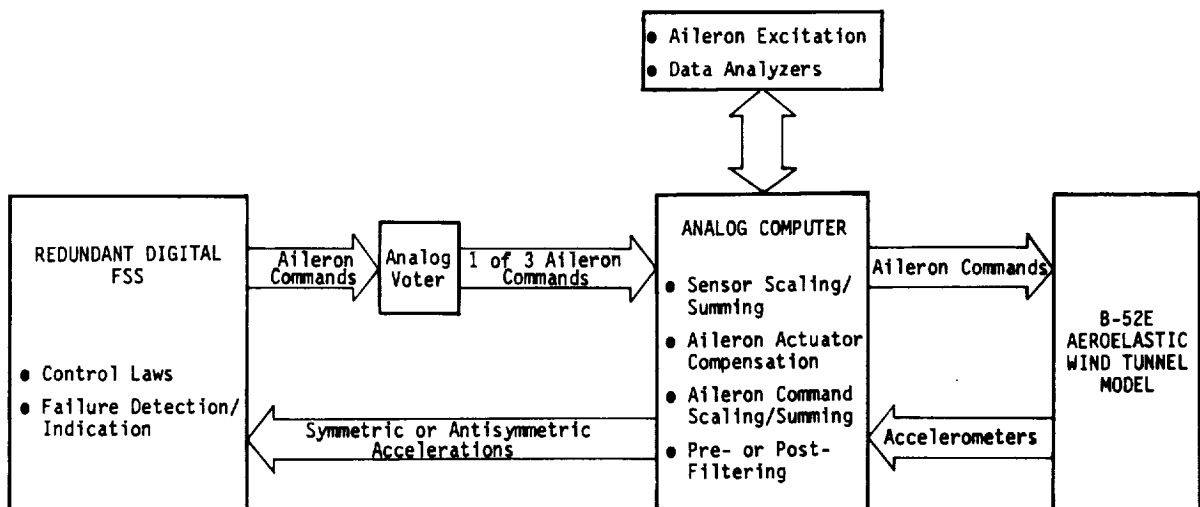


FIGURE 6-1 - SYSTEM INTERFACE CONFIGURATION

Since a considerable number of signals pass between the FSS, analog computer and analog voter, an interface panel was considered a necessity. This panel, shown on Figure 6-2, served as a common point at which all the electrical inter-connections were made.

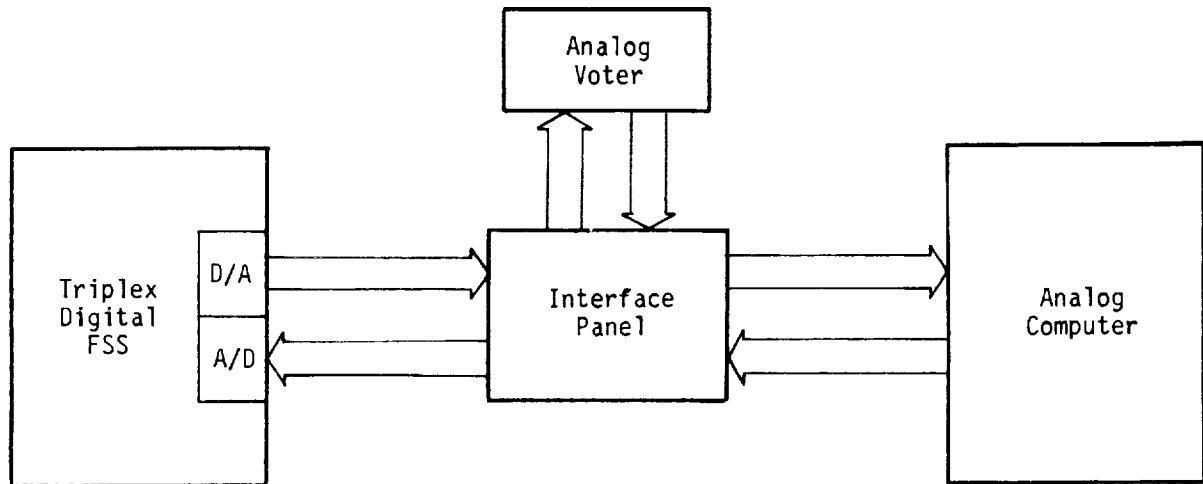


FIGURE 6-2 - INTERFACE PANEL SIGNAL PATHS

6.1.3 Final configuration - Several configurations were defined and evaluated for their ability to detect the required failures. In general, they involved comparing the voter output to the computer generated outputs with variations in how the signals were exchanged and cross-compared. The final configuration, which could successfully detect all required failures, is shown on Figure 6-3.

There were two types of signal paths in the final configuration of the FSS. The FSS filters were implemented by feeding the same accelerometer signals through three identical digital filters made up of an A-to-D and D-to-A converter and a digital computer. The outputs of the filters were then fed through an analog voter which produced the aileron commands. Since the voter output would always be a good signal unless it failed, it was fed back to each of the computers for comparison to other, possibly bad signals. The computers then performed the comparison in a circular fashion, using the output of the next computer. This "looking-over-each-other's-shoulder" approach allowed detection of any failure within the FSS itself. A test program would then be used to isolate the failed component.

Using this configuration the hardware required for implementation of the FSS was selected. Since the sampling rate was to be at least 250 samples per second, the computers had to be capable of computing the filtering equations and performing failure detection and timing logic in no more than 4 milli-seconds. HP 2100 mini-computers capable of performing most of its instructions in two

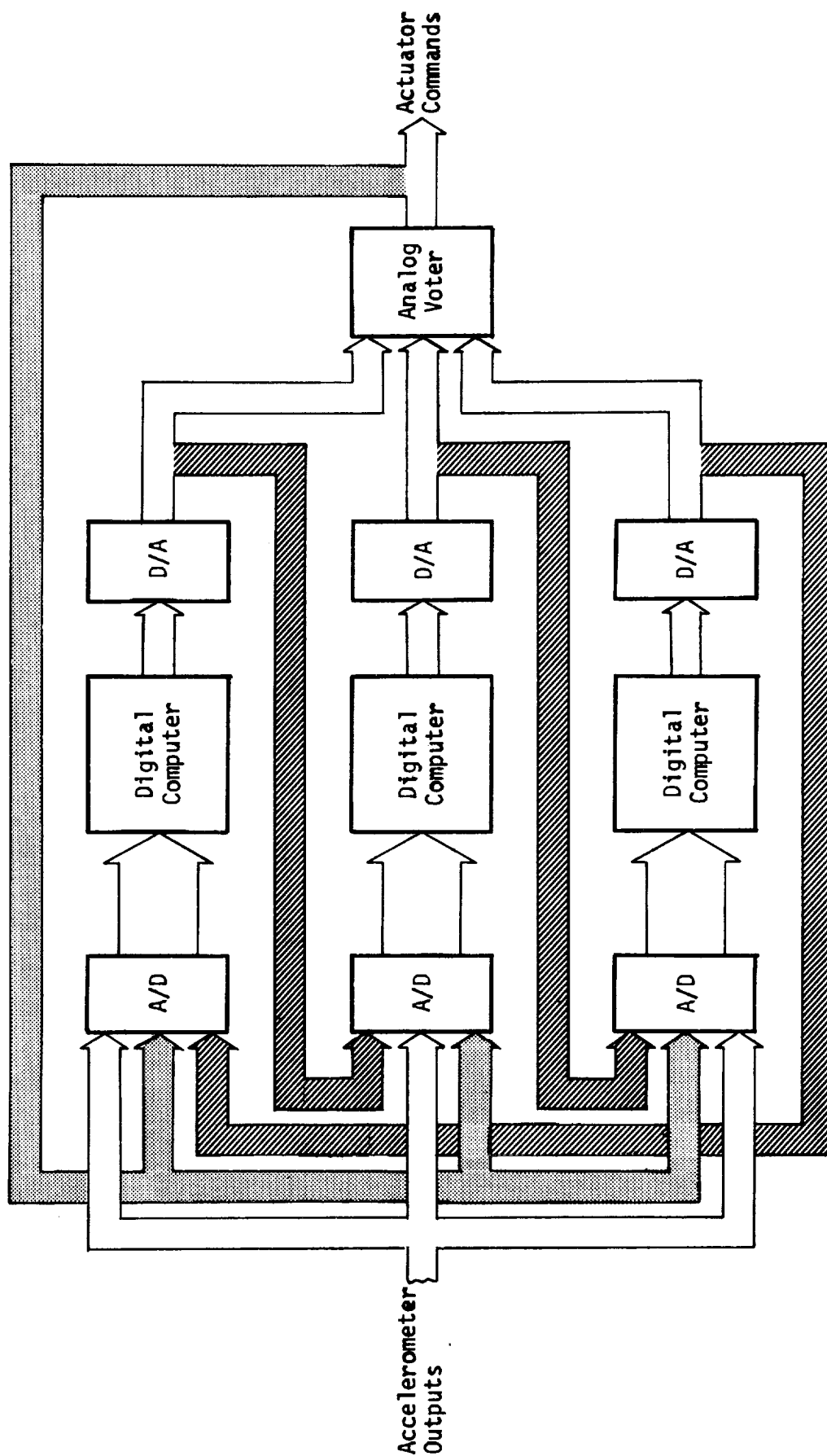


FIGURE 6-3 - REDUNDANT DIGITAL FLUTTER SUPPRESSION SYSTEM SIGNAL PATHS



micro-seconds and an integer multiply in eleven micro-seconds were selected. For an average instruction execution time of four micro-seconds, this computer could execute 1000 instructions in the allotted time, which was more than adequate. Hewlett-Packard A-to-D and D-to-A converters were also used both for interfacing ease and because their conversion speeds were higher than required.

## 6.2 Hardware Design

All hardware except the analog voter and the interface panel was readily available from laboratory equipment. The design of these two components is presented in the following paragraphs.

### 6.2.1 Analog voter design - The analog voter was required to select and output an unfaulted channel of the three input signals. In addition, it was to have unity gain at all frequencies and a dynamic range of $\pm 10$ volts.

A circuit was selected that produced the middle of the three inputs as its output. This circuit, shown on Figure 6-4, works by first selecting the maximums of the input signals taken in two's ( $V_A$ ,  $V_B$ ,  $V_C$ ). It then outputs the minimum of these three signals which would always be the middle of the three inputs. After a successful breadboard test, three identical channels of the voter circuit, along with input/output buffer amplifiers and a switchable inverter circuit were mechanized. Circuit diagrams of this circuit and the DC power supplies are given in Appendix B. Exterior details of the analog voter box are illustrated on Figure 6-5. The front panel has main power and on/off switches and input selector knobs for each of the three channels. The rear panel contains the FSS input, output and test input jacks and provides a mounting place for the voltage regulators. The switches for the inverters were mounted inside the box to prevent inadvertent contact.

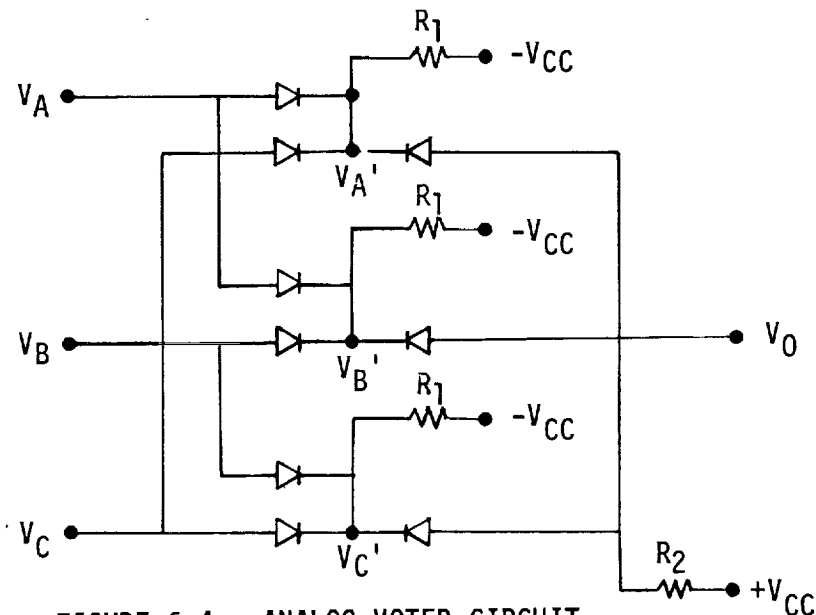
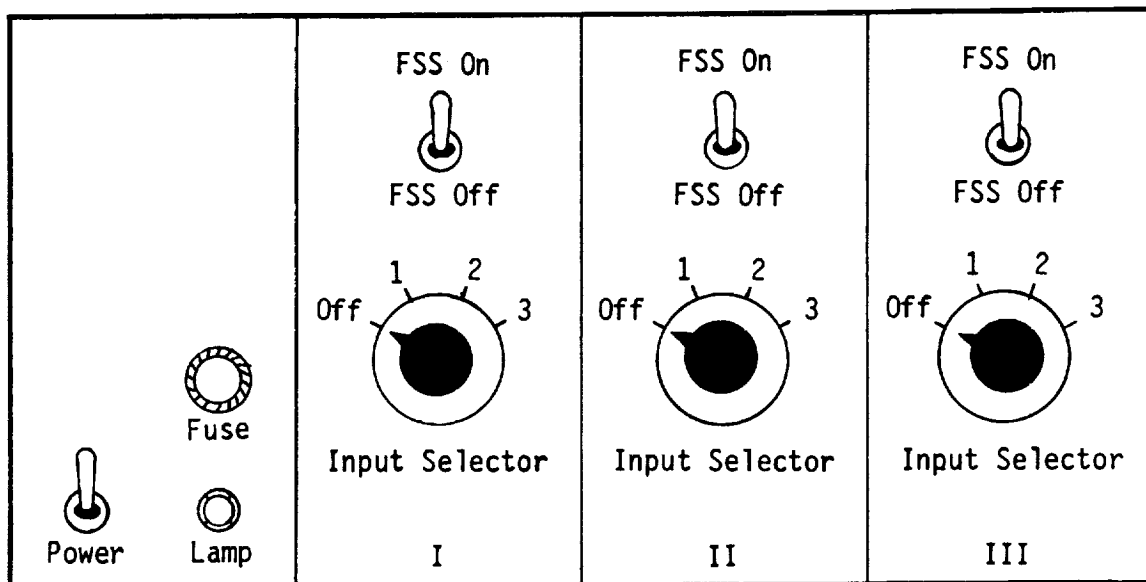
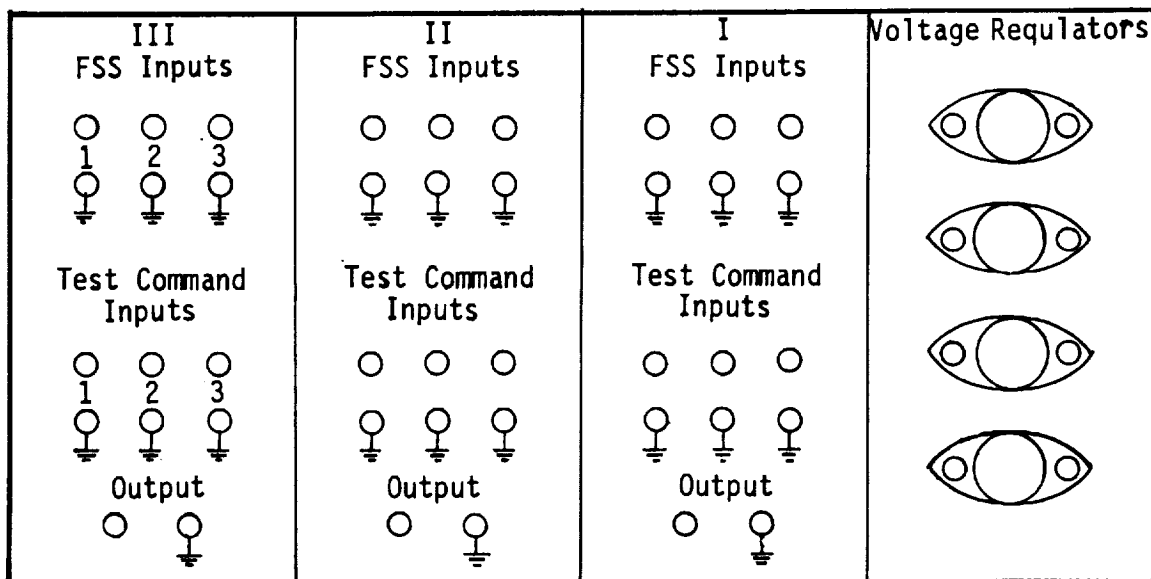


FIGURE 6-4 - ANALOG VOTER CIRCUIT



FRONT PANEL



BACK PANEL

FIGURE 6-5 - ANALOG VOTER BOX EXTERIOR DETAILS

- 6.2.2 Interface panel design - The interface panel was required to provide a common point at which all electrical interconnections between the redundant computer system, analog voter and analog computer could be made. The signals routed through the panel were symmetric and antisymmetric accelerations, voter inputs (FSS outputs), cross check inputs and voter outputs. The front panel details and wiring diagram of the interface panel are illustrated on Figure 6-6. The design provided connection to the analog voter and analog computer by use of banana jacks on the front panel and connection to the digital computer system through terminal strips on the rear of the panel. All inter-connection of signals was hardwired on the rear of the panel. A bracket to support the A-to-D and D-to-A converter cables was also provided.

### 6.3 Software Design

In order to implement the FSS filters on a digital computer the describing Laplace domain equations were transformed into difference equations. The difference equations along with the failure detection and other support software were then programmed on the computer in a form that would execute in the required time. Finally, the frequency response and failure detection performance of the FSS was assessed.

- 6.3.1 Software design requirements - There were two major design requirements which governed the overall software configuration. The frequency response of the digital filters was required to closely match the ideal response in the frequency range of the flutter mode. While performing the filter computations the FSS was also required to detect any failure within the FSS and give some indication to the operator.

- 6.3.2 Computer and signal processing equipment - The computers chosen to implement the FSS were capable of being programmed in several high-level software languages including FORTRAN and BASIC. However, in order to produce the most time-efficient software, a machine level language called assembly language was used. This language provided direct access to the fundamental instruction set of the computer which contained instructions to move data about in memory, perform arithmetic and logical operations and enable input-output data transfer to peripheral equipment. A brief description of the instruction set of the HP 2100 is provided in Appendix B.

The A-to-D and D-to-A converters were zero-order hold devices, that is, they represent the input or output signals in staircase fashion. The A-to-D converters were signed, 10-bit devices with an input range of  $\pm 10$  volts and the D-to-A converters were signed, 12-bit devices with an output range of  $\pm 10.24$  volts.

- 6.3.3 Selection of linear-to-discrete transform - In order to convert the Laplace domain equations describing the FSS filter to a form that could be programmed on a digital computer a transform

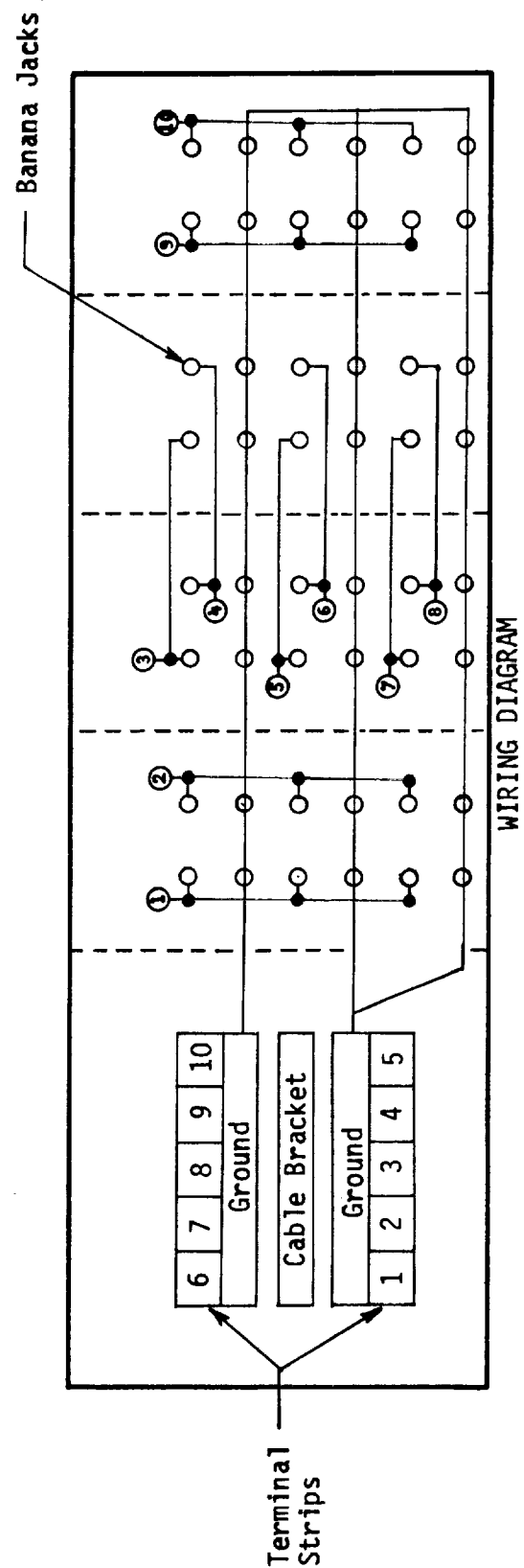
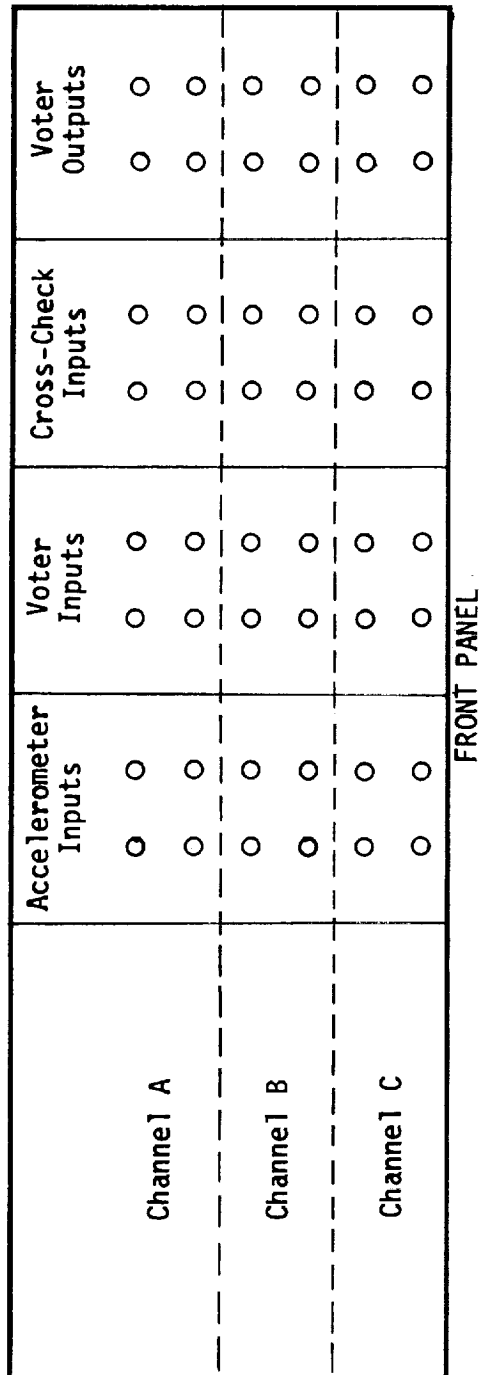


FIGURE 6-6 - INTERFACE PANEL FRONT DETAILS AND WIRING DIAGRAM

was necessary. The three widely used methods, namely, rectangular integration, trapezoidal integration and bilinear transform (Tustin's method), were considered in the present study. The process of using these three methods to transform a first-order lag is illustrated in Table 6-I. In the first two methods the Laplace equation was first converted into a block diagram made up of summing junctions, gains and integrators. The integration approximation was then substituted into the block diagram to give the discrete-time approximation (" $\Delta$  is the time delay operator where  $\Delta X_n = X_{n-1}$ "). From this approximation, the difference equation was written.

In Tustin's method the substitution is the same as for trapezoidal integration but it is made directly into the Laplace equation, resulting immediately in a difference equation. From this equation a block diagram was drawn.

Tustin's method has certain advantages over the other two techniques. By comparing the difference equations from Table 6-I it can be seen that Tustin's method avoids the delayed feedback form which results in the " $Y_{n-2}$ " term in the other equations. This "stale data" problem is the primary source of the other method's deficiencies. Therefore, Tustin's method was used as the analog-to-discrete transform. Difference equations for some common filter forms are given in Table 6-II.

- 6.3.4 Flutter suppression system filter implementation - Initially, the software required to interface with the D-to-A and A-to-D converters and to drive a real-time clock was developed. Since all of these devices were Hewlett-Packard equipment, standard interface cards and software were available. The real-time clock generates interrupts to the computer at a software selectable rate. These interrupts were counted in software to determine when the total cycle time had elapsed. At the beginning of each cycle the computer executed the filter equations and failure detection logic and counted interrupts until the cycle time had elapsed, whereupon the interrupt count was reset and a new cycle begun.

After successfully transferring analog signals end-to-end through the computer system, several single-element filters were programmed to gain experience with Tustin's method. Initially, the difference equations were programmed using floating point arithmetic operations. These filters performed well but consumed a lot of time, primarily because floating point arithmetic requires double-word length numbers and uses about 20 times more execution time than a regular instruction. To overcome this problem the filters were programmed using integer arithmetic operations which use single-word length numbers and about one-fourth the execution time. In order to use this method the input signal and difference equation coefficients must be scaled and the software has to check for an overflow after some arithmetic operations.

TABLE 6-1  
COMPARISON OF DISCRETE TRANSFORMS

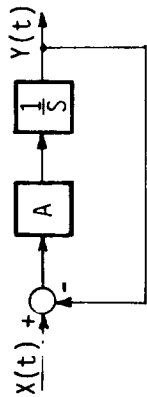
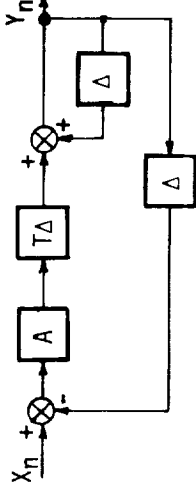
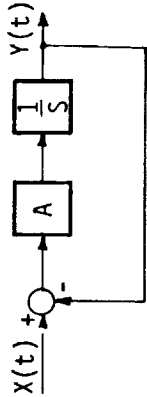
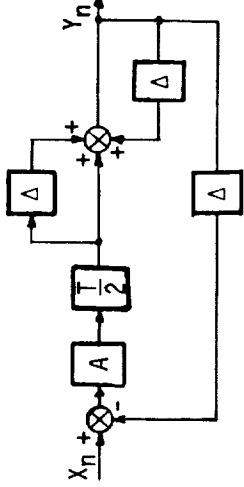

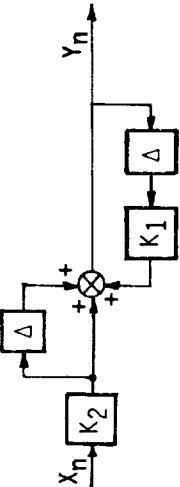
Method	LaPlace Representation	Continuous Time Representation	Transform	Discrete Time Representation
Rectangular Integration	$\frac{X}{Y} = \frac{A}{S+A}$		$\frac{1}{S} = T \left( \frac{\Delta}{1-\Delta} \right)$	 $Y_n = Y_{n-1} - ATY_{n-2} + ATX_{n-1}$
Trapezoidal Integration	$\frac{X}{Y} = \frac{A}{S+A}$		$\frac{1}{S} = \frac{T}{2} \left( \frac{1+\Delta}{1-\Delta} \right)$	 $Y_n = \left( 1 - \frac{AT}{2} \right) Y_{n-1} - \left( \frac{AT}{2} \right) Y_{n-2} + \left( \frac{AT}{2} \right) (X_n + X_{n-1})$
Bilinear Transform (Tustin's Method)	$\frac{X}{Y} = \frac{A}{S+A}$		$S = \frac{2}{T} \left( \frac{1-\Delta}{1+\Delta} \right)$	 $K_1 = (2 - AT)/(2 + AT)$ $K_2 = AT/(2 + AT)$ $Y_n = K_1 Y_{n-1} + K_2 (X_n + X_{n-1})$

TABLE 6-II  
DIFFERENCE EQUATIONS FOR COMMON FILTER ELEMENTS

Filter	Difference Equation
LAG $A/(S + A)$	$Y_n = K_1 Y_{n-1} + K_2 (X_n + X_{n-1})$ $K_1 = (2 - AT)/(2 + AT)$ $K_2 = AT/(2 + AT)$
WASHOUT $S/(S + A)$	$Y_n = K_1 Y_{n-1} + K_2 (X_n + X_{n-1})$ $K_1 = (2 - AT)/(2 + AT)$ $K_2 = 2/(2 + AT)$
LEAD-LAG $(S + B)/(S + A)$	$Y_n = K_1 Y_{n-1} + K_2 X_n + K_3 X_{n-1}$ $K_1 = (2 - AT)/(2 + AT)$ $K_2 = (2 + BT)/(2 + AT)$ $K_3 = (-2 + BT)/(2 + AT)$
SECOND ORDER $\frac{A^2}{S^2 + 2ABS + A^2}$	$Y_n = K_1 Y_{n-1} + K_2 Y_{n-2} + K_3 (X_n + 2X_{n-1} + X_{n-2})$ $K_1 = (8 - 2A^2T^2)/D$ $K_2 = (-4 + 4ABT - A^2T^2)/D$ $K_3 = A^2T^2/D$ $D = 4 + 4ABT + A^2T^2$
NOTCH $\frac{S^2 + 2ACS + A^2}{S^2 + 2ABS + A^2}$	$Y_n = K_1 Y_{n-1} + K_2 Y_{n-2} + K_3 X_n + K_4 X_{n-1} + K_5 X_{n-2}$ $K_1 = (8 - 2A^2T^2)/D$ $K_2 = (-4 + 4ABT - A^2T^2)/D$ $K_3 = (4 + 4ACT + A^2T^2)/D$ $K_4 = (-8 + 2A^2T^2)/D$ $K_5 = (4 - 4ACT + A^2T^2)/D$ $D = 4 + 4ABT + A^2T^2$

The FSS filters were programmed using the scaled integer technique and the difference equations found in Table 6-III. All the filter coefficients with magnitude less than one were scaled the maximum amount,  $2^{15}$ . Those coefficients greater in magnitude were scaled by  $2^{14}$  and the factor of two added after the multiplication by shifting the number left one bit. The result of each multiplication was a 32-bit word which was shifted left one bit to correct the scaling and then truncated to a 16-bit word. The filters were implemented in a cascade or series fashion with the output of one filter serving as the input to the next.

After the filters were programmed the end-to-end frequency response was evaluated. Initially, considerable effort was expended in adjusting the intermediate gains of the filter to eliminate overflow conditions. Even after all overflows had been eliminated the frequency response of the filter deviated significantly from the ideal, especially near the flutter frequency. The problem was found to be the limited range of the input device (10-bit A-to-D) and the wide difference in the frequency responses of the filter terms. The first-order lag at 10 rad/s has a very low gain at the flutter frequency of 125 radians/second. This reduces the resolution of the inputs from 10 bits to about six. When this signal was passed through the inverse notch at 125 rad/s, the round-off error distorted the output considerably. Changing the order of computation of the filter terms did not improve the result.

Since the series implementation would not work an alternate configuration was devised. This consisted of a parallel implementation of the filter by performing a partial fraction expansion on the filter. The resulting configuration is shown on Figure 6-7. The gains prior to the final summation were scaled by 70 and the D-to-A gain to reduce their magnitudes to less than one. The gain of 70 could then be moved to the analog computer and the internal gains scaled by  $2^{15}$  for integer multiplication, as before. The multiple terms in the denominator of the original filter produced a partial fraction expansion with only three unique terms. Since in Tustin's method overflow detection is not required in first-order lags, the only overflow detection was performed internal to the second-order term and at the output of the final summation. The difference equations to implement this filter are given in Table 6-IV.

These filter equations were programmed using a sample rate of 500/s and the system frequency response evaluated. The phase and gain matched the ideal responses closely except at the higher frequencies. The execution time delay caused the phase to lag the desired phase and the sampling rate caused the gain to go to zero at the nyquist frequency (250 Hz). A non-recursive approximation to a time advance was added in series with the output of the filter as follows:

$$Y_n = 1.875X_n - 1.25X_{n-1} + 0.375X_{n-2}.$$



**TABLE 6-III**  
**DIFFERENCE EQUATIONS FOR THE FLUTTER SUPPRESSION SYSTEM FILTER**

Filter	Difference Equation (T = .004)
$\frac{S}{S + 10}$	$Y_n = K_1 Y_{n-1} + K_2 (X_n - X_{n-1})$ $K_1 = 0.960784(2^{15}) = 31483$ $K_2 = 0.980392(2^{15}) = 32125$
$\frac{10}{S + 10}$	$Y_n = K_1 Y_{n-1} + K_2 (X_n + X_{n-1})$ $K_1 = 0.960784(2^{15}) = 31483$ $K_2 = 0.019078(2^{15}) = 643$
$\frac{150}{S + 150}$	$Y_n = K_1 Y_{n-1} + K_2 (X_n + X_{n-1})$ $K_1 = 0.538462(2^{15}) = 17644$ $K_2 = 0.230769(2^{15}) = 7562$
$\frac{22500}{1600} \frac{S^2 + 12S + 1600}{S^2 + 300S + 22500}$	$Y_n = G [K_1 Y_{n-1} + K_2 Y_{n-2} + K_3 X_n + K_4 X_{n-1} + K_5 X_{n-1}]$ $G = 14.0625$ $K_1 = 1.0769(2^{14}) = 17643$ $K_2 = -0.289941(2^{15}) = -9468$ $K_3 = 0.609704(2^{15}) = 19978$ $K_4 = -1.175858(2^{14}) = -19625$ $K_5 = 0.58130(2^{15}) = 19647$
$\frac{S^2 + 160S + 15625}{S^2 + 50S + 15625}$	$Y_n = K_1 Y_{n-1} + K_2 Y_{n-2} + K_3 X_n + K_4 X_{n-1} + K_5 X_{n-2}$ $K_1 = 1.6129(2^{14}) = 26426$ $K_2 = -0.827957(2^{15}) = -27130$ $K_3 = 1.18925(2^{14}) = 19485$ $K_4 = -1.6129(2^{14}) = -26426$ $K_5 = 0.63879(2^{15}) = 20929$

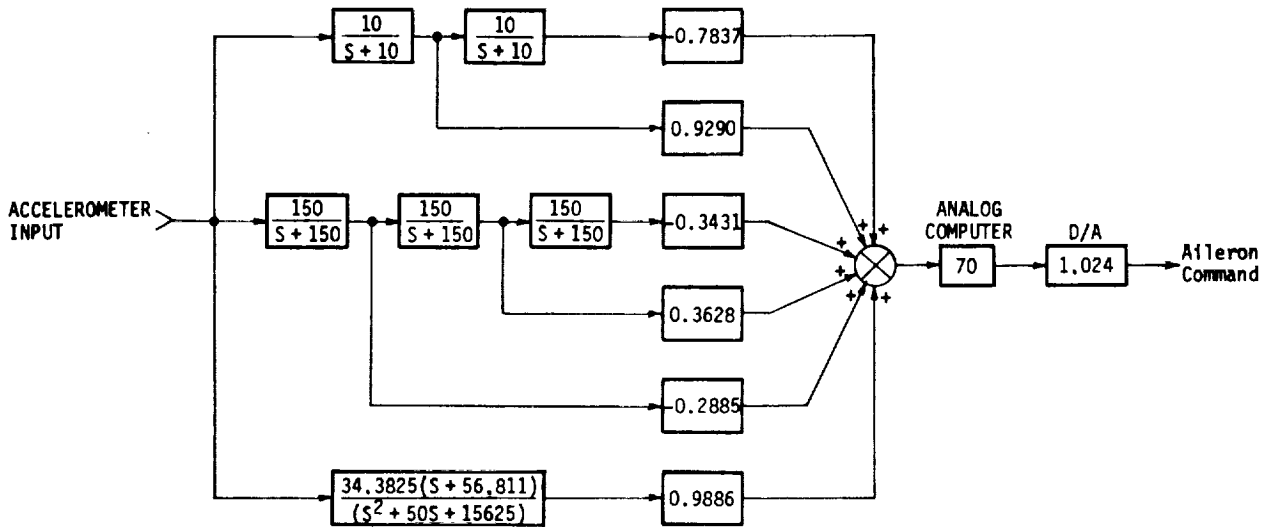


FIGURE 6-7 - PARALLEL EXPANSION OF THE FLUTTER SUPPRESSION SYSTEM FILTER

TABLE 6-IV  
DIFFERENCE EQUATIONS FOR THE PARALLEL FLUTTER SUPPRESSION SYSTEM FILTER

Filter	Difference Equations (T = 0.002)
$\frac{10}{s+10}$	$Y_n = K_1 Y_{n-1} + K_2 (X_n + X_{n-1})$ $K_1 = 0.980198(2^{15}) = 32118$ $K_2 = 0.009901(2^{15}) = 325$
$\frac{150}{s+150}$	$Y_n = K_1 Y_{n-1} + K_2 (X_n + X_{n-1})$ $K_1 = 0.73913(2^{15}) = 24220$ $K_2 = 0.130435(2^{15}) = 4274$
$\frac{34.3825(s+56.811)}{(s^2+50s+15625)}$	$Y_n = K_1 Y_{n-1} + K_2 Y_{n-2} + K_3 X_n + K_4 X_{n-1} + K_5 X_{n-2}$ $K_1 = 1.84751(2^{14}) = 30270$ $K_2 = -0.90616(2^{15}) = -29693$ $K_3 = 0.27276(2^{15}) = 8938$ $K_4 = 0.029323(2^{15}) = 961$ $K_5 = -0.243434(2^{15}) = -7977$

This prediction algorithm caused the output to be approximately what it would have been had no time elapsed between input and output. This improved the frequency response to an acceptable level.

In the parallel expansion of a filter a change in any term of the filter will affect the entire parallel filter. This prompted the development of an alternate parallel filter which did not include the washout or the first-order lag at 150 rad/s. These terms would then be mechanized on the analog computer for pre- or post filtering should this be necessary during the wind tunnel test. The configuration of this parallel filter is shown on Figure 6-8 and the difference equations appear in Table 6-V.

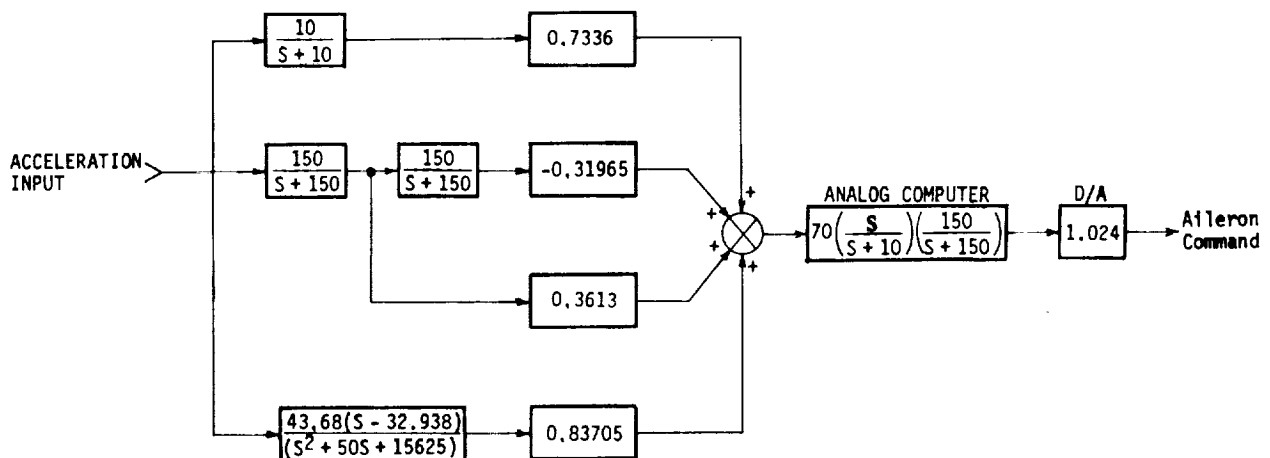


FIGURE 6-8 - PARALLEL EXPANSION OF THE PARTIAL FLUTTER SUPPRESSION SYSTEM FILTER

- 6.3.5 Failure detection and indication - The fail-operate and failure detection capabilities of the FSS were primarily determined by the hardware configuration as described in Paragraph 6.1. However, the detection and indication of a failure was performed in software. This software was then integrated with the filter software to complete the software design.

The failure detection software was programmed to detect two basic types of failures, erroneous system output and execution time overruns. The first type of failure was detected by comparing the absolute difference between the voter and computer outputs to a pre-determined threshold. If the error exceeded the threshold a failure was declared. Execution time overruns were detected by requiring the computer to set a flag at the end of execution of the program. If, at the start of the next execution interval this flag was not set, a failure was declared.

The occurrence of a failure or failures was indicated by flashing the computer's front panel lights. In order to make the flashing rate independent of the failure rate, failures were accumulated

TABLE 6-V  
DIFFERENCE EQUATIONS FOR THE PARTIAL PARALLEL FLUTTER SUPPRESSION SYSTEM  
FILTER

Filter	Difference Equation (T = 0.002)
$\frac{10}{s + 10}$	$Y_n = K_1 Y_{n-1} + K_2 (X_n + X_{n-1})$ $K_1 = 0.980198(2^{15}) = 32118$ $K_2 = 0.009901(2^{15}) = 325$
$\frac{150}{s + 150}$	$Y_n = K_1 Y_{n-1} + K_2 (X_n + X_{n-1})$ $K_1 = 0.73913(2^{15}) = 24220$ $K_2 = 0.130435(2^{15}) = 4274$
$\frac{43.68(s - 32.938)}{(s^2 + 50s + 15625)}$	$Y_n = K_1 Y_{n-1} + K_2 Y_{n-2} + K_3 X_n + K_4 X_{n-1} + K_5 X_{n-2}$ $K_1 = 1.8475(2^{14}) = 30270$ $K_2 = -0.90616(2^{15}) = -29693$ $K_3 = 0.31712(2^{15}) = 10391$ $K_4 = -0.02160(2^{15}) = -708$ $K_5 = -0.33872(2^{15}) = -11099$

for about one-half second. Unless no failures had occurred during that time interval the front panel lights were flashed at 1 Hz. This failure summing technique prevented the flash rate from being too fast or slow to be seen by the operator.

A separate program was written which allowed easy testing of each computer system to determine the origin of a failure. Listings of this program and the main program are given in Appendix B.

#### 6.4 System Performance

The performance of the entire system was evaluated to verify that all performance criteria had been met. The testing included the frequency response of the system with and without failures, analog voter performance and the successful detection of all required failures.

- 6.4.1 Filter frequency response - The frequency response of the FSS filters was evaluated using a digital transfer function analyzer. The resulting plots matched the theoretical response closely as shown on Figures 6-9 and 6-10. The deviations at the higher frequencies are attributable to effects of the sampling rate on phase and the output prediction algorithm on gain.
- 6.4.2 Analog voter performance - Initially analog voter performance was tested using a frequency response analyzer. Frequency responses of the analog voter with and without a failed channel showed unity gain characteristics up to 1000 Hz. In order to test the operation of the system with one channel failed, end-to-end frequency responses of the FSS filters were run. The resulting plots, shown on Figures 6-11 and 6-12, showed very little degradation due to a single failure. The variations in gain at 6.5 Hz and 100 Hz are attributable to the low amplitude of the output coupled with variations in voter electronics.
- 6.4.3 Failure detection performance - The ability of the FSS to detect internal failures was tested by introducing failures within the system and observing the results. The following failures were introduced by breaking wiring connections and switching off components:
- Failure of an A-to-D or D-to-A converter channel or the entire unit
  - Failure of a digital computer
  - Failure of the analog voter.

In all cases, with an input of reasonable magnitude, the FSS was able to detect and indicate to the operator that a failure had occurred.

- Input Scaling - 2.5 V/g
- Output Scaling - 0.02618 rad/V (1.5 deg/V)

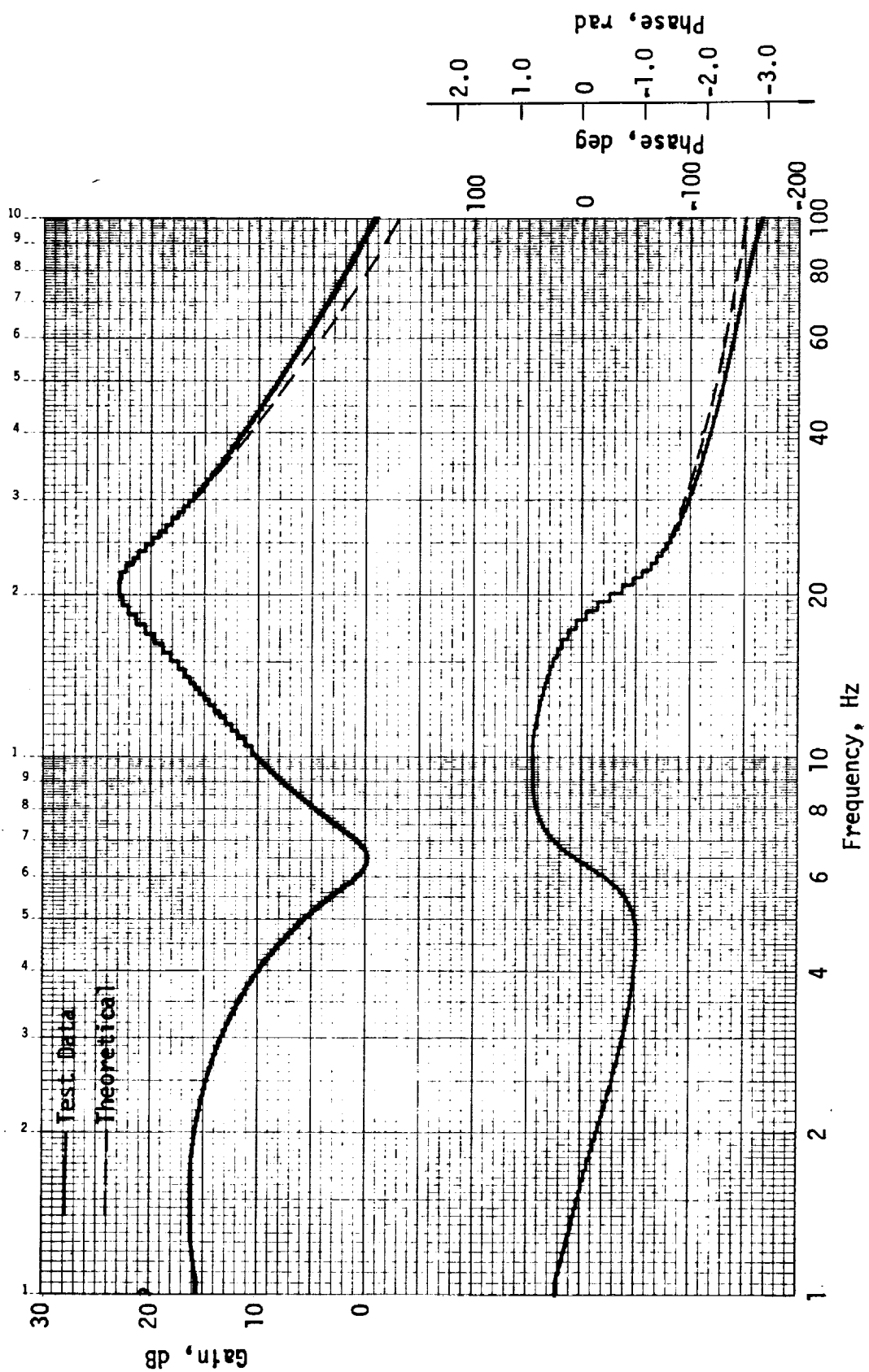


FIGURE 6-9 - FREQUENCY RESPONSE OF SYMMETRIC FLUTTER SUPPRESSION SYSTEM

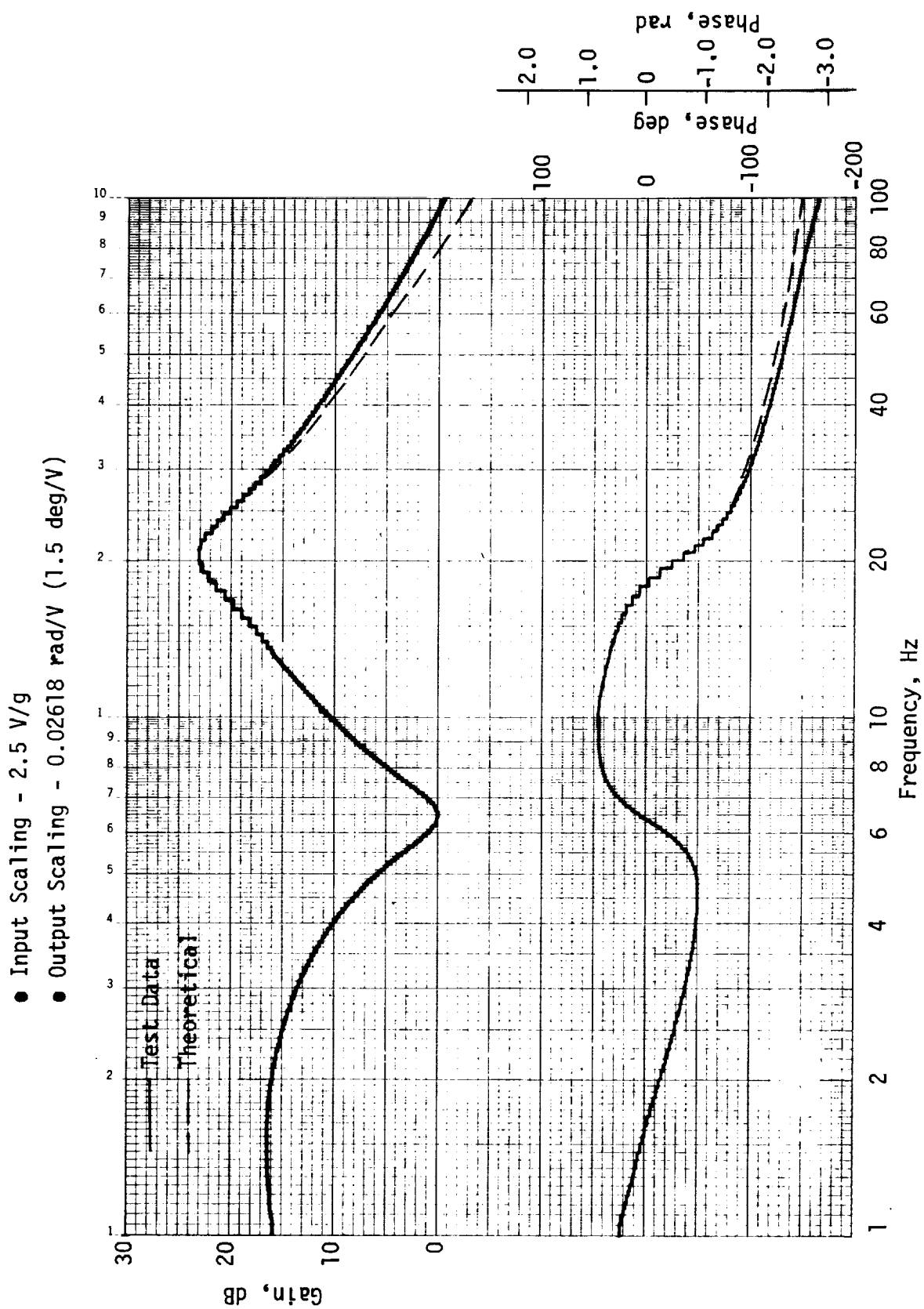


FIGURE 6-10 - FREQUENCY RESPONSE OF ANTISYMMETRIC FLUTTER SUPPRESSION SYSTEM

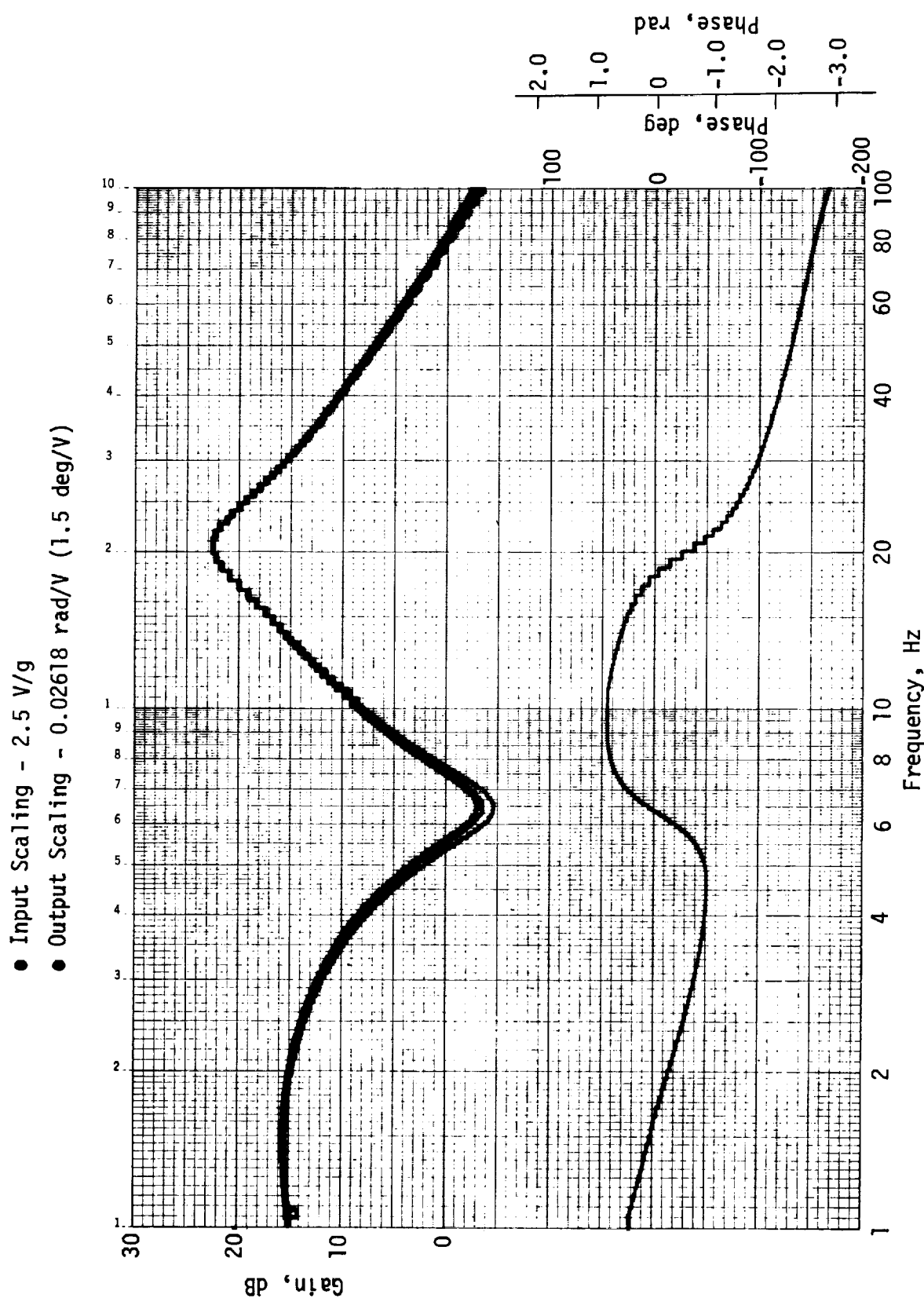


FIGURE 6-11 - FREQUENCY RESPONSE OF SYMMETRIC FLUTTER SUPPRESSION SYSTEM WITH EACH CHANNEL FAILED



● Input Scaling - 2.5 V/g

● Output Scaling - 0.02618 rad/V (1.5 deg/V)

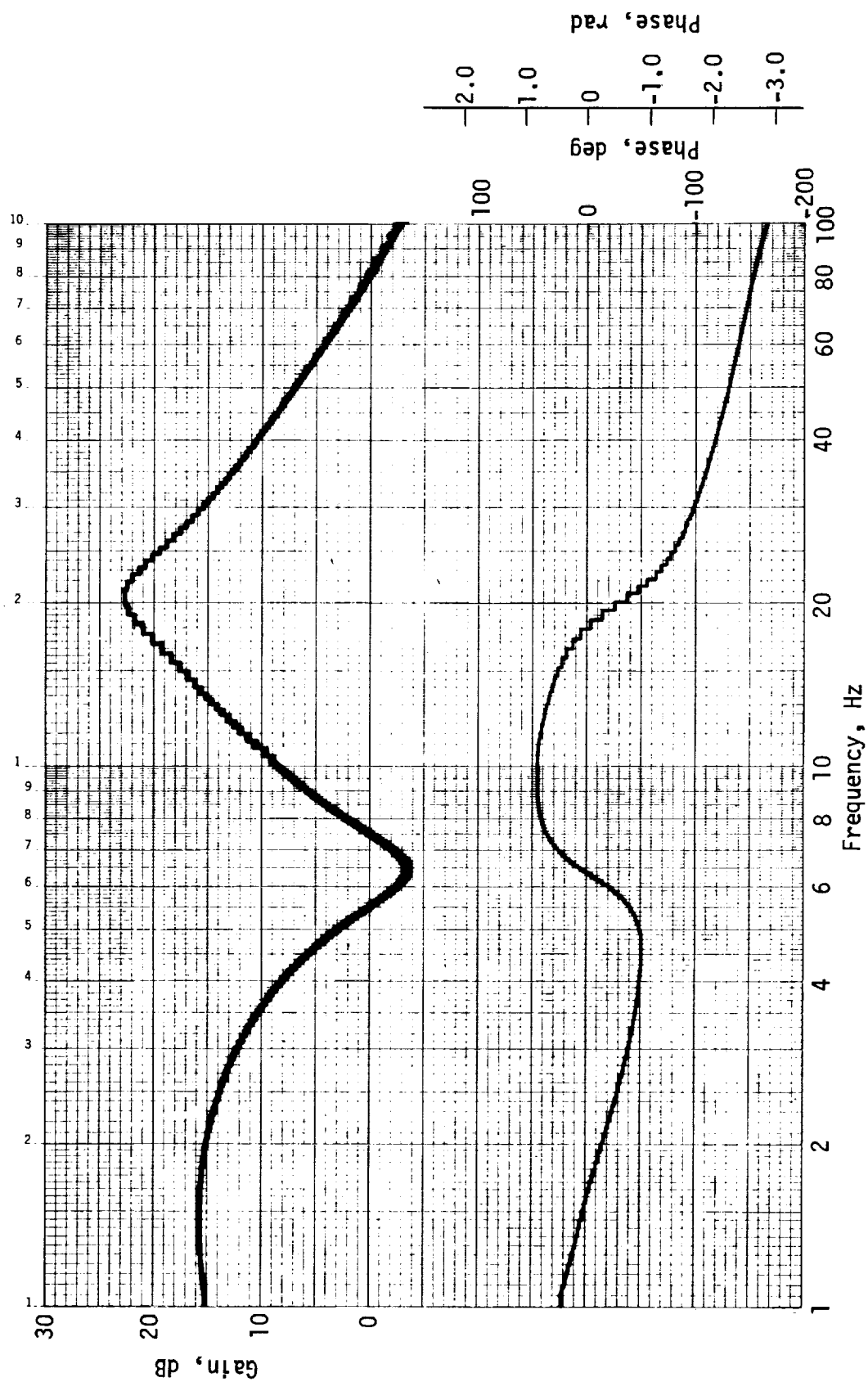


FIGURE 6-12 - FREQUENCY RESPONSE OF ANTISYMMETRIC FLUTTER SUPPRESSION SYSTEM WITH EACH CHANNEL FAILED



## 7.0 TEST SUPPORT AND RESULTS

This section describes the wind tunnel test of the FSS at NASA Langley Research Center. Support was provided for the initial setup and checkout and operation of the FSS during the wind tunnel test. Paragraph 7.1 describes the initial setup of the FSS prior to the test and the modifications made during preliminary testing in the wind tunnel. Results of the test are presented in Paragraph 7.2 and of the post-test analysis in Paragraph 7.3.

### 7.1 Flutter Suppression System Preparation and Model Modifications

Prior to the actual wind tunnel test the wind tunnel model and FSS hardware were integrated and tested. This allowed subsystem interfaces to be established, wiring to be completed and an end-to-end check to be performed. Included in the pretest activities was the programming of the analog computer and setup of the aileron actuation system. During preliminary testing several modifications were also identified which would provide a better correlation between analytical and actual model characteristics.

#### 7.1.1 Flutter suppression system preparation - Upon arrival at the test site, the FSS was complete with the exception of programming the analog computer and readying the aileron actuation system. The following functions were programmed on an EAI 580 analog computer:

- Aileron actuator compensation
- Accelerometer scaling and summing to form symmetric and anti-symmetric signals
- FSS pre- or post filtering
- Aileron command scaling and summing to form left and right commands
- Interface to aileron excitation generators (sweeps, steps) and data analyzers.

A patching diagram of the final configuration is provided in Appendix B.

The aileron actuation system is an electro-mechanical system made up of electric servo motors and position and rate transducers mechanically linked to the control surface (Reference 2). Position and rate feedback loops are closed through electronics located in the tunnel control room. The feedback gains were adjusted to give the desired command sensitivity and dynamics. The actuator compensation on the analog computer was then adjusted to cancel the actuator mode.

During initial integration of the model and the FSS it was found that the accelerometer outputs contained high frequency noise and had a strong DC drift with temperature. Since the input to a digital filter needs to be band-limited and centered in the input range of the A-to-D converter the alternate FSS was used during the wind tunnel test.

- 7.1.2 Model Modification - During preliminary wind tunnel testing two modifications were made to the model to produce closer correlation with the associated math models used during analysis. During initial setup the right aileron actuation system displayed considerably more inertia than the left. This caused large changes in actuator dynamics when the torque limit of the servo-motor was reached. During preliminary testing the wind tunnel turbulence produced large enough aileron commands to cause an instability. The aileron system was modified to reduce the inertia by re-routing and shortening the mechanical linkage between the servo-motor and the control surface. This resulted in an inertia roughly equivalent to the left aileron system. After this modification both acuation systems were tested and found to be capable of full deflections at the flutter frequency. The final actuator compensation was as follows:

$$C(s) = \frac{14348(s^2 + 200s + 95000)}{(s + 350)^2(s^2 + 1700s + 4.0 \times 10^6)} \quad \frac{\text{Rad}}{\text{Rad}}$$

As testing resumed it became apparent that flutter would occur at a higher dynamic pressure and model frequency than had been predicted by structural analysis. A comparison of GVT and analytical data (Table 7-I) showed that the analytical flutter pair was lower in frequency than the actual model. Because the mass properties of the model were well known, the torsional stiffness of the model was assumed to be the source of the problem. Since this could not be modified directly, the frequency was lowered to the analytical value by lowering the inboard flutter ballast 0.01524m (0.6 inches). This modification produced structural frequencies very close to analytical values but did not lower the flutter velocity.

TABLE 7-I  
COMPARISON OF GVT AND ANALYTICAL FREQUENCIES

Symmetric Mode	Frequency, Hz	
	GVT	Analysis
First Wing Bending	3.3	3.3
Second Wing Bending*	13.5	12.7
First Wing Torstion*	25.2	23.3

\*Flutter Pair

## 7.2 Test Results

The primary goal of the wind tunnel test was to demonstrate the capability of the FSS to suppress dual flutter modes (symmetric and antisymmetric) with violent, nearly-simultaneous onset, and, furthermore, that this system could be successfully implemented using digital computers as the feedback filters. A secondary goal was to investigate the characteristics of the redundant system under degraded system operation.

- 7.2.1 Flutter mode damping performance - The performance of the FSS in damping the flutter modes was evaluated initially by observing its effect just below flutter speed. This was done primarily to establish the open loop flutter speed and to gain confidence that the system was capable of stabilizing the flutter modes. Although the flutter dynamic pressure had been inaccurately predicted, 2873 N/m<sup>2</sup> (60 psf) instead of 3926 N/m<sup>2</sup> (82 psf), the FSS demonstrated good damping capability as shown on Figure 7-1. This strip-chart recording shows the response of the flutter mode building up with the FSS off and then becoming highly stable when it is turned on. This fact is also demonstrated on Figure 7-2 where the symmetric acceleration frequency response from an aileron sweep is shown. With the FSS off the response of the flutter mode at 19 Hz dominates the plot but is virtually eliminated when the system is turned on.

After verifying that the FSS was operating properly the dynamic pressure of the wind tunnel was increased to values above the flutter velocity. As speed was increased the flutter mode remained stable with some increase in control surface activity due to tunnel turbulence. At the structural limit of the model (4788 N/m<sup>2</sup> (100 psf)) the control surface activity was approximately 0.0873 rad (5 degrees) RMS with 0.1745 rad (10 degrees) peaks. Also, a mode at about 48 Hz was becoming increasingly active as the tunnel speed was increased. It appeared that this mode, probably either a structural mode excited by the actuator mode or the actuator mode itself, would have defined the system-on flutter boundary had the model's structural limit been higher. The maximum dynamic pressure tested was 4884 N/m<sup>2</sup> (102 psf) which represented an increase of 24 percent over the FSS off flutter dynamic pressure of 3926 N/m<sup>2</sup> (82 psf).

- 7.2.2 Degraded system performance - The performance of the system was evaluated while various degradations were introduced into the redundant portion of the FSS. Induced degradations included a single channel failure and gain reductions and phase changes in one channel while another was failed to maximum input level. The effects of these degradations on the output of the voter with sinusoidal inputs are illustrated in Table 7-II. The phase shift degradation was introduced by selecting the break frequency of a first-order lag in series with the FSS to give the desired phase change with unity gain at the flutter frequency ( $\approx 20$  Hz). The tests were conducted at 3831 N/m<sup>2</sup> (80 psf) where the model was stable but the effects of the FSS were obvious.

• Dynamic Pressure =  $3893 \text{ N/m}^2$  (81.3 psf)

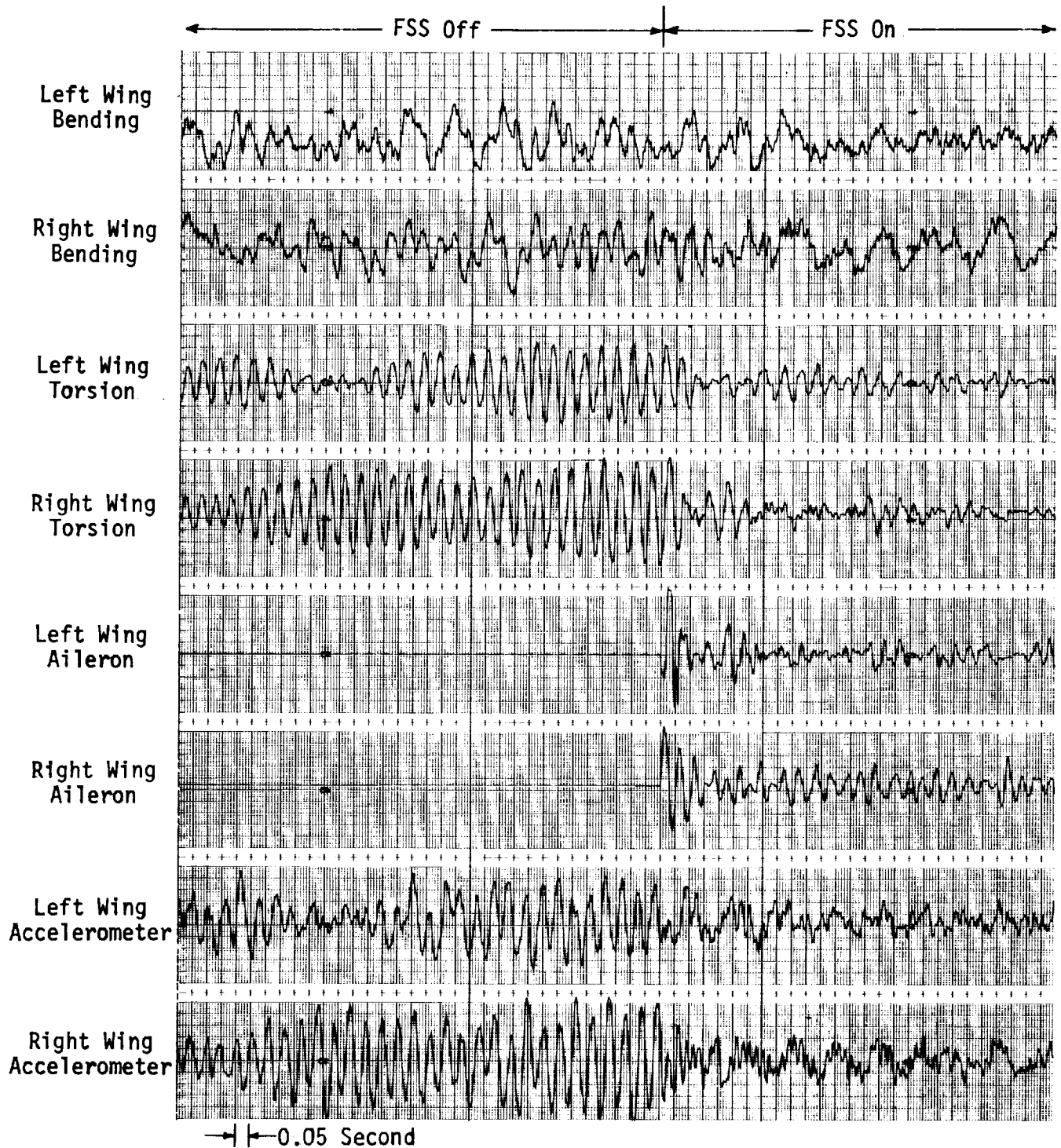


FIGURE 7-1 - MODEL RESPONSE WITH FLUTTER SUPPRESSION SYSTEM ON AND OFF

● Dynamic Pressure = 3831 N/m<sup>2</sup> (80 psf)

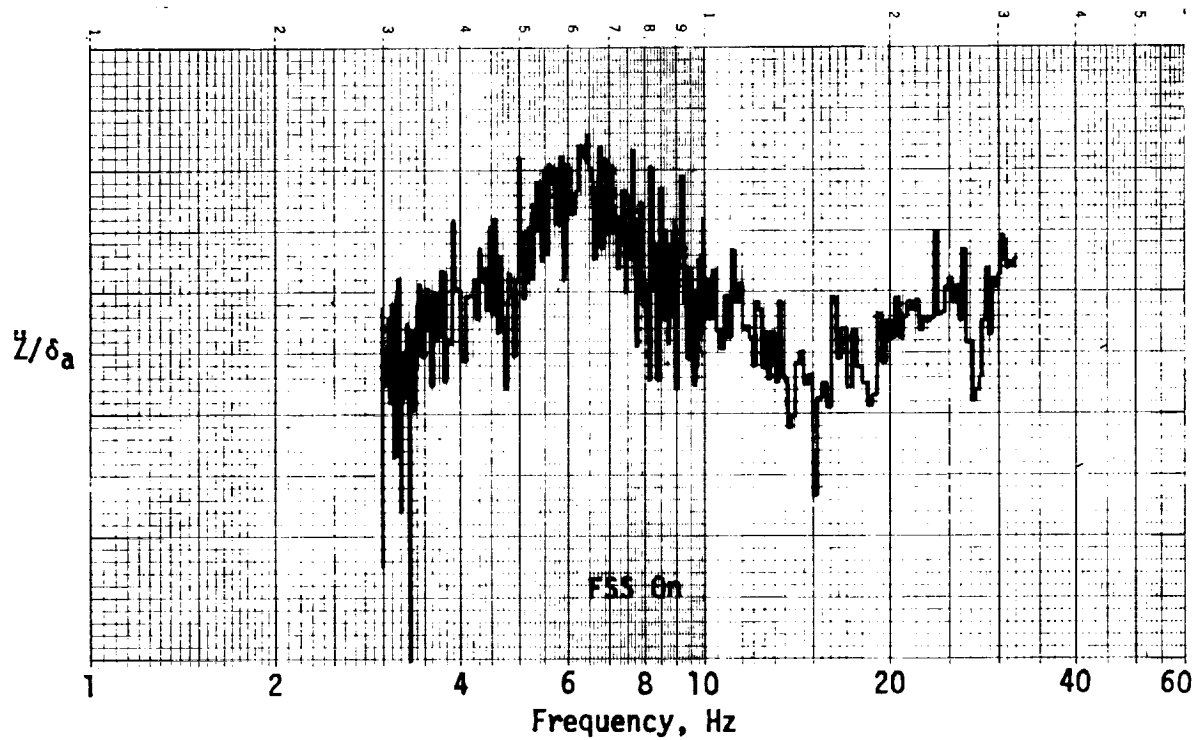
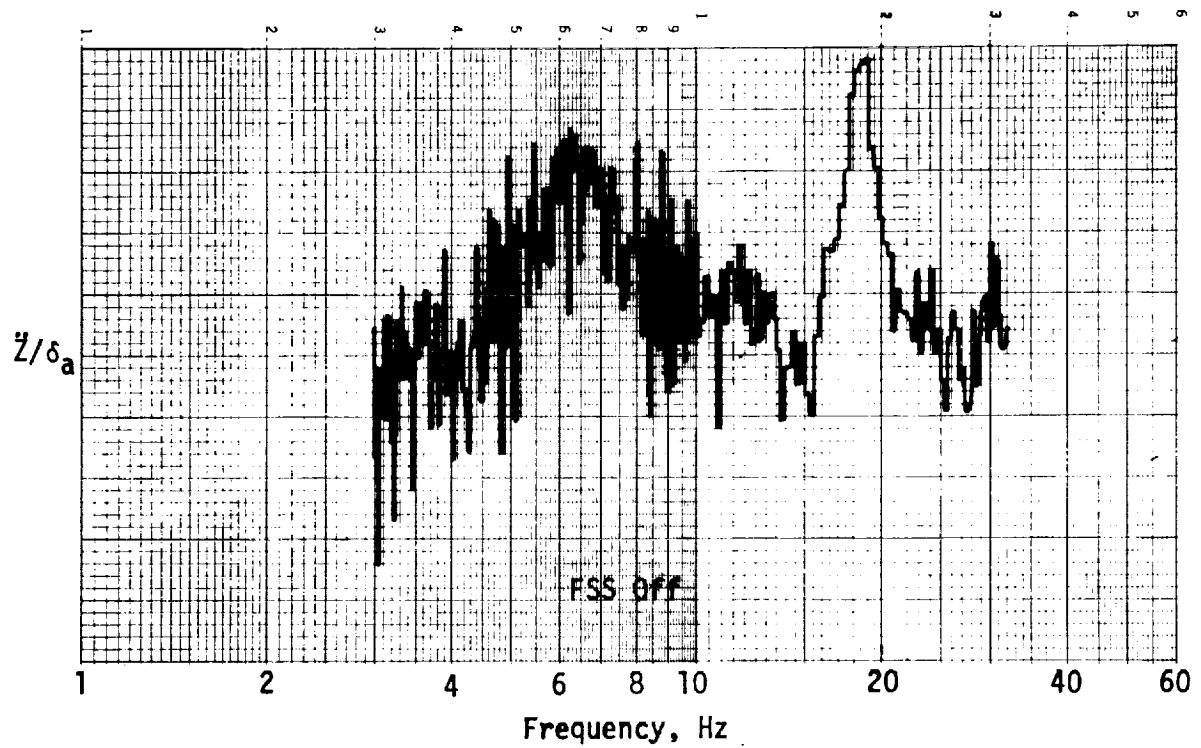
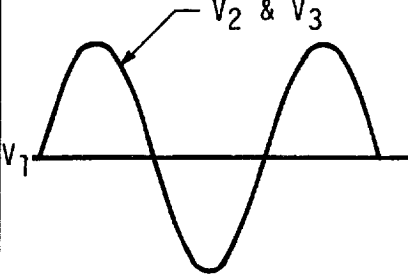
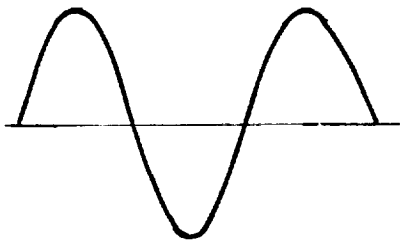
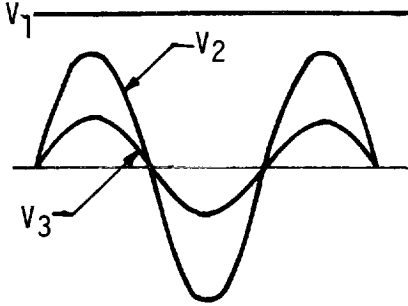
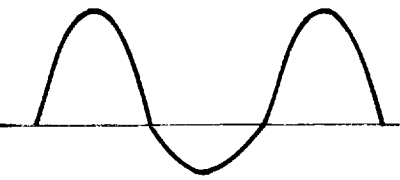
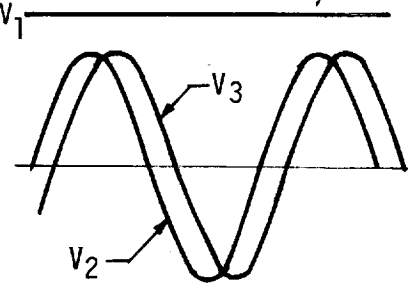
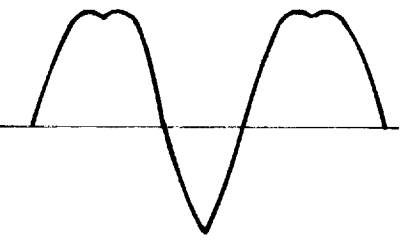


FIGURE 7-2 - ACCELERATION FREQUENCY RESPONSE WITH FLUTTER SUPPRESSION SYSTEM ON AND OFF

TABLE 7-II  
VOTER OUTPUTS WITH DEGRADED INPUTS

Failure	Input	Output
1. Failed (0) 2. Normal 3. Normal		
1. Failed (High) 2. Normal 3. Low Gain		
1. Failed (High) 2. Normal 3. Phase Shift		



Failing a single channel had no effect on the performance of the FSS as expected. The failed channel was tied to a high level (10 volts) and the gain on a second channel incrementally reduced. This had the effect of reducing the total FSS gain by half of the value of the single channel. That channel was then restored to full gain and a series of first-order lags with the appropriate gain inserted. This appeared to have the effect of changing the phase of the total FSS by half of this amount. These results indicated that first the FSS has fail-operate capability and that second, with one channel failed high, the FSS would be fairly insensitive to degradation in another channel.

### 7.3 Post Test Analysis

Analysis was conducted after the wind tunnel test to determine why the flutter speed was higher than predicted. The analytical performance of the improved math model was then compared to wind tunnel results.

7.3.1 Changes to structural model - As was noted earlier the difference in structural frequencies of the model and math model were probably due to a difference in torsional stiffness. Also the GVT data indicated that there was some flexibility in the sting mount, which had not been modeled. Two math models were developed to investigate the effects of, and sensitivity to, adding torsional stiffness and/or sting flexibility. The first model had only torsional stiffness added to give the same first torsion mode frequency. A second math model was developed that had some sting flexibility added and the torsional stiffness adjusted to math model frequencies.

7.3.2 Comparison with test results - The math model with torsional stiffness added had a flutter dynamic pressure of  $3735 \text{ N/m}^2$  (78 psf) only 3 percent low in velocity. The flutter characteristics were similar to the model as illustrated on Figure 7-3. This demonstrated the sensitivity of the model to torsional stiffness.

The second math model fluttered at about  $4788 \text{ N/m}^2$  (100 psf), well above the test results. Since the sting flexibility could only be guessed, the results were used as an indication of sensitivity to this parameter.

Using the math model with increased torsional stiffness, closed loop analysis was conducted to verify the performance of the FSS. As shown by the root locus on Figure 7-4, the flutter mode is driven very close to its zero when the FSS is turned on. This would tend to reduce its acceleration response to an aileron sweep dramatically, which was precisely what occurred in the actual test. The performance of the FSS in damping the flutter mode is illustrated on Figure 7-5. The system-on flutter speed is greater than  $4788 \text{ N/m}^2$  (100 psf) as was the case in the wind tunnel test.

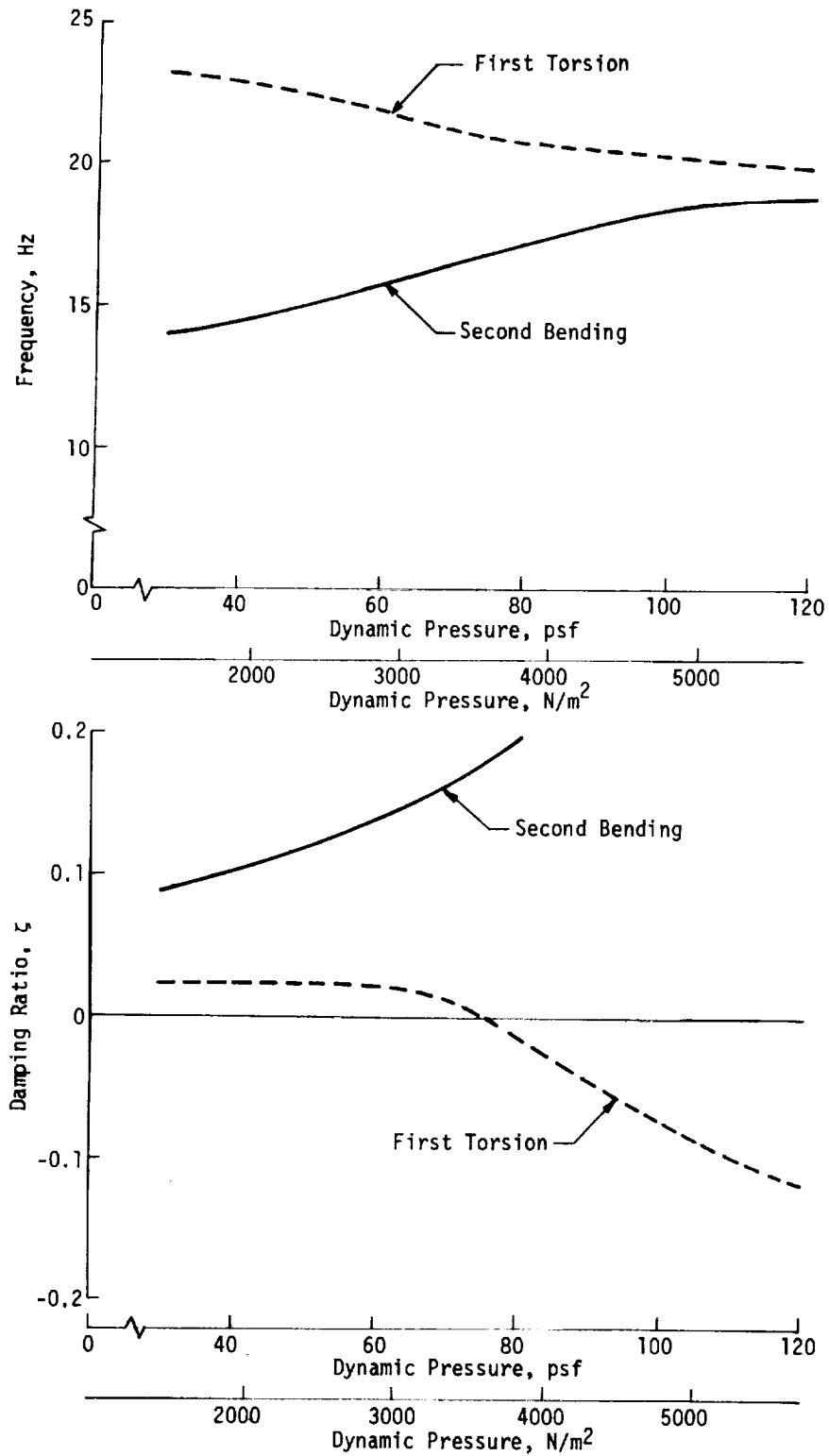


FIGURE 7-3 - SYMMETRIC FLUTTER CHARACTERISTICS - MODIFIED STIFFNESS

Actuator and FSS: Equations 5-1, 5-2 and 5-3

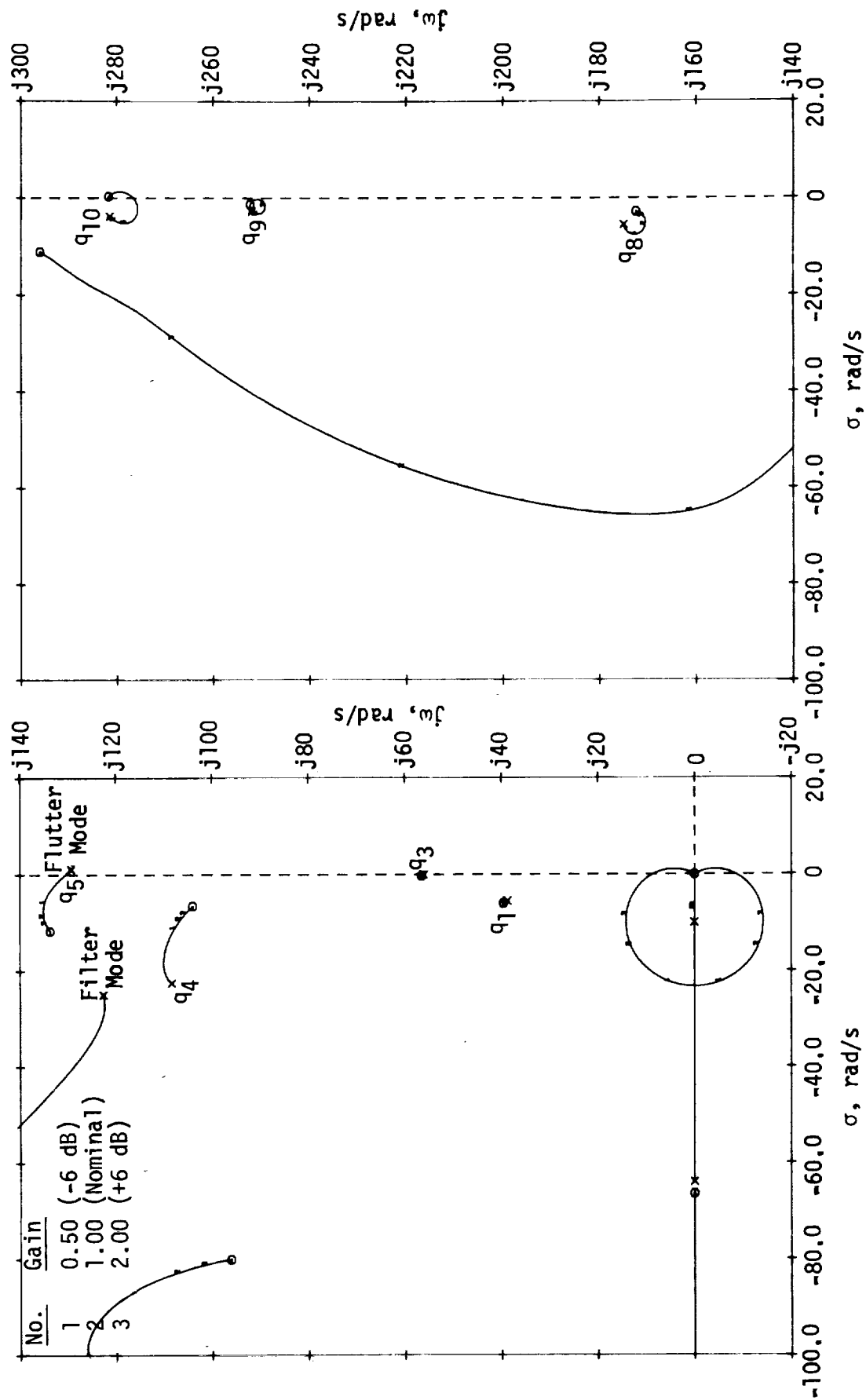


FIGURE 7-4 - ROOT LOCUS OF FLUTTER SUPPRESSION SYSTEM USING UPDATED EQUATIONS,  
DYNAMIC PRESSURE = 3831 N/m<sup>2</sup> (80 psf)

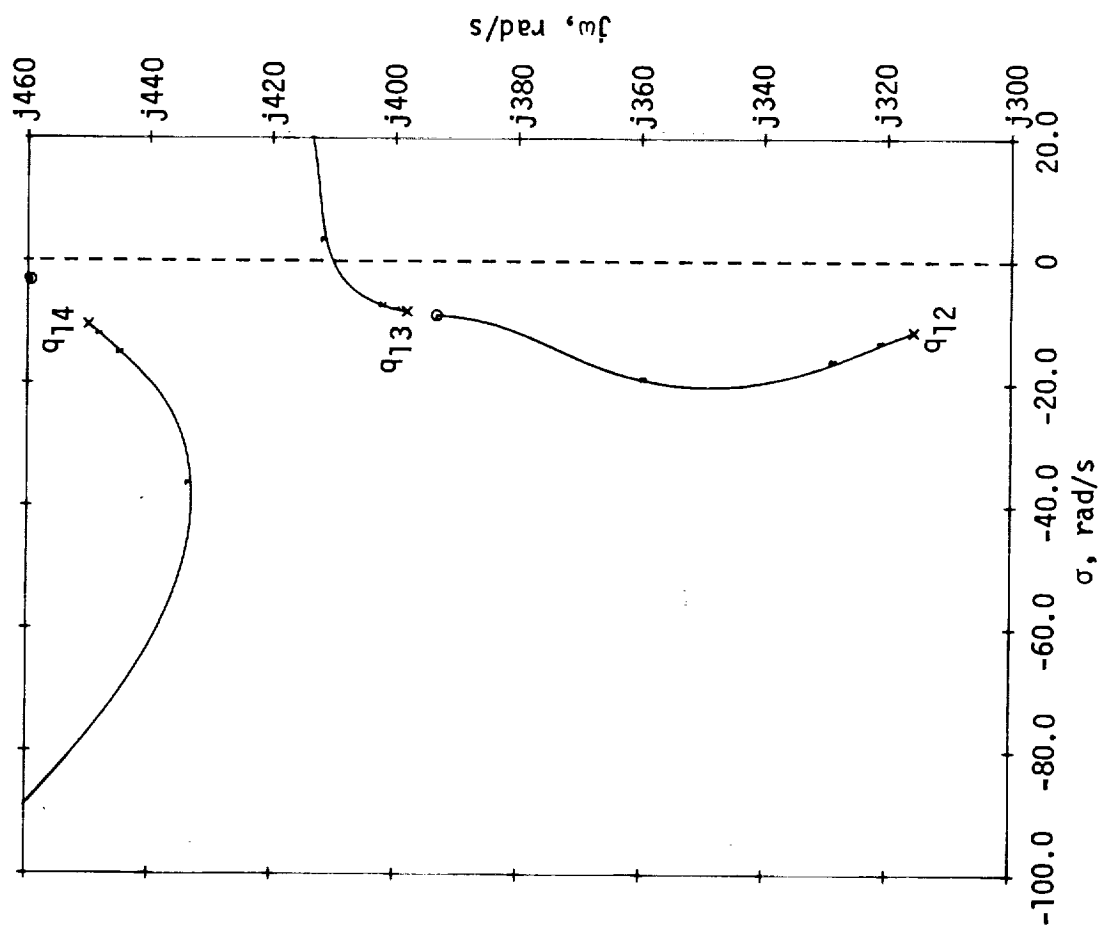


FIGURE 7-4 - ROOT LOCUS OF FLUTTER SUPPRESSION SYSTEM USING UPDATED EQUATIONS,  
DYNAMIC PRESSURE = 3831 N/m<sup>2</sup> (80 psf) (Concluded)

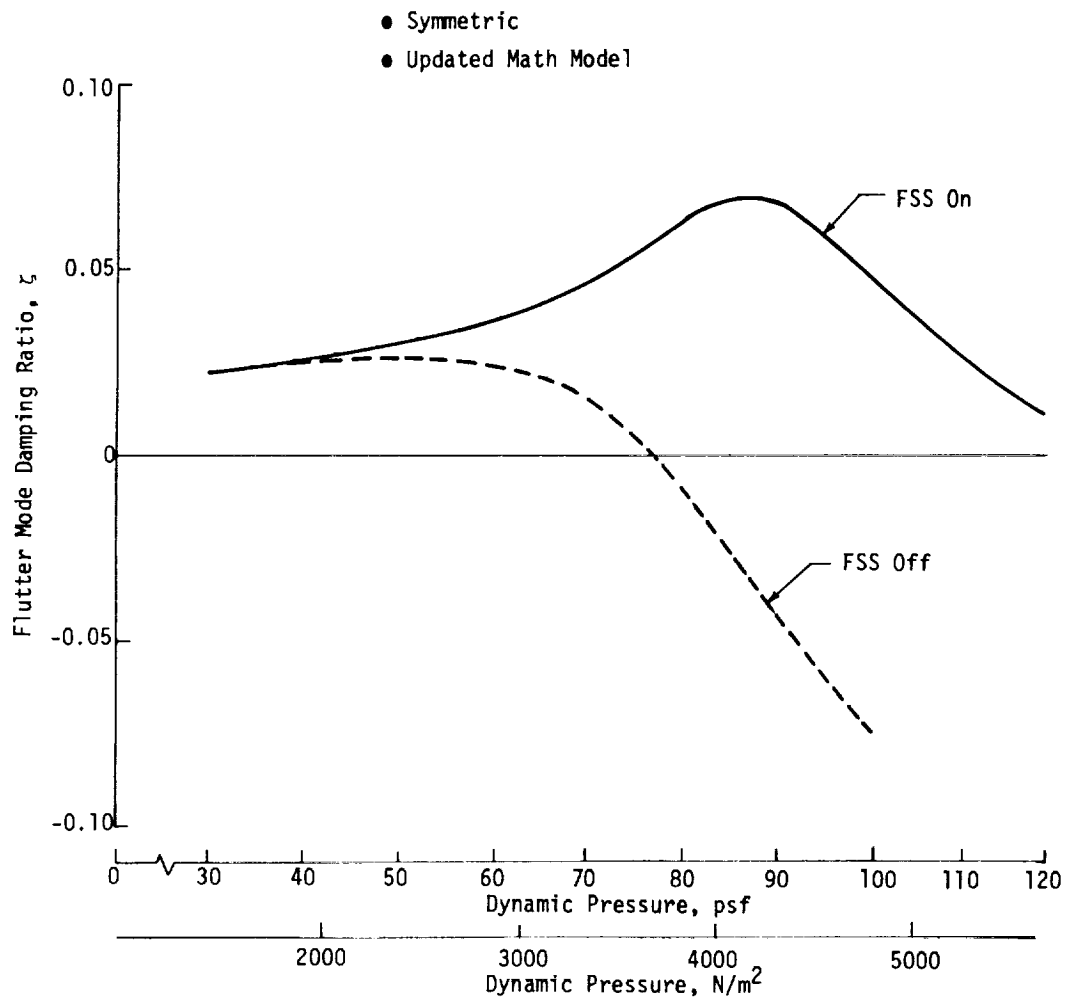


FIGURE 7-5 - FLUTTER SUPPRESSION SYSTEM SYSTEM FLUTTER MODE DAMPING PERFORMANCE

In short, the structural analysis indicated that the math model was sensitive to both torsional stiffness and sting flexibility. The closed loop analysis showed several points of correlation to the actual test results.

## 8.0 CONCLUSIONS AND RECOMMENDATIONS

### 8.1 Conclusions

Major conclusions resulting from this study are listed below:

1. The FSS was successful in stabilizing symmetric and antisymmetric flutter modes which exhibited violent onset and identical flutter velocities even though the experimental flutter velocity was considerably different than predicted analytically. This can be attributed to the wide stability margins of the FSS. Post wind tunnel test analysis indicated that the flutter speed of the mathematical model was sensitive to wing torsional stiffness and sting flexibility. Improved flutter velocity predictions were obtained when measured wing torsional stiffness and sting flexibility were incorporated in the model.
2. Digital implementation of control system filters which were synthesized using classical techniques can be performed with good frequency response fidelity, especially when a prediction algorithm is used to reduce time delay effects.
3. A triple redundant configuration which utilizes a circular failure detection scheme produces a fail-operate system capable of detecting any single internal failure with indication to the operator.
4. Using the parallel expansion technique in implementing digital filters eliminates the need to adjust internal gains to prevent under or overflows and thus reduces the total time needed to implement the filter.

### 8.2 Recommendations

The recommendations listed below are offered to suggest areas of future research and to ensure the success of these projects.

1. When testing flutter suppression systems every attempt should be made to attain an accurate mathematical model, particularly in regard to wing stiffness and sting flexibility.
2. Stability margins on future control systems should be as wide as possible in order to produce systems that are insensitive to variations in mathematical models.
3. The performance and flexibility of this system indicate that other ACT (Active Controls Technology) concepts such as gust and maneuver load alleviation and relaxed static stability could be synthesized using classical control techniques and implemented using digital computers.

4. As the technology advances, discrete time and advance control concepts (Z-transform, optimal control) should be used in the synthesis of control systems as well as in their implementation.



## 9.0

## REFERENCES

1. Williams, Edward H.: Design Control Specification for a One-Thirtieth Scale B-52E Flexible Model. Boeing Document D3-7387-1, June 15, 1967.
2. Severt, Frank D.: Analysis of Aeroelastic Model Stability Augmentation Systems. Document D3-8390-4, Boeing Company, March 1971. (Available as NASA CR-132354).
3. Severt, Francis D.; and Patel, Suresh M.: Analysis and Testing of Aeroelastic Model Stability Augmentation Systems--Final Report. Document D3-9245, Boeing Company, October 1973. (Available as NASA CR-132345).
4. Redd, L.T.; Gilman, J., Jr.; Cooley, D.E.; and Severt, F.D.: Wind-Tunnel Investigation of a B-52 Model Flutter Suppression System. J. Aircraft, Volume 11, No. 11, November 1974, pp. 659-663.
5. Thompson, G.O.; and Severt, F.D.: Wind Tunnel Investigation of Control Configured Vehicle Systems. Flutter Suppression and Structural Load Alleviation, AGARD CP-175, April 1975, pp. 4-1 - 4-8.

# APPENDIX A

## FLUTTER SUPPRESSION SYSTEM PERFORMANCE

This appendix contains additional performance data for the FSS using the original equations of motion. Modal damping and frequencies with the FSS on and off appear in Tables A-I to A-VI.

TABLE A-I  
MODAL DAMPING AND FREQUENCIES

- Symmetric
- Dynamic Pressure = 0 N/m<sup>2</sup> (0 psf)

Mode Number	FSS Off		FSS On	
	Frequency, Hz	Damping Ratio, $\zeta$	Frequency, Hz	Damping Ratio, $\zeta$
1	3.34	.0050	3.34	.0049
2	6.94	.0075	6.94	.0075
3	9.22	.0050	9.22	.0050
4	12.70	.0049	12.70	.0049
5	23.35	.0050	23.35	.0051
6	25.38	.0075	25.38	.0075
7	27.69	.0075	27.69	.0075
8	28.34	.0050	28.34	.0050
9	41.14	.0050	41.14	.0050
10	45.84	.0050	45.84	.0050
11	46.74	.0075	46.74	.0075
12	50.93	.0050	50.89	.0049
13	64.96	.0050	64.92	.0051
14	72.85	.0050	72.85	.0050
15	79.85	.0050	79.89	.0048
16	85.14	.0075	85.14	.0075
17	100.05	.0050	100.15	.0042
18	106.3	.0075	106.3	.0075
Filter	----	----	19.90	.2000

TABLE A-II  
MODAL DAMPING AND FREQUENCIES

- Symmetric
- Dynamic Pressure =  $1436 \text{ N/m}^2$  (30 psf)

Mode Number	FSS Off		FSS On	
	Frequency, Hz	Damping Ratio, $\zeta$	Frequency, Hz	Damping Ratio, $\zeta$
1	4.56	.126	4.49	.285
2	7.70	.0904	7.70	.0904
3	9.18	.0053	9.19	.0055
4	14.18	.0935	14.83	.0907
5	22.18	.0200	22.18	.0194
6	25.43	.0124	25.43	.0124
7	27.62	.0077	27.62	.0077
8	28.25	.0261	28.10	.0323
9	41.04	.0075	41.02	.0076
10	45.64	.0129	45.56	.0129
11	46.48	.0063	46.48	.0063
12	51.22	.0238	51.74	.0288
13	64.82	.0131	65.04	.0139
14	72.83	.0134	72.62	.0152
15	79.86	.0061	79.59	.0054
16	85.06	.0075	85.06	.0075
17	99.97	.0103	99.51	.0089
18	106.3	.0075	106.3	.0075
Filter	----	----	23.39	.338

TABLE A-III  
MODAL DAMPING AND FREQUENCIES

- Symmetric
- Dynamic Pressure =  $2873 \text{ N/m}^2$  (60 psf)

Mode Number	FSS Off		FSS On	
	Frequency, Hz	Damping Ratio, $\zeta$	Frequency, Hz	Damping Ratio, $\zeta$
1	5.61	.140	5.82	.207
2	8.37	.117	8.36	.117
3	9.13	.0044	9.14	.0058
4	16.29	.163	16.55	.103
5	20.27	.0015	20.74	.0301
6	25.48	.0151	25.48	.0151
7	27.55	.0077	27.55	.0077
8	28.12	.0329	27.51	.0435
9	40.90	.0087	40.83	.0096
10	45.38	.0153	45.20	.0168
11	46.14	.0057	46.14	.0058
12	51.49	.0326	52.82	.0422
13	64.65	.0171	65.21	.0164
14	72.77	.0175	72.19	.0233
15	79.87	.0066	79.28	.0065
16	84.98	.0073	84.98	.0073
17	99.85	.0126	98.93	.0123
18	106.3	.0076	106.3	.0076
Filter	----	----	32.91	.326

TABLE A-IV  
MODAL DAMPING AND FREQUENCIES

- Antisymmetric
- Dynamic Pressure =  $0 \text{ N/m}^2$  (0 psf)

Mode Number	FSS Off		FSS On	
	Frequency, Hz	Damping Ratio, $\zeta$	Frequency, Hz	Damping Ratio, $\zeta$
1	3.34	.0050	3.34	.0049
2	5.30	.0075	5.30	.0075
3	9.22	.0050	9.22	.0050
4	12.70	.0049	12.70	.0059
5	15.94	.0075	15.94	.0074
6	21.21	.0075	21.21	.0074
7	22.39	.0075	22.39	.0075
8	23.34	.0050	23.34	.0051
9	28.34	.0050	28.34	.0050
10	32.17	.0075	32.17	.0075
11	41.13	.0050	41.13	.0050
12	45.84	.0050	45.84	.0050
13	50.93	.0050	50.89	.0049
14	58.84	.0075	58.84	.0075
15	59.97	.0075	59.97	.0075
16	64.95	.0050	64.92	.0051
17	72.86	.0050	72.85	.0050
18	77.11	.0075	77.11	.0075
Filter	---	---	19.88	.198

TABLE A-V  
MODAL DAMPING AND FREQUENCIES

- Antisymmetric
- Dynamic Pressure =  $1436 \text{ N/m}^2$  (30 psf)

Mode Number	FSS Off		FSS On	
	Frequency, Hz	Damping Ratio, $\zeta$	Frequency, Hz	Damping Ratio, $\zeta$
1	4.49	.132	4.38	.298
2	6.05	.0827	6.05	.0827
3	9.18	.0051	9.19	.0054
4	14.17	.0926	14.84	.0885
5	16.33	.0583	16.33	.0583
6	20.77	.0495	20.77	.0495
7	22.17	.0194	22.18	.0188
8	22.23	.0075	22.23	.0075
9	28.25	.0257	28.12	.0321
10	32.13	.0116	32.13	.0116
11	41.04	.0074	41.01	.0076
12	45.64	.0127	45.56	.0128
13	51.22	.0237	51.62	.0284
14	58.88	.0098	58.88	.0098
15	59.98	.0081	59.98	.0081
16	64.83	.0129	65.05	.0135
17	72.84	.0132	72.65	.0152
18	77.10	.0074	77.10	.0074
Filter	---	---	23.39	.334

TABLE A-VI  
MODAL DAMPING AND FREQUENCIES

- Antisymmetric
- Dynamic Pressure = 2873 N/m<sup>2</sup> (60 psf)

Mode Number	FSS Off		FSS On	
	Frequency, Hz	Damping Ratio, $\zeta$	Frequency, Hz	Damping Ratio, $\zeta$
1	5.48	.149	5.76	.230
2	6.72	.0995	6.72	.0995
3	9.13	.0041	9.14	.0055
4	16.25	.161	16.54	.0963
5	16.85	.0860	16.85	.0862
6	20.15	.0629	20.15	.0627
7	20.26	-.0004	20.78	.0296
8	22.07	.0076	22.07	.0076
9	28.13	.0319	27.56	.0449
10	32.06	.0135	32.06	.0135
11	40.90	.0086	40.82	.0096
12	45.38	.0151	45.19	.0167
13	51.49	.0325	52.70	.0405
14	58.90	.0109	58.90	.0109
15	59.98	.0084	59.98	.0084
16	64.68	.0167	65.19	.0159
17	72.77	.0171	72.29	.0228
18	77.06	.0075	77.06	.0075
Filter	---	---	32.33	.316

## APPENDIX B

### FLUTTER SUPPRESSION SYSTEM IMPLEMENTATION

This appendix contains data pertaining to the implementation of the redundant, digital FSS for the B-52E aeroelastic wing tunnel model.

Detailed circuit diagrams of the analog voter and the analog voter DC power supplies are given on Figures B-1 and B-2.

Listings of the software implementing the full FSS filter and failure detection and timing logic are presented on pages B-4 through B-19. A listing of the program designed to isolate failed components in the FSS is given on pages B-20 through B-22.

An alphabetic list of assembly language instructions for the HP2100 mini-computer is given on pages B-23 through B-25.

The final analog computer patching diagram is presented on Figure B-3.



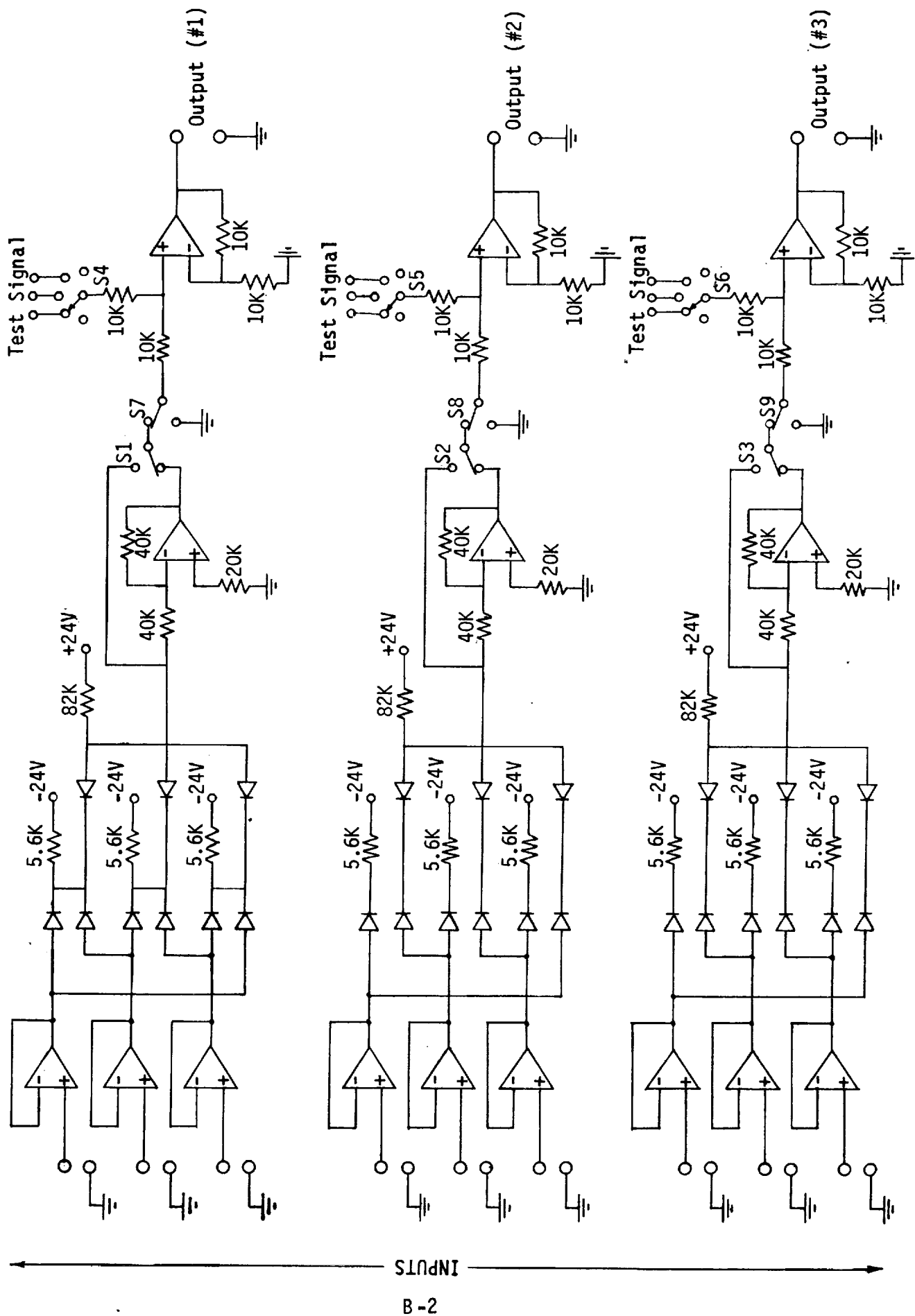


FIGURE B-1 - ANALOG VOTER CIRCUIT DIAGRAM

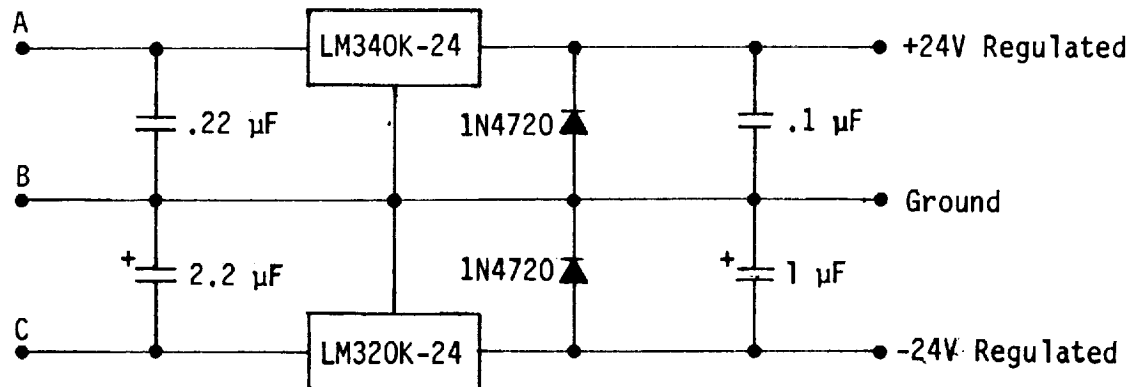
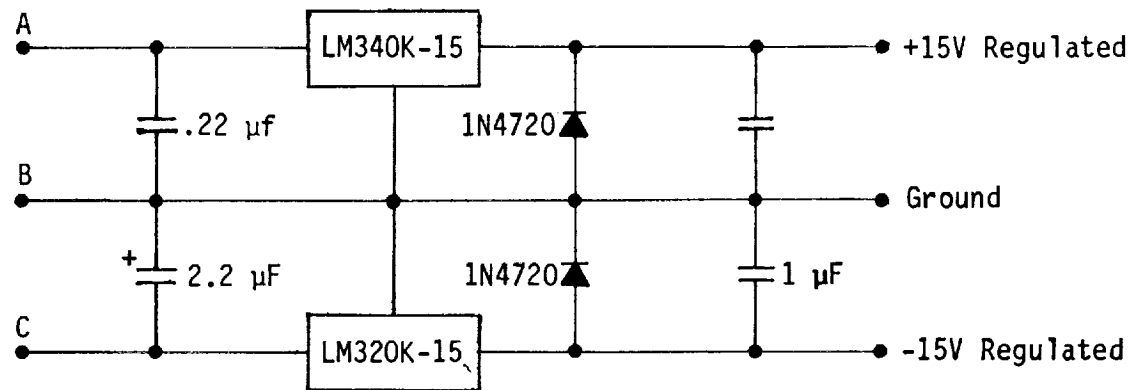
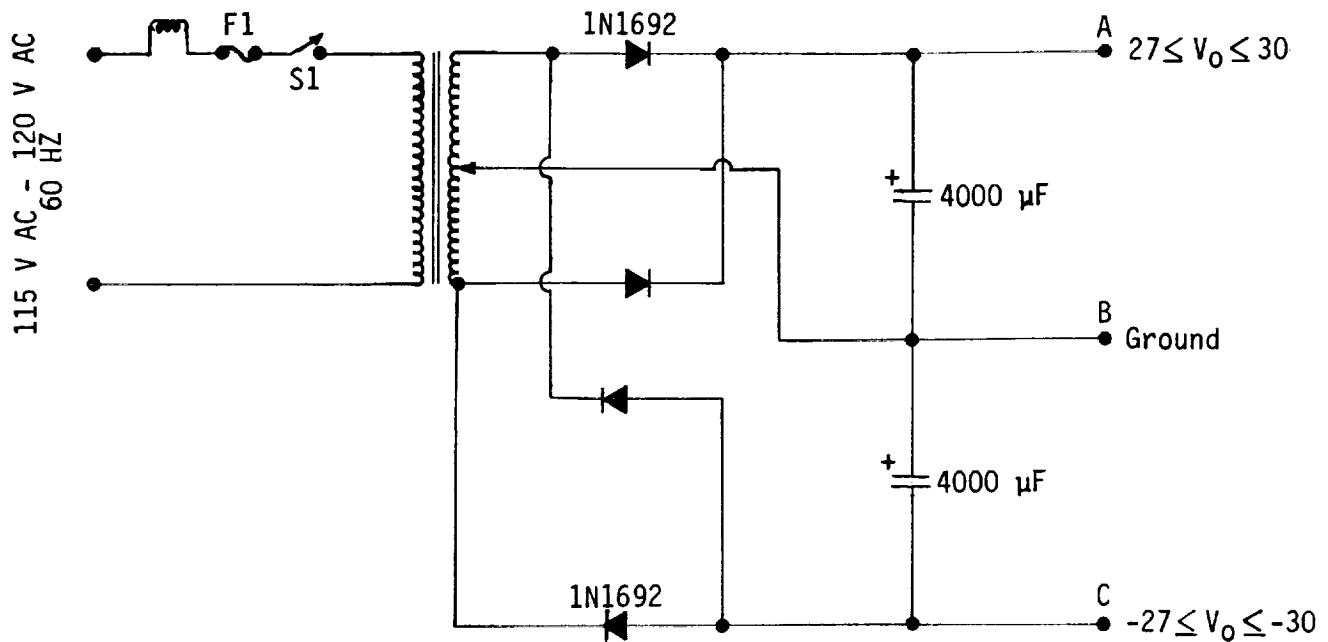


FIGURE B-2 - ANALOG VOTER POUR SUPPLIES CIRCUIT DIAGRAM

# FLUTTER SUPPRESSION SYSTEM COMPUTER PROGRAM

```

0001          ASMB,A,B,T,L
0002*THIS PROGRAM IS FOR DIGITAL FLUTTER SUPPRESSION SYS FOR B-52 MODEL
0003*FILE NAME IS " JFIL8 " CREATED BY JR MATTHEW 8/03/78
0004*BILINEAR TRANSFORMATION METHOD IS USED TO IMPLEMENT THIS FILTER
0005*HP 5610A A TO D CONVRTR AND HP 6940A MULTIPROG.ARE FOR USED FOR DATA IO
0006* SAMPLING PERIOD =.002 MILLISECONDS
0007*****
0008* INITIALIZE THE HP I/O DEVICES
0009*
0010 00100          ORG 1008
0011 00100 002400    CLA
0012 00101 070012    STA 128          INITIALIZE MEM LOC 128 TO ZERO(NOP)
0013 00102 070011    STA 118          INITIALIZE MEM LOC 118
0014 00103 061165    LDA INIT        LOAD INT REG'A' CONTROL WORD 170140B
0015 00104 102612    OTA 128
0016 00105 103712    STC 128,C
0017*****
0018*INITIALIZE TIME BASE GENERATOR TO 1.0 MILLISEC CLOCK PULSES
0019*
0020 00106 102100    STF 0
0021 00107 061170    LDA CW
0022 00110 102610    OTA 108
0023 00111 061173    LDA IJSH
0024 00112 070010    STA 108
0025 00113 061075    LDA CNT
0026 00114 070020    STA 208
0027*****
0028 00115 015066    START JSH RCNTR PROGRAM LOOP START AT THIS POINT
0029*
0030*****
0031* S REGISTER FLASH ROUTINE
0032*
0033* FLASHES AT 2HZ
0034*
0035 00116 000000    NOP
0036 00117 002400    CLA
0037 00120 065303    LDR AFF          'B'= A CHANNEL FINISHED FLAG
0038 00121 006020    SSB              FINISHED=-1,NOT FINISHED=0
0039 00122 024125    JMP ++3
0040 00123 035310    ISZ ERCNT
0041 00124 031312    IOR AFFER        SET BIT 2 IN FLASH WORD
0042 00125 000000    NOP
0043 00126 065304    LDB BFF          'B'= R CHANNEL FINISHED FLAG
0044 00127 006020    SSB              FINISHED=-1,NOT FINISHED=0
0045 00130 024133    JMP ++3
0046 00131 035310    ISZ ERCNT
0047 00132 031313    IOR BFFER        SET BIT 5 IN FLASH WORD
0048 00133 000000    NOP
0049 00134 065306    LDB ACF          'B'= A CHANNEL COMPARISON FLAG
0050 00135 006020    SSB              NO ERROR=-1,ERROR=0
0051 00136 024141    JMP ++3
0052 00137 035310    ISZ ERCNT
0053 00140 031314    IOR ACFER        SET BIT 8 IN FLASH WORD
0054 00141 000000    NOP
0055 00142 065307    LDB BCF          'B'= B CHANNEL COMPARISON FLAG
0056 00143 006020    SSB              NO ERROR=-1,ERROR=0

```

# FLUTTER SUPPRESSION SYSTEM COMPUTER PROGRAM (CONTINUED)

```

0057 00144 024147 JMP **3
0058 00145 035310 ISZ ERCNT
0059 00146 031315 IOR BCFER SET BIT 11 IN FLASH WORD
0060 00147 000000 NOP
0061 00150 065305 LOB CFF 'B'= COMPARISON FINISHED FLAG
0062 00151 006020 SSB FINISHED=-1, NOT FINISHED=0
0063 00152 024155 JMP **3
0064 00153 035310 ISZ ERCNT
0065 00154 031316 IOR CFFER SET BIT 14 IN FLASH WORD
0066 00155 000000 NOP
0067*
0068* CHECK FOR ERRORS AND DO FLASH OUTPUT
0069*
0070 00156 035311 ISZ ERCLK INCREMENT ERROR CLOCK SKIP IF = 0
0071 00157 024176 JMP CLEAR NOT TO CHECK FOR ERRORS
0072 00160 000000 NOP TIME TO CHECK FOR ERRORS
0073 00161 065310 LOB ERCNT 'B'= NUMBER OF ERRORS/SAMPLE PERIOD
0074 00162 006003 SZB, RSS ANY ERRORS?????
0075 00163 024170 JMP GOOD NO
0076 00164 106501 LIR 1B YES-GET FLASH WORD FROM S REGISTER
0077 00165 006021 SSB, RSS WAS FLASH WORD COMPLEMENTED LAST TIME
0078 00166 003000 CMA NO-COMPLEMENT FLASH WORD
0079 00167 024171 JMP FLASH YES-GO TO OUTPUT ROUTINE
0080 00170 002400 GOOD CLA CLEAR FLASH WORD
0081 00171 102601 FLASH OTA 1B PUT FLASH WORD INTO S REGISTER
0082 00172 065317 LOB FLCNT 'B'= -#CYCLES/FLASH
0083 00173 075311 STB ERCLK RESET ERROR CLOCK
0084 00174 006400 CLB
0085 00175 075310 STB ERCNT SET ERROR COUNT TO ZERO
0086 00176 006400 CLEAR CLB
0087 00177 075303 STB AFF CLEAR A CHANNEL FINISHED FLAG
0088 00200 075304 STB BFF CLEAR B CHANNEL FINISHED FLAG
0089 00201 075306 STB ACF CLEAR A CHANNEL COMPARISON FLAG
0090 00202 075307 STB BCF CLEAR B CHANNEL COMPARISON FLAG
0091 00203 075305 STB CFF CLEAR CHANNEL COMPARISON FLAG
0092 00204 000000 NOP
0093*****
0094*CHANNEL A FSS LOOP
0095*****
0096*READ INPUT FROM CH 0, INPU PORT 11B
0097*
0098 00205 061157 LDA CHA SELECT CHANNEL 0 OF A/D DEVICE (I/O PORT 11B)
0099 00206 102611 OTA 11B OUTPUT 'A' REG TO I/O PORT 11B
0100 00207 103711 STC 11B,C DEVICE COMMAND TO I/O 11B
0101 00210 102311 SFS 11B
0102 00211 024210 JMP **1
0103 00212 102511 LIA 11B READ I/O BUFFER CONTENT IN 'A' REG
0104 00213 011166 AND MASK ZERO OUT/ CH.ID ON BITS 0 THRU 5
0105 00214 071145 STA INPTA
0106*****
0107*CHANNEL A FSS FILTER IMPLEMENTATION
0108*****
0109* STAGE A11 LAG (10/(S+10))
0110*
0111 00215 000000 NOP
0112 00216 061126 LDA Y1A11 Y1A11 IN 'A'=Y(N-1)T;

```

# FLUTTER SUPPRESSION SYSTEM COMPUTER PROGRAM (CONTINUED)

```

0113 00217 100200 MPY K1A11      'B'=Y(N-1)T*K1A11(2**-1)
      00220 001204
0114 00221 100021 ASL 1          'B'=Y(N-1)*K1A11
0115 00222 045127 ADB KXA11      'B'= Y(N-1)*K1A11+X(N-1)T*K2A11
0116 00223 075144 STB TEMP
0117 00224 061145 LDA INPTA      'A'=X(NT),,, 'INPTA'
0118 00225 100200 MPY K2A11      'B'=X(NT)*K2A11(2**-1)
      00226 001205
0119 00227 100021 ASL 1          'B'=X(NT)*K2A11
0120 00230 075127 STB KXA11      KXA11=X(N-1)T*K2A11 FOR NEXT ITERATION
0121 00231 045144 ADB TEMP      'B'=(X(NT)+X(N-1)T)*K2A11 + Y(N-1)T*K1A11
0122 00232 075126 STB Y1A11     Y1A11=Y(NT),, OUTPUT OF THIS STAGE
0123 00233 000000 NOP
0124*****
0125* STAGE A12 LAG (10/(S+10))
0126*
0127 00234 000000 NOP
0128 00235 061130 LDA Y1A12      Y1A12 IN 'A'=Y(N-1)T;;
0129 00236 100200 MPY K1A12      'B'=Y(N-1)T*K1A12(2**-1)
      00237 001206
0130 00240 100021 ASL 1          'B'=Y(N-1)*K1A12
0131 00241 045131 ADB KXA12      'B'= Y(N-1)*K1A12+X(N-1)T*K2A12
0132 00242 075144 STB TEMP
0133 00243 061126 LDA Y1A11      'A'=X(NT)=OUTPUT FROM STAGE A11
0134 00244 100200 MPY K2A12      'B'=X(NT)*K2A12(2**-1)
      00245 001207
0135 00246 100021 ASL 1          'B'=X(NT)*K2A12
0136 00247 075131 STB KXA12      KXA12=X(N-1)T*K2A12 FOR NEXT ITERATION
0137 00250 045144 ADB TEMP      'B'=(X(NT)+X(N-1)T)*K2A12 + Y(N-1)T*K1A12
0138 00251 075130 STB Y1A12     Y1A12=Y(NT),, OUTPUT OF THIS STAGE
0139 00252 000000 NOP
0140*****
0141* STAGE A21 LAG 150/(S+150)
0142*
0143 00253 061132 LDA Y1A21      'A'=Y(N-1)
0144 00254 100200 MPY K1A21      'B'=Y(N-1)*K1A21(2**-1)
      00255 001210
0145 00256 100021 ASL 1          'B'=Y(N-1)*K1A21
0146 00257 045133 ADB KXA21      'B'=Y(N-1)*K1A21+X(N-1)*K2A21
0147 00260 075144 STB TEMP
0148 00261 061145 LDA INPTA      'A'= X(NT),,,FSS CHANNEL A INPUT
0149 00262 100200 MPY K2A21      'B'=X(NT)*K2A21(2**-1)
      00263 001211
0150 00264 100021 ASL 1          'B' X(NT)*K2A21
0151 00265 075133 STB KXA21      KXA21=X(N-1)*K2A21 FOR NEXT ITERATION
0152 00266 045144 ADB TEMP      'B'=(X(NT)+X(N-1)T)*K2A21 + Y(N-1)T*K1A21
0153 00267 075132 STB Y1A21     Y1A21=Y(NT),, OUTPUT OF THIS STAGE
0154 00270 000000 NOP
0155*****
0156* STAGE A22 LAG 150/(S+150)
0157*
0158 00271 061134 LDA Y1A22      'A'=Y(N-1)
0159 00272 100200 MPY K1A22      'B'=Y(N-1)*K1A22(2**-1)
      00273 001212
0160 00274 100021 ASL 1          'B'=Y(N-1)*K1A22
0161 00275 045135 ADB KXA22      'B'=Y(N-1)*K1A22+X(N-1)*K2A22

```

# FLUTTER SUPPRESSION SYSTEM COMPUTER PROGRAM (CONTINUED)

```

0162 00276 075144 STB TEMP
0163 00277 061132 LDA Y1A21
0164 00300 100200 MPY K2A22
00301 001213
0165 00302 100021 ASL 1
0166 00303 075135 STB KXA22
0167 00304 045144 ADB TEMP
0168 00305 075134 STB Y1A22
0169 00306 000000 NOP
0170*****
0171* STAGE A23 LAG 150/(S+150)
0172*
0173 00307 061136 LDA Y1A23
0174 00310 100200 MPY K1A23
00311 001214
0175 00312 100021 ASL 1
0176 00313 045137 ADB KXA23
0177 00314 075144 STB TEMP
0178 00315 061134 LDA Y1A22
0179 00316 100200 MPY K2A23
00317 001215
0180 00320 100021 ASL 1
0181 00321 075137 STB KXA23
0182 00322 045144 ADB TEMP
0183 00323 075136 STB Y1A23
0184 00324 000000 NOP
0185*****
0186** STAGE A31 FIRST-ORDER/SECOND-ORDER
0187** 32.1325(S+56.811)/(S2+S0S+15625)
0188**
0189 00325 000000 NOP
0190 00326 061141 LDA Y2A31
0191 00327 100200 MPY K2A31
00330 001217
0192 00331 100021 ASL 1
0193 00332 075150 STB TEMP1
0194 00333 061140 LDA Y1A31
0195 00334 071141 STA Y2A31
0196 00335 100200 MPY K1A31
00336 001216
0197 00337 100021 ASL 1
0198 00340 075151 STB TEMP2
0199 00341 061143 LDA X3A31
0200 00342 100200 MPY K5A31
00343 001222
0201 00344 100021 ASL 1
0202 00345 075152 STB TEMP3
0203 00346 061142 LDA X2A31
0204 00347 071143 STA X3A31
0205 00350 100200 MPY K4A31
00351 001221
0206 00352 100021 ASL 1
0207 00353 075153 STB TEMP4
0208 00354 061145 LDA INPTA
0209 00355 001121 ARS,ARS
0210 00356 001100 ARS

'A' = X(NT) = OUTPUT FROM STAGE A21
'B' = X(NT) * K2A22 (2** - 1)

'B' = X(NT) * K2A22
KXA22 = X(N-1) * K2A22 FOR NEXT ITERATION
'B' = (X(NT) + X(N-1) * T) * K2A22 + Y(N-1) * T * K1A22
Y1A22 = Y(NT),, OUTPUT OF THIS STAGE

'A' = Y(N-1)
'B' = Y(N-1) * K1A23 (2** - 1)

'B' = Y(N-1) * K1A23
'B' = Y(N-1) * K1A23 + X(N-1) * K2A23

'A' = X(NT) = OUTPUT FROM STAGE A22
'B' = X(NT) * K2A23 (2** - 1)

'B' = X(NT) * K2A23
KXA23 = X(N-1) * K2A23 FOR NEXT ITERATION
'B' = (X(NT) + X(N-1) * T) * K2A23 + Y(N-1) * T * K1A23
Y1A23 = Y(NT),, OUTPUT OF THIS STAGE

'A' = Y(N-2)

'B' = Y(N-2) * K2A31

'A' = Y(N-1)
PUT Y(N-1) INTO Y(N-2) FOR NEXT IT
'B' = Y(N-1) * K1A31 (2** - 2)

'B' = Y(N-1) * K1A31 (2** - 1)

'A' = X(N-2)

'B' = X(N-2) * K5A31

'A' = X(N-1)
PUT X(N-1) INTO X(N-2) FOR NEXT IT

'B' = X(N-1) * K4A31

'A' = X(N),,, FSS CHANNEL A INPUT

'A' = X(N) / 8 PREVENT OVERFLOW AT 2

```

# FLUTTER SUPPRESSION SYSTEM COMPUTER PROGRAM (CONTINUED)

```

0211 00357 071142 STA X2A31          PUT X(N) INTO X(N-1) FOR NEXT ITER
0212 00360 100200 MPY K3A31
      00361 001220
0213 00362 100021 ASL 1              'B'=X(N)*K3A31
0214 00363 045152 ADB TEMP3          'B'=" + X(N-2)*K5A31
0215 00364 000000 NOP
0216 00365 045153 ADB TEMP4          'B'=" + X(N-1)*K4A31
0217 00366 000000 NOP
0218 00367 045150 ADB TEMP1          'B'=" + Y(N-2)*K2A31
0219 00370 000000 NOP
0220 00371 005100 BRS 1              'B'="(2**-1)
0221 00372 045151 ADB TEMP2          'B'=" + Y(N-1)*K1A31(2**-1)
0222 00373 000000 NOP
0223 00374 005000 BLS 1              'B'=Y(N)-----DON'T KNOW LAST
0224 00375 075140 STB Y1A31          Y1A31=Y(NT),,OUTPUT OF THIS STAGE
0225 00376 000000 NOP
0226*****
0227* SUMMATION OF FILTER OUTPUTS
0228*
0229 00377 061126 LDA Y1A11          'A'=OUTPUT FROM STAGE A11
0230 00400 100200 MPY KOA11
      00401 001224
0231 00402 100021 ASL 1              'B'= A11*KOA11
0232 00403 075150 STB TEMP1
0233 00404 061130 LDA Y1A12          'A'=OUTPUT FROM STAGE A12
0234 00405 100200 MPY KOA12
      00406 001223
0235 00407 100021 ASL 1              'B'= A12*KOA12
0236 00410 075151 STB TEMP2
0237 00411 061132 LDA Y1A21          'A'=OUTPUT FROM STAGE A21
0238 00412 100200 MPY KOA21
      00413 001227
0239 00414 100021 ASL 1              'B'= A21*KOA21
0240 00415 075152 STB TEMP3
0241 00416 061134 LDA Y1A22          'A'=OUTPUT FROM STAGE A22
0242 00417 100200 MPY KOA22
      00420 001226
0243 00421 100021 ASL 1              'B'= A22*KOA22
0244 00422 075153 STB TEMP4
0245 00423 061136 LDA Y1A23          'A'=OUTPUT FROM STAGE A23
0246 00424 100200 MPY KOA23
      00425 001225
0247 00426 100021 ASL 1              'B'= A23*KOA23
0248 00427 075154 STB TEMP5
0249 00430 061140 LDA Y1A31          'A'=OUTPUT FROM STAGE A31
0250 00431 100200 MPY KOA31
      00432 001230
0251 00433 100021 ASL 1              'B'= A31*KOA31
0252 00434 045154 ADB TEMP5          'B'=" +A23*KOA23
0253 00435 045153 ADB TEMP4          'B'=" +A22*KOA22
0254 00436 045152 ADB TEMP3          'B'=" +A21*KOA21
0255 00437 045151 ADB TEMP2          'B'=" +A12*KOA12
0256 00440 045150 ADB TEMP1          'B'=" +A11*KOA11
0257 00441 103201 SOC C
0258 00442 015106 JSB OVFL0
0259 00443 075155 STB OUTA          SATURATE IF OVERFLOW OCCURRS

```

# FLUTTER SUPPRESSION SYSTEM COMPUTER PROGRAM (CONTINUED)

```

0260 00444 000000 NOP
0261*****
0262*CHANNEL A OUTPUT ROUTINE
0263*
0264*APPLY PREDICTOR ALGORITHM TO OUTPUT SIGNAL
0265*
0266*  $Y(N) = K1P1 * X(N) + K2P1 * X(N-1) + K3P1 * X(N-2)$ 
0267*
0268 00445 000000 NOP
0269 00446 061147 LDA INPA2 'A' = OUTA(N-2)
0270 00447 100200 MPY K3PA1
0271 00450 001203 'R' = OUTA(N-2) * K3PA1 (2** - 1)
0272 00451 100021 ASL 1
0273 00452 075150 STR TEMP1
0274 00453 061146 LDA INPA1 'A' = OUTA(N-1)
0275 00454 071147 STA INPA2 PUT OUTA(N-1) INTO OUTA(N-2) FOR NEXT I
0276 00455 100200 MPY K2PA1
0277 00456 001202 'B' = OUTA(N-1) * K2PA1 (2** - 1)
0278 00457 100021 ASL 1
0279 00460 075144 STB TEMP
0280 00461 061155 LDA OUTA 'A' = OUTA(N)
0281 00462 071146 STA INPA1 PUT OUTA(N) INTO OUTA(N-1) FOR ITERATION
0282 00463 100200 MPY K1PA1
0283 00464 001201 'R' = OUT(N) * K1P1 (2** - 1)
0284 00465 100021 ASL 1 'R' = " + OUTA(N-1) * K2PA1 (2** - 1)
0285 00466 045144 ADR TEMP 'B' = " + OUTA(N-2) * K3PA1 (2** - 1)
0286 00467 045150 ADR TEMP1 'B' = PREDICTED OUTPUT .002 MILLISEC AM
0287 00470 100021 ASL 1 CHECK FOR OVERFLOW
0288 00471 103201 SOC C
0289 00472 015106 JSB OVFL0
0290*****
0291*OUTPUT CHANNEL A ON D/A CHANNEL ZERO
0292*
0293 00473 101044 LSR 4 LSR TO INCLUDE CH 008 ID. IN BITS 12 THRU 15
0294 00474 102312 SFS 128
0295 00475 024474 JMP *-1
0296 00476 106612 OTB 128 12 BIT DATA & 4BIT CH ID. TO OUTPUT BUFFER I
0297 00477 103712 STC 128,C
0298 00500 000000 NOP
0299*****
0300*SET CHANNEL A FINISHED FLAG
0301*
0302 00501 061320 LDA FLAG
0303 00502 071303 STA AFF
0304 00503 000000 NOP
0305*****
0306*CHANNEL B FSS LOOP
0307*
0308 00504 061160 LDA CHB SELECT CHANNEL 1 OF A/D DEVICE (I/O PORT 138)
0309 00505 102611 OTA 118 OUTPUT 'A' REG TO I/O PORT 118
0310 00506 103711 STC 118,C DEVICE COMMAND TO I/O 118
0311 00507 102311 SFS 118
0312 00510 024507 JMP *-1
0313 00511 102511 LIA 118 READ I/O BUFFER CONTENT IN 'A' REG

```



# FLUTTER SUPPRESSION SYSTEM COMPUTER PROGRAM (CONTINUED)

```

0313 00512 011166 AND MASK ZERO OUT/ CH.ID ON BITS 0 THRU 5
0314 00513 071247 STA INPTB
0315*****
0316*CHANNEL B FSS FILTER IMPLEMENTATION
0317*****
0318* STAGE B11 LAG (10/(S+10))
0319*
0320 00514 000000 NOP
0321 00515 061231 LDA Y1B11 Y1B11 IN 'A'=Y(N-1)T
0322 00516 100200 MPY K1B11 'B'=Y(N-1)T*K1B11(2**=1)
      00517 001256
0323 00520 100021 ASL 1 'B'=Y(N-1)*K1B11
0324 00521 045232 ADB KXB11 'B'= Y(N-1)*K1B11+X(N-1)T*K2B11
0325 00522 075144 STB TEMP
0326 00523 061247 LDA INPTB 'A'=X(NT),,, 'INPTB'
0327 00524 100200 MPY K2B11 'B'=X(NT)*K2B11(2**=1)
      00525 001257
0328 00526 100021 ASL 1 'B'=X(NT)*K2B11
0329 00527 075232 STB KXB11 KXB11=X(N-1)T*K2B11 FOR NEXT ITERATION
0330 00530 045144 ADB TEMP 'B'=(X(NT)+X(N-1)T)*K2B11 + Y(N-1)T*K1B11
0331 00531 075231 STB Y1B11 Y1B11=Y(NT),,OUTPUT OF THIS STAGE
0332 00532 000000 NOP
0333*****
0334* STAGE B12 LAG (10/(S+10))
0335*
0336 00533 000000 NOP
0337 00534 061233 LDA Y1B12 Y1B12 IN 'A'=Y(N-1)T
0338 00535 100200 MPY K1B12 'B'=Y(N-1)T*K1B12(2**=1)
      00536 001260
0339 00537 100021 ASL 1 'B'=Y(N-1)*K1B12
0340 00540 045234 ADB KXB12 'B'= Y(N-1)*K1B12+X(N-1)T*K2B12
0341 00541 075144 STB TEMP
0342 00542 061231 LDA Y1B11 'A'=X(NT)=OUTPUT FROM STAGE B11
0343 00543 100200 MPY K2B12 'B'=X(NT)*K2B12(2**=1)
      00544 001261
0344 00545 100021 ASL 1 'B'=X(NT)*K2B12
0345 00546 075234 STB KXB12 KXB12=X(N-1)T*K2B12 FOR NEXT ITERATION
0346 00547 045144 ADB TEMP 'B'=(X(NT)+X(N-1)T)*K2B12 + Y(N-1)T*K1B12
0347 00550 075233 STB Y1B12 Y1B12=Y(NT),,OUTPUT OF THIS STAGE
0348 00551 000000 NOP
0349*****
0350* STAGE B21 LAG 150/(S+150)
0351*
0352 00552 061235 LDA Y1B21 'A'=Y(N-1)
0353 00553 100200 MPY K1B21 'B'=Y(N-1)*K1B21(2**=1)
      00554 001262
0354 00555 100021 ASL 1 'B'=Y(N-1)*K1B21
0355 00556 045236 ADB KXB21 'B'=Y(N-1)*K1B21+X(N-1)*K2B21
0356 00557 075144 STB TEMP
0357 00560 061247 LDA INPTB 'A'= X(NT);,,FSS CHANNEL B INPUT
0358 00561 100200 MPY K2B21 'B'=X(NT)*K2B21(2**=1)
      00562 001263
0359 00563 100021 ASL 1 'B'= X(NT)*K2B21
0360 00564 075236 STB KXB21 KXB21=X(N-1)*K2B21 FOR NEXT ITERATION
0361 00565 045144 ADB TEMP 'B'=(X(NT)+X(N-1)T)*K2B21 +Y(N-1)T*K1B21
0362 00566 075235 STB Y1B21 Y1B21=Y(NT),,OUTPUT OF THIS STAGE

```

# FLUTTER SUPPRESSION SYSTEM COMPUTER PROGRAM (CONTINUED)

```

0363 00567 000000 NOP
0364*****
0365* STAGE B22 LAG 150/(S+150)
0366*
0367 00570 061237 LDA Y1B22 'A'=Y(N-1)
0368 00571 100200 MPY K1B22 'B'=Y(N-1)*K1B22(2**-1)
      00572 001264
0369 00573 100021 ASL 1 'B'=Y(N-1)*K1B22
0370 00574 045240 ADB KXB22 'B'=Y(N-1)*K1B22+X(N-1)*K2B22
0371 00575 075144 STB TEMP
0372 00576 061235 LDA Y1B21 'A'=X(NT)=OUTPUT FROM STAGE B21
0373 00577 100200 MPY K2B22 'B'=X(NT)*K2B22(2**-1)
      00600 001265
0374 00601 100021 ASL 1 'B'=X(NT)*K2B22
0375 00602 075240 STB KXB22 KXB22=X(N-1)*K2B22 FOR NEXT ITERATION
0376 00603 045144 ADB TEMP 'B'=(X(NT)+X(N-1)T)*K2B22 +Y(N-1)T*K1B22
0377 00604 075237 STB Y1B22 Y1B22=Y(NT),,OUTPUT OF THIS STAGE
0378 00605 000000 NOP
0379*****
0380* STAGE B23 LAG 150/(S+150)
0381*
0382 00606 061241 LDA Y1B23 'A'=Y(N-1)
0383 00607 100200 MPY K1B23 'B'=Y(N-1)*K1B23(2**-1)
      00610 001266
0384 00611 100021 ASL 1 'B'=Y(N-1)*K1B23
0385 00612 045242 ADB KXB23 'B'=Y(N-1)*K1B23+X(N-1)*K2B23
0386 00613 075144 STB TEMP
0387 00614 061237 LDA Y1B22 'A'=X(NT)=OUTPUT FROM STAGE B22
0388 00615 100200 MPY K2B23 'B'=X(NT)*K2B23(2**-1)
      00616 001267
0389 00617 100021 ASL 1 'B'=X(NT)*K2B23
0390 00620 075242 STB KXB23 KXB23=X(N-1)*K2B23 FOR NEXT ITERATION
0391 00621 045144 ADB TEMP 'B'=(X(NT)+X(N-1)T)*K2B23 +Y(N-1)T*K1B23
0392 00622 075241 STB Y1B23 Y1B23=Y(NT),,OUTPUT OF THIS STAGE
0393 00623 000000 NOP
0394*****
0395** STAGE B31 FIRST-ORDER/SECOND-ORDER
0396** 32.1325(S+56.811)/(S2+50S+15625)
0397**
0398 00624 000000 NOP
0399 00625 061244 LDA Y2B31 'A'=Y(N-2)
0400 00626 100200 MPY K2B31
      00627 001271
0401 00630 100021 ASL 1 'B'=Y(N-2)*K2B31
0402 00631 075150 STB TEMP1
0403 00632 061243 LDA Y1B31 'A'=Y(N-1)
0404 00633 071244 STA Y2B31 PUT Y(N-1) INTO Y(N-2) FOR NEXT IT
0405 00634 100200 MPY K1B31 'B'=Y(N-1)*K1B31(2**-2)
      00635 001270
0406 00636 100021 ASL 1 'B'=Y(N-1)*K1B31(2**-1)
0407 00637 075151 STB TEMP2
0408 00640 061246 LDA X3B31 'A'=X(N-2)
0409 00641 100200 MPY K5B31
      00642 001274
0410 00643 100021 ASL 1 'B'=X(N-2)*K5B31
0411 00644 075152 STB TEMP3

```

# FLUTTER SUPPRESSION SYSTEM COMPUTER PROGRAM (CONTINUED)

0412	00645	061245	LDA X2B31	'A'=X(N-1)
0413	00646	071246	STA X3B31	PUT X(N-1) INTO X(N-2) FOR NEXT IT
0414	00647	100200	MPY K4B31	
	00650	001273		
0415	00651	100021	ASL 1	'B'=X(N-1)*K4B31
0416	00652	075153	STB TEMP4	
0417	00653	061247	LDA INPTB	'A'=X(N),,,,FSS CHANNEL B INPUT
0418	00654	001121	ARS,ARS	
0419	00655	001100	ARS	'A'=X(N)/8 PREVENT OVERFLOW AT 2
0420	00656	071245	STA X2B31	PUT X(N) INTO X(N-1) FOR NEXT ITER
0421	00657	100200	MPY K3B31	
	00660	001272		
0422	00661	100021	ASL 1	'B'=X(N)*K3B31
0423	00662	045152	ADB TEMP3	'B'= " + X(N-2)*K5B31
0424	00663	000000	NOP	
0425	00664	045153	ADB TEMP4	'B'= " + X(N-1)*K4B31
0426	00665	000000	NOP	
0427	00666	045150	ADB TEMP1	'B'= " + Y(N-2)*K2B31
0428	00667	000000	NOP	
0429	00670	005100	BRS 1	'B'= "(2**=1)
0430	00671	045151	ADB TEMP2	'B'= " +Y(N-1)*K1B31(2**=1)
0431	00672	000000	NOP	
0432	00673	005000	BLS 1	'B'= Y(N)-----DON'T KNOW LAST
0433	00674	075243	STB Y1B31	Y1B31=Y(NT),,OUTPUT OF THIS STAGE
0434	00675	000000	NOP	
0435	*****			
0436	SUMMATION OF FILTER OUTPUTS			
0437	*****			
0438	00676	061231	LDA Y1B11	'A'=OUTPUT FROM STAGE B11
0439	00677	100200	MPY KOB11	
	00700	001276		
0440	00701	100021	ASL 1	'B'= B11*KOB11
0441	00702	075150	STB TEMP1	
0442	00703	061233	LDA Y1B12	'A'=OUTPUT FROM STAGE B12
0443	00704	100200	MPY KOB12	
	00705	001275		
0444	00706	100021	ASL 1	'B'= B12*KOB12
0445	00707	075151	STB TEMP2	
0446	00710	061235	LDA Y1B21	'A'=OUTPUT FROM STAGE B21
0447	00711	100200	MPY KOB21	
	00712	001301		
0448	00713	100021	ASL 1	'B'= B21*KOB21
0449	00714	075152	STB TEMP3	
0450	00715	061237	LDA Y1B22	'A'=OUTPUT FROM STAGE B22
0451	00716	100200	MPY KOB22	
	00717	001300		
0452	00720	100021	ASL 1	'B'= B22*KOB22
0453	00721	075153	STB TEMP4	
0454	00722	061241	LDA Y1B23	'A'=OUTPUT FROM STAGE B23
0455	00723	100200	MPY KOB23	
	00724	001277		
0456	00725	100021	ASL 1	'B'= B23*KOB23
0457	00726	075154	STB TEMP5	
0458	00727	061243	LDA Y1B31	'A'=OUTPUT FROM STAGE B31
0459	00730	100200	MPY KOB31	
	00731	001302		

# FLUTTER SUPPRESSION SYSTEM COMPUTER PROGRAM (CONTINUED)

```

0460 00732 100021 ASL 1 'B' = B31*K0B31
0461 00733 045154 ADB TEMP5 'B' = " + B23*K0B23
0462 00734 045153 ADB TEMP4 'B' = " + B22*K0B22
0463 00735 045152 ADB TEMP3 'B' = " + B21*K0B21
0464 00736 045151 ADB TEMP2 'B' = " + B12*K0B12
0465 00737 045150 ADB TEMP1 'B' = " + B11*K0B11
0466 00740 103201 SOC C
0467 00741 015106 JSB OVFL0 SATURATE IF OVERFLOW OCCURRS
0468 00742 075252 STB OUTB
0469 00743 000000 NOP
0470*****
0471*CHANNEL B OUTPUT ROUTINE
0472*
0473*APPLY PREDICTOR ALGORITHM TO OUTPUT SIGNAL
0474*
0475* Y(N)=K1P1*X(N)+K2P1*X(N-1)+K3P1*X(N-2)
0476*
0477 00744 000000 NOP
0478 00745 061251 LDA INPB2 'A'=OUTB(N-2)
0479 00746 100200 MPY K3PB1
0480 00750 100021 ASL 1 'B'=OUTB(N-2)*K3PB1(2**-1)
0481 00751 075150 STB TEMP1
0482 00752 061250 LDA INPB1 'A'=OUTB(N-1)
0483 00753 071251 STA INPB2 PUT OUTB(N-1) INTO OUTB(N-2) FOR NEXT I
0484 00754 100200 MPY K2PB1
0485 00755 001254 'B'=OUTB(N-1)*K2PB1(2**-1)
0486 00757 075144 STB TEMP
0487 00760 061252 LDA OUTB 'A'=OUTB(N)
0488 00761 071250 STA INPB1 PUT OUTB(N) INTO OUTB(N-1) FOR ITERATION
0489 00762 100200 MPY K1PB1
0490 00764 100021 ASL 1 'B'=OUTB(N)*K1PB1(2**-1)
0491 00765 045144 ADB TEMP 'B' = " + OUTB(N-1)*K2PB1(2**-1)
0492 00766 045150 ADB TEMP1 'B' = " + OUTB(N-2)*K3PB1(2**-1)
0493 00767 100021 ASL 1 'B' = PREDICTED OUTPUT .002 MILLISEC AH
0494 00770 103201 SOC C CHECK FOR OVERFLOW
0495 00771 015106 JSB OVFL0
0496*****
0497*OUTPUT CHANNEL B ON D/A CHANNEL ONE
0498*
0499 00772 002404 CLA,INA
0500 00773 101104 RRR 4 ROTATE TO INCLUDE CH 1B ID. IN BITS 12 THRU 15
0501 00774 102312 SFS 12B
0502 00775 024774 JMP *-1
0503 00776 106612 OTB 12B 12 BIT DATA & 4BIT CH ID. TO OUTPUT BUFFER I
0504 00777 103712 STC 12B,C
0505 01000 000000 NOP
0506*****
0507* SET CHANNEL B FINISHED FLAG
0508*
0509 01001 061320 LDA FLAG
0510 01002 071304 STA BFF
0511 01003 000000 NOP
0512*****

```

# FLUTTER SUPPRESSION SYSTEM COMPUTER PROGRAM (CONTINUED)

```

0513* DIGITAL CROSS CHECK OF A & B CHANNELS ON ANOTHER COMPUTER'S
0514* OUTPUT VERSUS OUTPUT OF ANALOG VOTER
0515* DATA IS SHIFTED TO THE RIGHT TO ELIMINATE ALL BUT
0516* THE SIGN BIT AND 2 SIGNIFICANT BITS
0517*
0518 01004 061161 LDA CH2
0519 01005 102611 OTA 118 SELECT CHANNEL 2 OF A/D
0520 01006 103711 STC 118,C
0521 01007 102311 SFS 118
0522 01010 025007 JMP *-1
0523 01011 102511 LIA 118 'A'= CHANNEL A VOTER OUTPUT
0524 01012 065162 LDB CH3
0525 01013 106611 OTB 118 SELECT CHANNEL 3 OF A/D
0526 01014 103711 STC 118,C
0527 01015 102311 SFS 118
0528 01016 025015 JMP *-1
0529 01017 106511 LIB 118 'B'= CHANNEL A COMPUTER OUTPUT
0530 01020 015116 JSB PROCS PROCESS DATA
0531 01021 075321 STB CHAER
0532 01022 061163 LDA CH4
0533 01023 102611 OTA 118 SELECT CHANNEL 4 OF A/D
0534 01024 103711 STC 118,C
0535 01025 102311 SFS 118
0536 01026 025025 JMP *-1
0537 01027 102511 LIA 118 'A'= CHANNEL B VOTER OUTPUT
0538 01030 065164 LDB CH5
0539 01031 106611 OTB 118 SELECT CHANNEL 5 OF A/D
0540 01032 103711 STC 118,C
0541 01033 102311 SFS 118
0542 01034 025033 JMP *-1
0543 01035 106511 LIB 118 'B'= CHANNEL A COMPUTER OUTPUT
0544 01036 015116 JSB PROCS PROCESS DATA
0545 01037 075322 STB CHBER
0546*
0547* CHECK FOR EXCESSIVE ERROR AND SET APPROPRIATE FLAGS
0548*
0549 01040 061321 LDA CHAER 'A'= CHAN A VOTER - CHAN A OUTPUT
0550 01041 002002 SZA IS ERROR ZERO
0551 01042 025045 JMP **3 NO
0552 01043 061320 LDA FLAG YES
0553 01044 071306 STA ACF SET CHANNEL A 'OK' FLAG
0554 01045 000000 NOP DON'T SET CHANNEL 'OK' FLAG
0555 01046 061322 LDA CHBER 'A'= CHAN B VOTER - CHAN B OUTPUT
0556 01047 002002 SZA IS ERROR ZERO
0557 01050 025053 JMP **3 NO
0558 01051 061320 LDA FLAG YES
0559 01052 071307 STA BCF SET CHANNEL B 'OK' FLAG
0560 01053 000000 NOP DON'T SET CHANNEL B 'OK' FLAG
0561 01054 061320 LDA FLAG
0562 01055 071305 STA CFF SET COMPARISON FINISHED FLAG
0563 01056 000000 NOP
0564** DUMMY COUNTER ROUTINE 4.9MICROSECONDS COUNT
0565 01057 002400 CLA
0566 01060 071176 STA NUMBR
0567 01061 035176 ISZ NUMBR SKIP IF NUMBR=0, NUMBR=-32768
0568 01062 025061 JMP *-1 JUMP TO INCREMENT

```

# FLUTTER SUPPRESSION SYSTEM COMPUTER PROGRAM (CONTINUED)

```

0569 01063 000000 NOP
0570 01064 102044 HLT 44B
0571 01065 025065 END JMP *
0572*
0573* RESET THE COUNTER
0574 01066 000000 RCNTR NOP
0575 01067 061174 LDA MNUM
0576 01070 071175 STA CNTDN
0577 01071 061176 LDA NUMBR
0578 01072 071156 STA LCNT
0579 01073 103710 STC 10B,C
0580 01074 125066 JMP RCNTR,I
0581*
0582* INCREMENT THE COUNTER
0583 01075 001076 CNT DEF CNTR
0584 01076 000000 CNTR NOP
0585 01077 106710 CLC 10B
0586 01100 035175 ISZ CNTDN
0587 01101 025104 JMP **3
0588 01102 102077 HLT 77B HALT AFTER ONE PASS & CHECK DATA IN 'NUMBR'
0589 01103 024115 JMP START
0590 01104 103710 STC 10B,C
0591 01105 125076 JMP CNTR,I
0592*
0593*****
0594* THE OVERFLOW SUBROUTINE
0595* THE INPUT IS IN THE B REGISTER
0596 01106 000000 OVFLD NOP
0597 01107 006020 SSB
0598 01110 025113 JMP **3
0599 01111 065171 LDB PLUS
0600 01112 025114 JMP **2
0601 01113 065172 LDB MINUS
0602 01114 103101 CLO
0603 01115 125106 JMP OVFLD,I
0604*****
0605*****
0606* SUBROUTINE TO SUBTRACT A-REG FROM B-REG AND TAKE ABSOLUTE
0607* VALUE AND SHIFT DATA RIGHT 12 PLACES
0608*
0609 01116 000000 PROCS NOP
0610 01117 003004 CMA,INA
0611 01120 044000 ADB 0B
0612 01121 006020 SSB
0613 01122 007004 CMB,INB
0614 01123 000000 NOP
0615 01124 101055 LSR 13
0616 01125 125116 JMP PROCS,I
0617*
0618* FILTER INITIAL CONDITIONS CHANNEL A
0619*
0620 01126 000000 Y1A11 OCT 0
0621 01127 000000 KXA11 OCT 0
0622*
0623 01130 000000 Y1A12 OCT 0
0624 01131 000000 KXA12 OCT 0

```

# FLUTTER SUPPRESSION SYSTEM COMPUTER PROGRAM (CONTINUED)

```

0625*
0626 01132 000000 Y1A21 OCT 0
0627 01133 000000 KXA21 OCT 0
0628*
0629 01134 000000 Y1A22 OCT 0
0630 01135 000000 KXA22 OCT 0
0631*
0632 01136 000000 Y1A23 OCT 0
0633 01137 000000 KXA23 OCT 0
0634*
0635 01140 000000 Y1A31 OCT 0
0636 01141 000000 Y2A31 OCT 0
0637 01142 000000 X2A31 OCT 0
0638 01143 000000 X3A31 OCT 0
0639*
0640 01144 000000 TEMP OCT 0
0641 01145 000000 INPTA OCT 0
0642 01146 000000 INPA1 OCT 0
0643 01147 000000 INPA2 OCT 0
0644 01150 000000 TEMP1 OCT 0
0645 01151 000000 TEMP2 OCT 0
0646 01152 000000 TEMP3 OCT 0
0647 01153 000000 TEMP4 OCT 0
0648 01154 000000 TEMP5 OCT 0
0649 01155 000000 OUTA OCT 0
0650 01156 000000 LCNT OCT 0
0651*****
0652* CONSTANTS FOR I/O AND .004 CYCLE TIME
0653*
0654 01157 100000 CHA OCT 100000
0655 01160 100001 CHB OCT 100001
0656 01161 100002 CH2 OCT 100002
0657 01162 100003 CH3 OCT 100003
0658 01163 100004 CH4 OCT 100004
0659 01164 100005 CH5 OCT 100005
0660 01165 170140 INIT OCT 170140
0661 01166 177700 MASK OCT 177700
0662 01167 010000 DACH OCT 010000
0663 01170 000001 CW OCT 1
0664 01171 077777 PLUS OCT 77777
0665 01172 100000 MINUS OCT 100000
0666 01173 114020 IJSB JSB 20B,I
0667 01174 177776 MNUM DEC -2
0668 01175 177776 CNTDN DEC -2
0669 01176 000000 NUMBR DEC 0
0670 01177 037777 MAX02 OCT 37777 32768/2-1
0671 01200 000100 ONHUN OCT 100
0672*****
0673** PREDICTOR ALGORITHM CONSTANTS TAU=T/2=.002MILLISECONDS
0674*
0675* CHANNEL A
0676*
0677 01201 074000 K1PA1 DEC 30720 =1.875(2**14)
0678 01202 130000 K2PA1 DEC -20480 =-1.25(2**14)
0679 01203 014000 K3PA1 DEC 6144 =.375(2**14)
0680*****

```

# FLUTTER SUPPRESSION SYSTEM COMPUTER PROGRAM (CONTINUED)

```

0681* CHANNEL A FILTER CONSTANTS
0682* CONSTANTS FOR .002 CYCLE TIME
0683*
0684 01204 076566 K1A11 DEC 32118 =.9801980198(2**15)
0685 01205 000505 K2A11 DEC 325 =.0099009901(2**15)
0686*
0687 01206 076566 K1A12 DEC 32118 =.9801980198(2**15)
0688 01207 000505 K2A12 DEC 325 =.0099009901(2**15)
0689*
0690 01210 057234 K1A21 DEC 24220 =.7391304348(2**15)
0691 01211 010262 K2A21 DEC 4274 =.1304347826(2**15)
0692*
0693 01212 057234 K1A22 DEC 24220 =.7391304348(2**15)
0694 01213 010262 K2A22 DEC 4274 =.1304347826(2**15)
0695*
0696 01214 057234 K1A23 DEC 24220 =.7391304348(2**15)
0697 01215 010262 K2A23 DEC 4274 =.1304347826(2**15)
0698*
0699 01216 073076 K1A31 DEC 30270 =1.847507236(2**14)
0700 01217 106003 K2A31 DEC -29693 =-.9061583110(2**15)
0701 01220 021352 K3A31 DEC 8938 =.2727598821(2**15)
0702 01221 001701 K4A31 DEC 961 =.0293225116(2**15)
0703 01222 160327 K5A31 DEC -7977 =-.2434343704(2**15)
0704*****
0705* CHANNEL A OUTPUT SUMMATION CONSTANTS
0706*
0707 01223 115657 KOA12 DEC -25681 =-56.176/1.024*70(2**15)
0708 01224 073350 KOA11 DEC 30440 =66.588/1.024*70(2**15)
0709 01225 152025 KOA23 DEC -11243 =-24.593/1.024*70(2**15)
0710 01226 027101 KOA22 DEC 11841 =26.003/1.024*70(2**15)
0711 01227 155422 KOA21 DEC -9454 =-20.681/1.024*70(2**15)
0712 01230 077213 KOA31 DEC 32395 =70.863/1.024*70(2**15)
0713*****
0714* FILTER INITIAL CONDITIONS CHANNEL A
0715*
0716 01231 000000 Y1B11 OCT 0
0717 01232 000000 KX911 OCT 0
0718*
0719 01233 000000 Y1B12 OCT 0
0720 01234 000000 KX812 OCT 0
0721*
0722 01235 000000 Y1B21 OCT 0
0723 01236 000000 KX821 OCT 0
0724*
0725 01237 000000 Y1B22 OCT 0
0726 01240 000000 KX822 OCT 0
0727*
0728 01241 000000 Y1B23 OCT 0
0729 01242 000000 KX823 OCT 0
0730*
0731 01243 000000 Y1B31 OCT 0
0732 01244 000000 Y2B31 OCT 0
0733 01245 000000 X2B31 OCT 0
0734 01246 000000 X3B31 OCT 0
0735*
0736 01247 000000 INPTB OCT 0

```



# FLUTTER SUPPRESSION SYSTEM COMPUTER PROGRAM (CONTINUED)

```

0737 01250 000000 INPB1 OCT 0
0738 01251 000000 INPB2 OCT 0
0739 01252 000000 OUTB OCT 0
0740*****
0741** PREDICTOR ALGORITHM CONSTANTS    TAU=T/2=.002MILLISECONDS
0742*
0743* CHANNEL B
0744*
0745 01253 074000 K1PB1 DEC 30720          =1.875(2**14)
0746 01254 130000 K2PB1 DEC -20480         =-1.25(2**14)
0747 01255 014000 K3PB1 DEC 6144          =.375(2**14)
0748*****
0749* CHANNEL B FILTER CONSTANTS
0750* CONSTANTS FOR .002 CYCLE TIME
0751*
0752 01256 076566 K1B11 DEC 32118          =.9801980198(2**15)
0753 01257 000505 K2B11 DEC 325           =.0099009901(2**15)
0754*
0755 01260 076566 K1B12 DEC 32118          =.9801980198(2**15)
0756 01261 000505 K2B12 DEC 325           =.0099009901(2**15)
0757*
0758 01262 057234 K1B21 DEC 24220          =.7391304348(2**15)
0759 01263 010262 K2B21 DEC 4274          =.1304347826(2**15)
0760*
0761 01264 057234 K1B22 DEC 24220          =.7391304348(2**15)
0762 01265 010262 K2B22 DEC 4274          =.1304347826(2**15)
0763*
0764 01266 057234 K1B23 DEC 24220          =.7391304348(2**15)
0765 01267 010262 K2B23 DEC 4274          =.1304347826(2**15)
0766*
0767 01270 073076 K1B31 DEC 30270          =1.847507236(2**14)
0768 01271 106003 K2B31 DEC -29693         =-.9061583110(2**15)
0769 01272 021352 K3B31 DEC 8938          =.2727598821(2**15)
0770 01273 001701 K4B31 DEC 961           =.0293255116(2**15)
0771 01274 160327 K5B31 DEC -7977         =-.2434343704(2**15)
0772*****
0773* CHANNEL B OUTPUT SUMMATION CONSTANTS
0774*
0775 01275 115657 K0B12 DEC -25681          =-56.176/1.024*70(2**15)
0776 01276 073350 K0B11 DEC 30440          =66.588/1.024*70(2**15)
0777 01277 152025 K0B23 DEC -11243         =-24.593/1.024*70(2**15)
0778 01300 027101 K0B22 DEC 11841          =26.003/1.024*70(2**15)
0779 01301 155422 K0B21 DEC -9454          =-20.681/1.024*70(2**15)
0780 01302 077213 K0B31 DEC 32395          =70.863/1.024*70(2**15)
0781*****
0782* S REGISTER FLASH ROUTINE CONSTANTS
0783*
0784* INITIAL CONDITIONS
0785*
0786 01303 177777 AFF OCT -1
0787 01304 177777 BFF OCT -1
0788 01305 177777 CFF OCT -1
0789 01306 177777 ACF OCT -1
0790 01307 177777 BCF OCT -1
0791 01310 000000 ERCNT OCT 0
0792 01311 177777 ERCLK OCT -1

```

# FLUTTER SUPPRESSION SYSTEM COMPUTER PROGRAM (CONCLUDED)

```

0793*
0794*CONSTANTS
0795*
0796 01312 000002  AFFER OCT 2
0797 01313 000020  BFFER OCT 20
0798 01314 000200  ACFER OCT 200
0799 01315 002000  BCFER OCT 2000
0800 01316 020000  CFFER OCT 20000
0801 01317 177603  FLCNT DEC -125
0802 01320 177777  FLAG OCT -1
0803*****
0804* CROSS-CHECK INITIAL CONDITIONS
0805*
0806 01321 000000  CHAER OCT 0
0807 01322 000000  CHBER OCT 0
0808***** THE *** END *****
0809                                END

```

# HARDWARE TEST PROGRAM

```

0001          ASMB,A,B,T,L
0002* FILE NAME  &JTEST   CREATED 8/31/78 BY JRMATTHEW
0003*****
0004* PROGRAM TO TEST ADC AND DAC CHANNELS 0-7
0005* SET BIT 15 FOR CONTINUOUS INPUT AND OUTPUT OF DATA
0006* OR CLEAR BIT 15 FOR DISCRETE INPUT AND OUTPUT OF DATA
0007* IN S REGISTER WHEN HALT 20B OCCURRS AND PUSH RUN
0008*
0009 10000          ORG 10000B
0010 10000 103100   CLF 0          TURN OFF INTERRUPT SYSTEM
0011 10001 062004   LDA INIT      INITIALIZE DAC
0012 10002 102612   OTA 12B
0013 10003 103712   STC 12B,C
0014 10004 170140   INIT OCT 170140
0015 10005 102020   MAIN HLT 20B   SET OR CLEAR BIT 15 AS ABOVE INSTUCTIONS
0016 10006 102501   LIA 1B
0017 10007 002020   SSA
0018 10010 026013   JMP COUT      JUMP TO CONTINUOUS ROUTINE
0019 10011 026030   JMP DOUT      JUMP TO DISCRETE ROUTINE
0020 10012 102077   HLT 77B
0021*****
0022* ROUTINE TO INPUT AND OUTPUT DATA CONTINUOUSLY FROM
0023* SELECTED ADC AND DAC CHANNELS
0024*
0025* HALT 22B INDICATES TOP OF ROUTINE--ENTER ADC CHANNEL INTO
0026* BITS 0-2 AND DAC CHANNEL INTO BITS 3-5 AND PUSH RUN
0027*
0028* SET BIT 0 TO STOP CLEAR TO CONTINUE
0029*
0030 10013 102022   COUT HLT 22B   READY FOR CHANNEL INFO
0031 10014 016071   JSB GCHAN      PROCESS CHANNEL INFO
0032 10015 016056   LOOP JSB ADC   GET INPUT FROM ADC
0033 10016 062027   LOA INPUT
0034 10017 102601   OTA 1B         PUT INPUT INTO S REGISTER
0035 10020 072026   STA OUTPT
0036 10021 016044   JSB DAC        OUTPUT INPUT DATA TO DAC
0037 10022 102501   LIA 1B
0038 10023 000010   SLA
0039 10024 026005   JMP MAIN
0040 10025 026015   JMP LOOP
0041*
0042 10026 000000   OUTPT OCT 0
0043 10027 000000   INPUT OCT 0
0044*****
0045* ROUTINE TO OUTPUT DATA IN S REGISTER TO DAC AND INPUT DATA
0046* FROM ADC USING CHANNELS IN BITS 0-2 FOR ADC AND 3-5 FOR DAC
0047* INPUT IS IN A REGISTER
0048*
0049* HALT 21B MEANS TOP OF ROUTINE ENTER CHANNEL INFO
0050*
0051* HALT 40B ENTER OUTPUT DATA
0052*
0053* HALT 31B SET BIT 15 TO STOP CLEAR TO CONTINUE
0054*
0055 10030 102021   DOUT HLT 21B   ENTER CHANNEL INFO
0056 10031 016071   JSB GCHAN      PROCESS CHANNEL INFO

```

# HARDWARE TEST PROGRAM (CONTINUED)

```

0057 10032 102040 HLT 40B          ENTER DATA
0058 10033 102501 LIA 1B          GET DATA
0059 10034 072026 STA OUTPT
0060 10035 016044 JSB DAC          OUTPUT DATA TO DAC
0061 10036 016056 JSB ADC          INPUT DATA FROM ADC
0062 10037 062027 LDA INPUT        PUT INPUT INTO A REGISTER
0063 10040 102031 HLT 31B          SET BIT 15 TO STOP CLEAR TO CONTINUE
0064 10041 002020 SSA
0065 10042 026005 JMP MAIN
0066 10043 026030 JMP DOUT
0067*****
0068* DAC OUTPUT ROUTINE USING SLOT 12B
0069*
0070 10044 000000 DAC NOP
0071 10045 066026 LDB OUTPT        'B'=OUTPUT
0072 10046 101044 LSR 4            SHIFT RIGHT 4 AND CLEAR UPPER BITS
0073 10047 062111 LDA DACCH        'A'=DAC CHANNEL IN BITS 12-15
0074 10050 030001 IOR 1B          'A'=OVERLAY OF OUTPUT AND CHANNEL
0075 10051 102312 SFS 12B          LAST OUTPUT COMPLETE?
0076 10052 026051 JMP *-1         NO-CHECK AGAIN
0077 10053 102612 OTA 12B          YES-OUTPUT DATA
0078 10054 103712 STC 12B,C
0079 10055 126044 JMP DAC,I       RETURN
0080*****
0081* ADC INPUT ROUTINE USING SLOT 11B
0082*
0083 10056 000000 ADC NOP
0084 10057 062110 LDA ADCCH        'A'=OUTPUT CHANNEL CONTROL WORD
0085 10060 102611 OTA 11B          SELECT CHANNEL
0086 10061 103711 STC 11B,C
0087 10062 102311 SFS 11B          INPUT COMPLETE ?
0088 10063 026062 JMP *-1         NO-CHECK AGAIN
0089 10064 102511 LIA 11B          YES-'A'=INPUT
0090 10065 012070 AND MASK        MASK OUT CHANNEL ID
0091 10066 072027 STA INPUT
0092 10067 126056 JMP ADC,I       RETURN
0093*
0094 10070 177700 MASK OCT 177700
0095*****
0096* GETS ADC AND DAC CHANNEL NUMBERS FROM S REGISTER
0097*
0098* ADC CHANNEL IN BITS 0-2
0099*
0100* DAC CHANNEL IN BITS 3-5
0101*
0102 10071 000000 GCHAN NOP
0103 10072 102501 LIA 1B          GET CHANNEL INFO
0104 10073 070001 STA 1B          PUT INTO 'B'
0105 10074 012105 AND MASK1        'A'=BITS 0-2
0106 10075 032106 IOR MASK2        'A'=10000N N=ADC CHANNEL NUMBER
0107 10076 072110 STA ADCCH        STORE ADC CONTROL WORD
0108 10077 060001 LDA 1B
0109 10100 012107 AND MASK3        'A'=BITS 3-5
0110 10101 001727 ALF,ALF
0111 10102 001200 RAL
0112 10103 072111 STA DACCH        'A' HAS DAC CHANNEL IN BITS 12-15
                                         STORE DAC CONTROL WORD

```

# HARDWARE TEST PROGRAM (CONCLUDED)

```
0113 10104 126071    JMP GCHAN,I          RETURN
0114*
0115 10105 000007    MASK1 OCT 7
0116 10106 100000    MASK2 OCT 100000
0117 10107 000070    MASK3 OCT 70
0118 10110 000000    ADCCH OCT 0
0119 10111 000000    DACCH OCT 0
0120*****
0121                      END
```

## ALPHABETIC LIST OF INSTRUCTIONS FOR HP2100 COMPUTER

ABS	Define absolute value
ADA	Add to A
ADB	Add to B
ALF	Rotate A left 4
ALR	Shift A left 1, clear sign
ALS	Shift A left 1
AND	"And" to A
ARS	Shift A right 1, sign carry
ASC	Generate ASCII characters
ASL	Arithmetic long shift left
ASR	Arithmetic long shift right
BLF	Rotate B left 4
BLR	Shift B left 1, clear sign
BLS	Shift B left 1
BRS	Shift B right 1, carry sign
BSS	Reserve block of storage starting at symbol
CCA	Clear and complement A (1's)
CCB	Clear and complement B (1's)
CCE	Clear and complement E (set E = 1)
CLA	Clear A
CLB	Clear B
CLC	Clear I/O control bit
CLE	Clear E
CLF	Clear I/O flag
CLO	Clear overflow bit
CMA	Complement A
CMB	Complement B
CME	Complement E
COM	Reserve block of common storage
CPA	Compare to A, skip if unequal
CPB	Compare to B, skip if unequal
DEC	Defines decimal constants
DEF	Defines address
DEX	Defines extended precision constants
DIV	Divide
DLD	Double load
DST	Double store
ELA	Rotate E and A left 1
ELB	Rotate E and B left 1
END	Terminate program
ENT	Entry point
ERA	Rotate E and A right 1
ERB	Rotate E and B right 1

# ALPHABETIC LIST OF INSTRUCTIONS FOR HP2100 COMPUTER (CONTINUED)

EQU	Equate symbol
EXT	External reference
FAD	Floating add
FDV	Floating divide
FMP	Floating multiply
FSB	Floating subtract
HED	Print heading at top of each page
HLT	Halt
IFN	When N appears in Control Statement, assemble ensuing instructions
IFZ	When Z appears in Control Statement, assemble ensuing instructions
INA	Increment A by 1
INB	Increment B by 1
IOR	Inclusive "or" to A
ISZ	Increment, then skip if zero
JMP	Jump
JSB	Jump to subroutine
LDA	Load into A
LDB	Load into B
LIA	Load into A from I/O channel
LIB	Load into B from I/O channel
LSL	Logical long shift left
LSR	Logical long shift right
LST	Resume list output (follows a UNL)
MIA	Merge "or" into A from I/O channel
MIB	Merge "or" into B from I/O channel
MPY	Multiply
NAM	Names relocatable program
NOP	No operation
OCT	Defines octal constant
ORB	Establish origin in base page
ORG	Establish program origin
ORR	Reset program location counter
OTA	Output from A to I/O channel
OTB	Output from B to I/O channel
RAL	Rotate A left 1
RAR	Rotate A right 1
RBL	Rotate B left 1
RBR	Rotate B right 1
REP	Repeat next statement
RRL	Rotate A and B left
RRR	Rotate A and B right

## ALPHABETIC LIST OF INSTRUCTIONS FOR HP2100 COMPUTER (CONCLUDED)

RSS	Reverse skip sense
SEZ	Skip if E = 0
SFC	Skip if I/O flag = 0 (clear)
SFS	Skip if I/O flag = 1 (set)
SKP	Skip to top of next page
SLA	Skip if LSB of A = 0
SLB	Skip if LSB of B = 0
SOC	Skip if overflow bit = 0 (clear)
SOS	Skip if overflow bit = 1 (set)
SPC	Space n lines
SSA	Skip if sign A = 0
SSB	Skip if sign B = 0
STA	Store A
STB	Store B
STC	Set I/O control bit
STF	Set I/O flag
STO	Set overflow bit
SUP	Suppress list output of additional code lines
SWP	Switch the (A) and (B)
SZA	Skip if A = 0
SZB	Skip if B = 0
UNL	Suppress list output
UNS	Resume list output of additional code lines
XIF	Terminate an IFN or IFZ group of instructions
XOR	Exclusive "or" to A



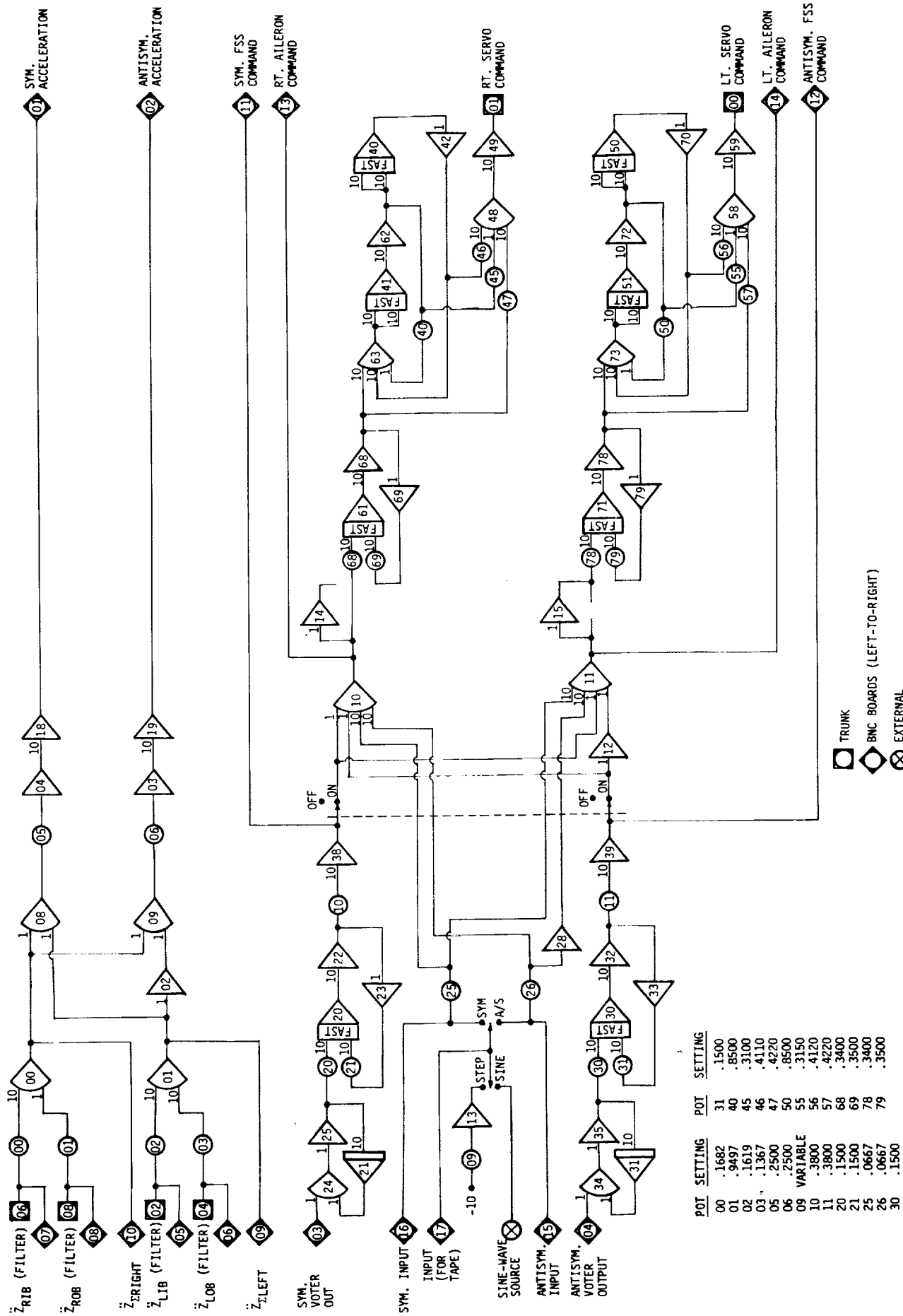


FIGURE B-3 - ANALOG COMPUTER PATCHING DIAGRAM

1. Report No. NASA CR-159155		2. Government Accession No.		3. Recipient's Catalog No.	
4. Title and Subtitle Developing, Mechanizing and Testing a Digital Active Flutter Suppression System for a Modified B-52 Wind-Tunnel Model				5. Report Date January 1980	
				6. Performing Organization Code	
7. Author(s) John Matthew				8. Performing Organization Report No. D3-1168-1	
				10. Work Unit No.	
9. Performing Organization Name and Address Boeing Military Airplane Company 3801 S. Oliver Wichita, Kansas 67210				11. Contract or Grant No. NAS1-14031	
				13. Type of Report and Period Covered Contractor Report, Final July 1975 to January 1980	
12. Sponsoring Agency Name and Address National Aeronautics and Space Administration Washington, DC 20546				14. Sponsoring Agency Code	
15. Supplementary Notes  Langley Technical Monitor: Robert V. Doggett, Jr.					
16. Abstract  A study was conducted to develop and mechanize a digital flutter suppression system for a significantly modified version of the 1/30-scale B-52E aeroelastic wind tunnel model. A model configuration was identified that produced symmetric and antisymmetric flutter modes that occur at $2873\text{N/m}^2$ (60 psf) dynamic pressure with violent onset. The flutter suppression system, using one trailing edge control surface and two accelerometers on each wing, extended the flutter dynamic pressure of the model beyond the design limit of $4788\text{N/m}^2$ (100 psf). The hardware and software required to implement the flutter suppression system were designed and mechanized using digital computers in a fail-operate configuration. The model equipped with the system was tested in the Transonic Dynamics Tunnel at NASA Langley Research Center and results showed the flutter dynamic pressure of the model was extended beyond $4884\text{N/m}^2$ (102 psf).					
17. Key Words (Suggested by Author(s))  Flutter Suppression Digital Control Laws Active Control Technology			18. Distribution Statement  Unclassified - Unlimited  Subject Category 39		
19. Security Classif. (of this report) Unclassified	20. Security Classif. (of this page) Unclassified		21. No. of Pages	22. Price*	